Establishment and application of a high-content screening assay to protect postmitotic podocytes in the zebrafish pronephros

I n a u g u r a l d i s s e r t a t i o n

zur

Erlangung des akademischen Grades eines

Doktors der Naturwissenschaften (Dr. rer. nat.)

der

Mathematisch-Naturwissenschaftlichen Fakultät

der

Universität Greifswald

vorgelegt von

Maximilian Schindler

Greifswald, 12.07.2022

Dekan:	Prof. Dr. rer. nat. Gerald Kerth
1. Gutachter:	Prof. Dr. rer. nat. Steffen Harzsch
2. Gutachter:	Prof. Dr. rer. nat. Nicole Endlich
3. Gutachter:	Prof. Dr. med. Jun Oh
4. Gutachter:	Prof. Dr. med. Jochen Reiser
Tag der Promotion:	19.12.2022

Content

1 List of figures

2 Abbreviations

3D	Three-dimensional
ADR	Adriamycin
DMSO	Dimethylsulfoxide
dpf	Days post fertilization
ESKD	End stage kidney disease
fabp10a	Fatty acid-binding protein 10 a
FP	Foot processes
FSGS	Focal and segmental glomerulosclerosis
GBM	Glomerular basement membrane
GFB	Glomerular filtration barrier
eGFP	Enhanced Green fluorescent protein
HE	Hematoxilin and eosin
HDAC	Histone deacetylase
hpf	Hours post fertilization
IM	Imaging Machine
kDa	Kilodalton
MTZ	Metronidazole
NTR	Nitroreductase
PAN	Puromycin aminonucleoside
PEC	Parietal epithelial cell
PP	Primary process
RT-(q)PCR	Reverse transcriptase-(quantitative) polymerase chain reaction
VDP-eGFP	Vitamin D-binding, enhanced green fluorescent fusion protein
WT1	Wilms tumor protein 1

3 Summary

Podocytes are highly specialized kidney cells that are attached to the outer aspect of the glomerular capillaries and are damaged in more than 75% of patients with an impaired renal function. This specific cell type is characterized by a complex 3D morphology which is essential for proper filtration of the blood. Any changes of this unique morphology are directly associated with a deterioration of the size-selectivity of the filtration barrier. Since podocytes are postmitotic, there is no regenerative potential and the loss of these cells is permanent. Therefore, identification of small molecules that are able to protect podocytes is highly important. The aim of this work was to establish an *in vivo* high-content drug screening in zebrafish larvae. At first, we looked for a reliable podocyte injury model which is fast, reproducible and easy to induce. Since adriamycin is commonly used in rodents to damage podocytes, we administered it to the larvae and analyzed the phenotype by *in vivo* microscopy, (immuno-) histology and RT-(q)PCR. However, adriamycin did not result in a podocyte-specific injury in zebrafish larvae. Subsequently, we decided to use a genetic ablation model which specifically damages podocytes in zebrafish larvae. Treatment of transgenic zebrafish larvae with 80 µM metronidazole for 48 hours generated an injury resembling focal and segmental glomerulosclerosis which is characterized by podocyte foot process effacement, cell depletion and proteinuria. Following this, we established an *in vivo* high-content screening system by the use of a specific screening zebrafish strain. This screening strain expresses a circulating 78 kDa eGFP-labeled Vitamin D-binding fusion protein, which passes the filtration barrier only after glomerular injury. Therefore, we had an excellent readout to follow podocyte injury *in vivo*. We generated a custom image analysis software that

measures the fluorescence intensity of podocytes and the vasculature automatically on a large scale. Furthermore, we screened a specific drug library consisting of 138 compounds for protective effects on larval podocytes using this *in vivo* high-content system. The analysis identified several initial hits and the subsequent validation experiments identified belinostat as a reliable and significant protective agent for podocytes. These results led to a patent request and belinostat is a promising candidate for a clinical use and will be tested in mammalian podocyte injury models.

4 Introduction

Kidney function in mammals is critically dependent on an intact filtration barrier in the renal glomerulus. The filtration barrier consists of a fenestrated endothelium, a glomerular basement membrane (GBM) and podocytes covering the outer aspect of the glomerular tuft. Podocytes are highly specialized, postmitotic cells with a complex three-dimensional (3D) morphology including interdigitating foot processes attached to the GBM (Fig. 1). Between these exceptionally organized foot processes, a slit membrane is spanned with the transmembrane protein nephrin [1]. This zipper-like morphology represents an important part of the blood-urine barrier and is essential for the size-selectivity, which is limited to 70 kDa [2].

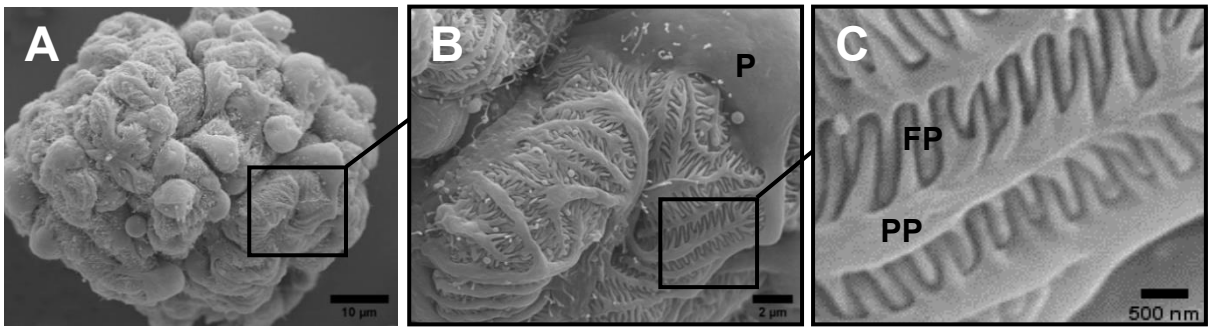

Figure 1: Scanning electron microscopy of the murine renal filtration barrier. A whole glomerulus is depicted in **A**. Podocytes (P) cover the glomerular capillaries with their 3D cytoarchitecture (**B**). Primary processes (PP) ramify into interdigitating foot processes (FP) with the actual filtration barrier in between foot processes (**C**). Photo: Dr. Nadine Artelt and Dr. Rabea Schlüter.

Any changes of this complex morphology like the loss of nephrin, impairment of other components of the slit membrane or a broadening of foot processes (effacement) lead to a loss of the size-selectivity of the filtration barrier [3, 4]. This allows the passage of high molecular weight proteins such as albumin, which is termed as proteinuria and is a clinical hallmark of kidney disease [5]. Moreover, not only effacement but also detachment of podocytes leads to a leaky filtration barrier. Since podocytes have no regenerative potential due to their postmitotic state, a loss of these cells is permanent. Therefore, knowledge about processes resulting in filtration barrier injury and substances that are able to ameliorate these changes is essential. In order to study this aim, our research group uses a well-accepted animal model, the zebrafish larva. This model allows manipulations and investigations of the filtration barrier directly *in vivo*. Larvae of the small teleost zebrafish, *Danio rerio,* have become a widely used vertebrate model in many research fields in the last decades [6–9]. A rapid *ex utero* development, optical transparency, a high fertility and comparably low maintenance costs grant critical advantages as *in vivo* model over mammalian organisms. Moreover, around 70% of all human genes have at least one orthologue in the zebrafish genome, which makes this model very attractive for life sciences [10]. Particularly in the field of kidney research, the zebrafish larva has been established as an important tool to study glomerular development, physiology and responses to injury [11–14]. The larval zebrafish pronephros develops one glomerulus which fuses from two migrating progenitor cell populations at the midline [11]. This glomerulus is composed of a fenestrated endothelium, a GBM and highly differentiated podocytes with interdigitating foot processes that are connected by a slit membrane, like in mammals (Fig. 2) [15–18]. Podocytes become terminally differentiated as soon as 4 days post fertilization (dpf)

and thus, the glomerular filtration barrier (GFB) reaches its restrictive properties for large molecular weight proteins [15].

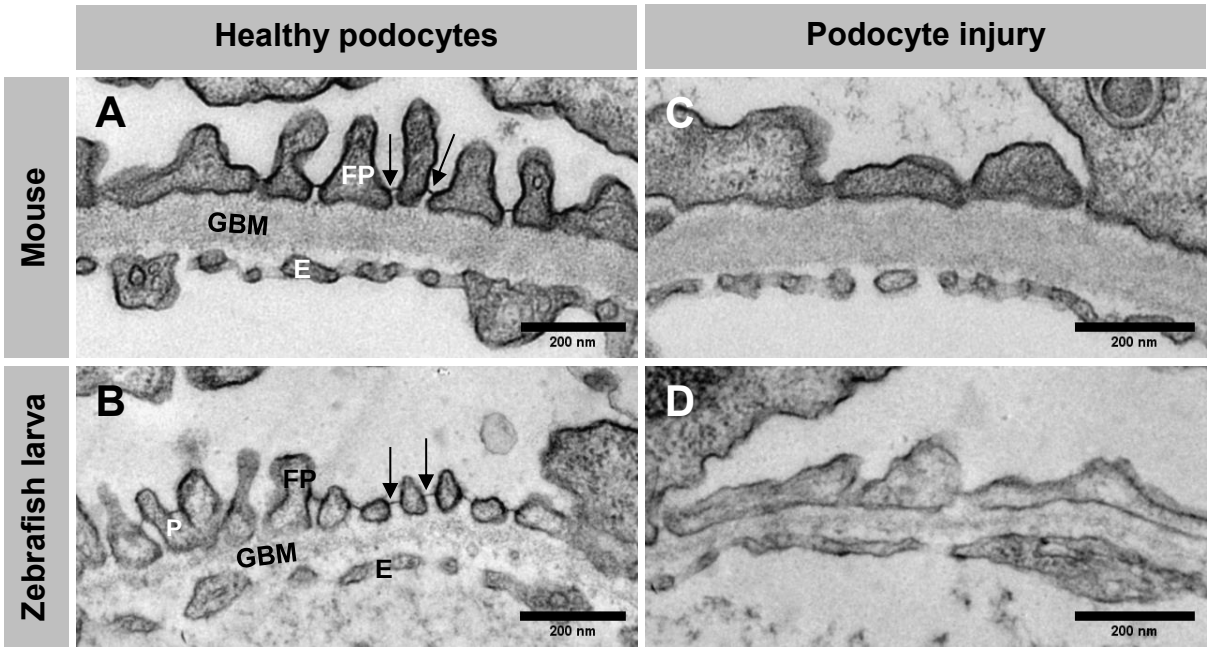

Figure 2: Transmission electron microscopy of the glomerular filtration barrier. The glomerular filtration barrier is a highly conserved structure between mammals and zebrafish (**A**, **B**). A fenestrated endothelium (E), a three-layered glomerular basement membrane (GBM) and interdigitating foot processes (FP) of podocytes which bridge the filtration slit with a slit membrane are central structures. Upon podocyte injury, foot processes flatten and merge, a phenotype called effacement (**C**, **D**). The size selectivity of the filtration barrier is impaired. Photos: Dr. Nadine Artelt, Dr. Antje Blumenthal, Maximilian Schindler.

Additionally, transgenic introduction of cell specific fluorescent reporters and/or enzyme expression via the Tol2 transposon or the CRISPR/Cas9 systems provides further advantages, especially for *in vivo* microscopy [19–21]. Podocyte-specific expression of the enhanced green fluorescent protein (eGFP) or mCherry allows direct assessment of the cell condition *in vivo* and on histologic sections (Fig. 3).

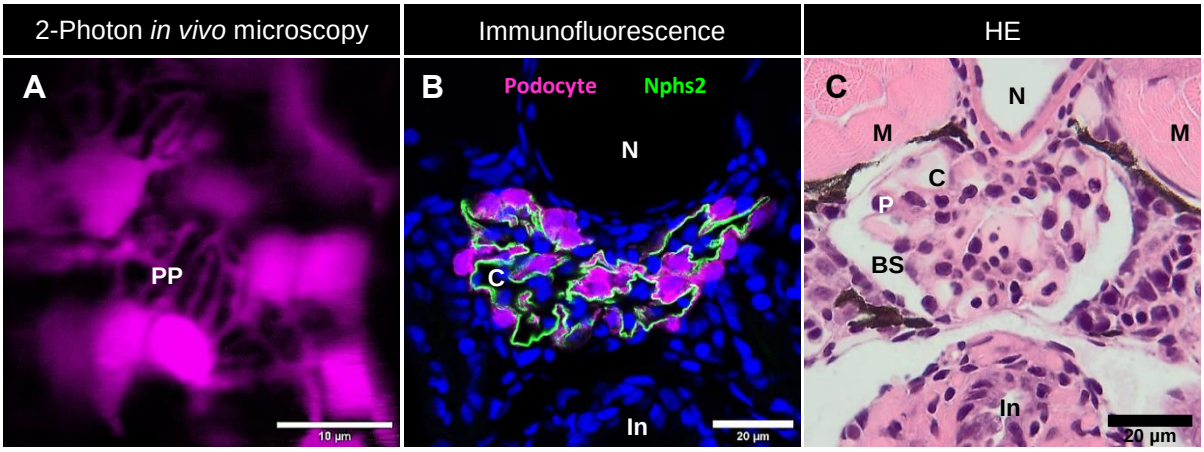

Figure 3: Zebrafish larvae offer outstanding possibilities for microscopy. Due to transparency, tissue accessibility and fluorescent reporters, podocytes (P) and primary processes (PP) can be resolved *in vivo* (**A**). Important slit membrane proteins such as podocin (Nphs2) can be visualized by confocal laser-scanning microscopy **(B**). Glomerular morphology presents itself best on plastic sections of zebrafish larvae (**C**). N = Notochord, In = Intestine, C = Capillary lumen, M = Myotomes, BS = Bowman´s space. Photos: Maximilian Schindler.

Furthermore, the group of Anand-Apte created a transgenic reporter line, that expresses a circulating fusion protein of the Vitamin D-binding protein and eGFP (VDP-eGFP) with a size of 78 kDa [22]. Although initially created to investigate the blood-brain-barrier, this fusion protein is unable to pass the glomerular filtration barrier in zebrafish larvae under healthy steady-state conditions. Upon podocyte injury, the VDP-eGFP cannot longer be retained in the blood and is cleared through the GFB. This results in a loss of eGFP fluorescence in the blood and can be utilized as surrogate parameter for proteinuria, a hallmark of podocytopathies (Fig. 4) [23].

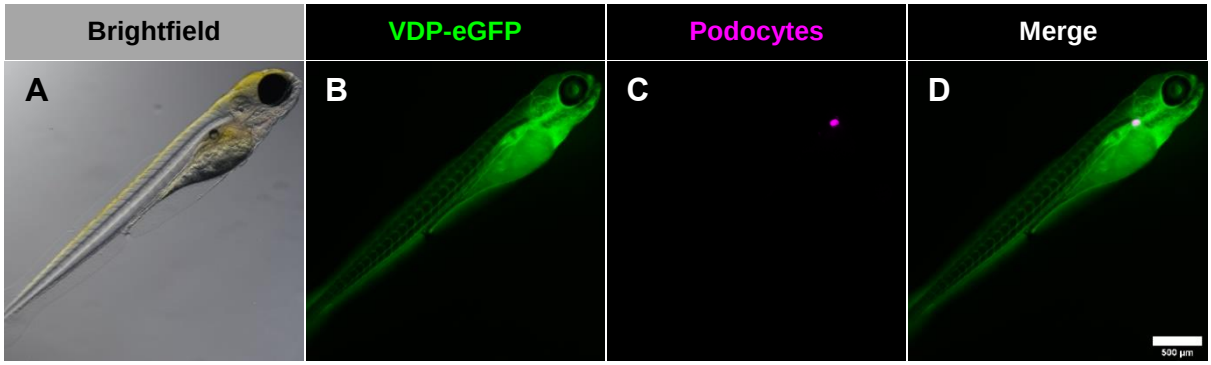

Figure 4: Transgenic zebrafish can be utilized to assess glomerular parameters *in vivo*. On the basis of brightfield images, the gross morphology can be evaluated (**A**). The 78-kDa, circulating VDP-eGFP is retained in the vasculature in healthy larvae and passes the glomerular filter after podocyte injury (**B**). Presence and fluorescence intensities of podocytes can be assessed in the living larva (**C**). Podocyte and vascular fluorescence can be combined as read-outs for glomerular integrity (**D**). Photos: Maximilian Schindler.

Unfortunately, kidney diseases are on an alarming rise worldwide and are a severe burden for patients as well as health care systems [24]. Disruptions of the glomerulus are responsible for 90% of end stage kidney disease (ESKD) cases [25]. Focal and segmental glomerulosclerosis (FSGS) is a histopathological pattern in the glomerulus that often results in ESKD [26]. Initial podocyte injury leads to foot process effacement, podocyte loss and glomerular matrix accumulation which clinically presents as nephrotic syndrome [27]. Unfortunately, the regenerative potential of podocytes is strongly limited due to their postmitotic state and the kidney function of patients progressively declines. Renal replacement therapies such as transplantation or hemodialysis are often the only option but implicate a severe deterioration in quality of life and a dramatic increase of mortality [28, 29]. However, no curative drugs that directly target podocytes are available until now and patients suffering from FSGS are treated non-specifically with immunosuppressants (e. g. Dexamethasone, Cyclosporin A) or drugs that reduce blood pressure (angiotensin-converting enzyme or renin-angiotensin-aldosterone system inhibitors) [30]. This lack of specific treatment creates a large demand for drugs that directly target podocytes

and potentially decelerate or even stop disease progression of podocytopathies. Large scale drug screens are a promising approach to find new drugs that might close this gap of podocyte protection. However, most models lack scalability which is a limiting factor for high-throughput screenings. Cell culture based systems can provide a high homogeneity in screening experiments and robust podocyte injury models are available [31, 32]. Nevertheless, podocytes as terminally differentiated cells tend to de-differentiate upon immortalization in cell culture and lose important podocyte markers such as Wilms tumor protein 1 (Wt1) and Podocalyxin [33]. The complex and necessary physiological environment of podocytes *in vivo* including glomerular blood pressure, blood composition and cellular crosstalk are barely possible to mimic *in vitro*. On the other hand, screening experiments in mammalian models such as mice and rats might bring results that have a short road to a clinical translation because of the high resemblances of the GFB. Podocyte injury in rodents requires injections of podocyte toxins, such as adriamycin (ADR) or puromycin aminonucleosides (PAN) [34, 35]. Despite the evident ethical concerns that come along with injury models in mammals via injections, these models can barely be combined with a high-throughput.

For these reasons, we used transgenic zebrafish larvae as an *in vivo* model for this work, since it combines a high-throughput with necessary properties such as blood pressure in the glomerulus. In order to establish a screening for beneficial effects on differentiated podocytes, a suitable podocyte injury model is a compelling first necessity. Podocyte-specific injury in zebrafish larvae is a difficult task but has been successfully achieved via injections of either ADR or PAN [36, 37]. However, injections in zebrafish larvae require plenty of time and experimental skill and can thus hardly be scaled to a high-throughput. Since zebrafish larvae are able to absorb

drugs directly from the water (transdermal, oral or by diffusion), induction of podocyte injury by treatment via the water is a possibility offered by this model.

Aim of this work

In order to study damage as well as loss of podocytes and substances that protect podocytes and the filtration barrier, we aimed to establish an *in vivo* high-content screening protocol based on transgenic zebrafish larvae. First, a reliable and scalable podocyte injury model had to be established. To this end, we first examined the effect of ADR on larval podocytes. Furthermore, we used the pharmacogenetic nitroreductase/metronidazole (NTR/MTZ) model to induce a podocyte specific injury in zebrafish larvae. Using a dedicated screening microscope, we further aimed to create an imaging-based, high-content readout system for the presence of podocytes and the constitution of the GFB. After calibration of the screening method, a library of small molecules was screened for their protective effects on larval podocytes.

5 Zebrafish strains

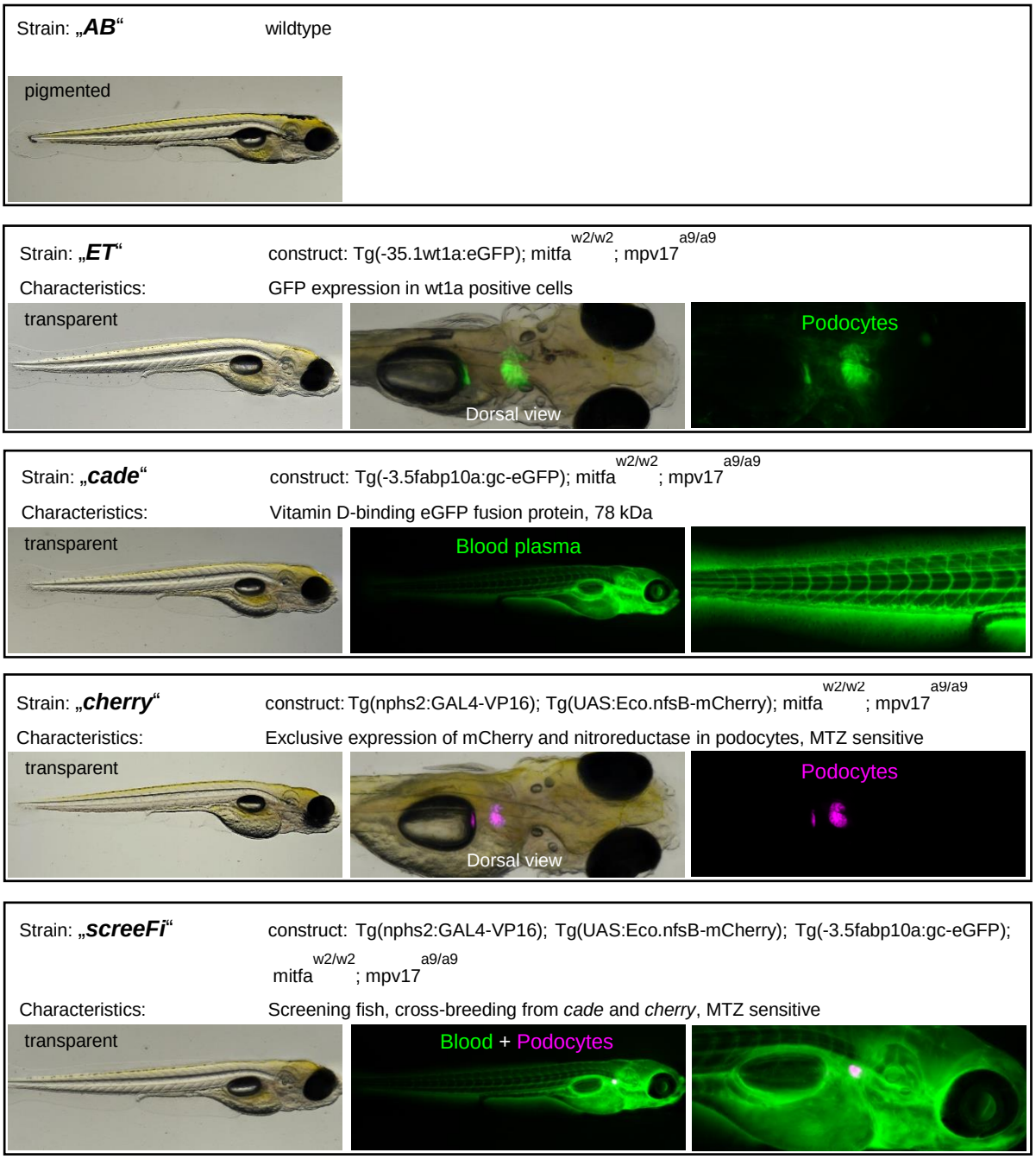

Figure 5: List of zebrafish strains used in this work. Photos: Maximilian Schindler

6 Publications

Publication I

Adriamycin does not damage podocytes of zebrafish larvae

Published in PLOS ONE, peer-reviewed, open access journal

Maximilian Schindler, Antje Blumenthal, Marcus Johannes Moeller, Karlhans Endlich, Nicole Endlich

DOI: 10.1371/journal.pone.0242436

PLOS ONE

RESEARCH ARTICLE

Adriamycin does not damage podocytes of zebrafish larvae

Maximilian Schindler[1], **Antje Blumenthal**[1], **Marcus Johannes Moeller**[2], **Karlhans Endlich**[1], **Nicole Endlich**[1]*

1 Department of Anatomy and Cell Biology, University Medicine Greifswald, Greifswald, Germany,
2 Department of Nephrology and Clinical Immunology, RWTH Aachen University Clinic, Aachen, Germany

* nicole.endlich@uni-greifswald.de

OPEN ACCESS

Citation: Schindler M, Blumenthal A, Moeller MJ, Endlich K, Endlich N (2020) Adriamycin does not damage podocytes of zebrafish larvae. PLoS ONE 15(11): e0242436. https://doi.org/10.1371/journal.pone.0242436

Editor: Sridhar Muthusami, Karpagam Academy of Higher Education, INDIA

Received: June 18, 2020

Accepted: November 3, 2020

Published: November 13, 2020

Data Availability Statement: All relevant data are within the paper and its Supporting Information files.

Funding: This work was supported by a grant of the Federal Ministry of Education and Research (BMBF, grant 01GM1518B, STOP-FSGS) to Nicole Endlich (NE) and (BMBF, grant 01GM1901A, STOP-FSGS) to Marcus Johannes Moeller (MJM). URL: https://www.gesundheitsforschung-bmbf.de/de/stop-fsgs-translationaler-forschungsverbund-zur-verbesserung-der-diagnostik-und-therapie-9349.php The funders had no role in study design,

Abstract

Podocytes are highly specialized epithelial cells that are essential for an intact glomerular filtration barrier in the kidney. Several glomerular diseases like focal segmental glomerulosclerosis (FSGS) are initially due to podocyte injury and loss. Since causative treatments for FSGS are not available until today, drug screening is of great relevance. In order to test a high number of drugs, FSGS needs to be reliably induced in a suitable animal model. The zebrafish larva is an ideal model for kidney research due to the vast amount of offsprings, the rapid development of a simple kidney and a remarkable homology to the mammalian glomerulus. Zebrafish larvae possess a size-selective glomerular filtration barrier at 4 days post fertilization including podocytes with interdigitating foot processes that are connected by a slit membrane. Adriamycin is an anthracycline which is often used in mice and rats to induce a FSGS-like phenotype. In this study, we aimed to induce a similar phenotype to zebrafish larvae by adding adriamycin to the tank water in different concentrations. Surprisingly, zebrafish larvae did not develop glomerular injury and displayed an intact filtration barrier after treatment with adriamycin. This was shown by (immuno-) histology, our filtration assay, *in vivo* imaging by 2-photon microcopy, RT-(q)PCR as well as transmission electron microscopy. To summarize, adriamycin is unable to induce a podocyte-related damage in zebrafish larvae and therefore major effort must be made to establish FSGS in zebrafish larvae to identify effective drugs by screenings.

Introduction

Chronic kidney disease (CDK) with a global prevalence of 9.1% and an increase by 29.3% since 1990 is a major burden for both patients and public healthcare [1]. Within CKD, Glomerulopathies are the main causes for the development of nephrotic syndromes worldwide [2]. Especially, focal segmental glomerulosclerosis (FSGS) is a severe glomerular pathohistological condition which often results in end stage renal disease [3]. FSGS is strongly associated with podocyte damage, hypertrophy and a loss of these post-mitotic cells [4]. Activated parietal epithelial cells, accumulation of extracellular matrix and finally glomerular scarring follow podocyte injury [5]. Since regenerative mechanisms of podocytes are poorly understood, the renal filtration barrier is permanently affected. Until now, no causative drugs or therapies are

data collection and analysis, decision to publish, or preparation of the manuscript.

Competing interests: The authors have declared that no competing interests exist.

available underlining the urgent need of screening methods that identify drugs for glomerulopathies.

In the past, it became clear that the zebrafish larva is an excellent model to study kidney development, function and morphology [6, 7]. Today, it is apparent that the zebrafish could be an ideal model for drug screening due to a large number of advantages compared to mice and rats. The quick development of hundreds of *ex utero* fertilized eggs per week, a simple kidney (pronephros) as well as transparency open many possibilities in that field. The zebrafish larva develops a filtrating pronephros approximately 40 hours post fertilization (hpf) which is composed of only one single glomerulus connected to two tubules [8]. Moreover, the morphology of the zebrafish glomerulus shows high similarities to that of mammals. Additionally, the interdigitating podocytes of the zebrafish larvae express slit membrane specific proteins like nephrin and podocin that are the prerequisite for a size selectivity of the filtration barrier. Thus, the knockdown of nephrin or podocin by specific Morpholinos resulted in a disrupted filtration barrier and a proteinuric phenotype in zebrafish larvae [9]. The renal filtration of zebrafish larvae can even be observed *in vivo* by utilizing a strain that expresses eGFP fused to the vitamin-D binding protein as an indicator for a proper filtration barrier [10].

In order to induce glomerular injury in animal models, adriamycin (ADR or Doxorubicin) is widely used. ADR is an anthracycline that is commonly utilized to induce FSGS in rodents [11–13]. The efficacy of ADR is strongly dependent on the rodent strain it is used on. While being effective on most rat strains, only a few mouse strains are susceptible to ADR nephropathy [14]. Beside this, side effects like cardiomyopathy, a small range for the dose and a high degree of technical administration expertise are disadvantages of this model [15]. Regarding zebrafish, administration of ADR at an early stage to the tank water induced developmental defects of the pronephros [16]. Injection of ADR in 3 dpf old larvae resulted in severe cardiovascular off target effects and was deemed unsuitable as an injury model [17].

The aim of this study was to induce injury to the pronephric glomerulus of zebrafish larvae in order to mimic FSGS and therefore to create a drug screening model. To this end, ADR was administered into the tank water of 7 dpf old larvae. Subsequently, zebrafish larvae were analyzed by RT-(q)PCR, a filtration assay, in histological sections and *in vivo* 2-photon microscopy. In contrast to rodent models, zebrafish larvae did not respond to ADR treatment with a FSGS-like phenotype.

Materials and methods

Zebrafish husbandry

Zebrafish were held at standard conditions in tanks with circulating water at 27˚C and and a light cycle of 14:10 h (14 light: 10 dark). Mating was induced in small groups in mating tanks overnight and eggs were collected in the morning. Larvae were raised in E3 medium at 28.5˚C, as previously described [18]. In order to track podocytes, the ET strain (Tg(-35.1wt1a:eGFP); mitfa$^{w2/w2}$; mpv17$^{a9/a9}$, kindly provided by Dr. C. Englert, Jena, Germany) was used for all experiments except for the filtration assay [18, 19]. This was conducted with DBP larvae (Tg (-3.5fabp10a:gc-eGFP), which was kindly provided by Dr. B. Anand-Apte, Cleveland, USA [20]. Larvae were fed twice a day from 6 to 9 dpf with GEMMA Micro 75 (Zebcare, Neederwert, Netherlands). Anesthesia for *in vivo* imaging and euthanasia was conducted with tricaine (Sigma-Aldrich, St. Louis, Missouri, USA).

All prerequisites of the German animal protection law were met and experiments were performed in accordance with the guidelines of the federal agencies in Mecklenburg-Western Pomerania (LALLF M-V). The responsible ethics committee within the LALLF M-V approved the experiments with zebrafish larvae older than 6 dpf.

Adriamycin treatment

At 7 dpf the E3 medium was changed to E3 containing 0 (Ctrl), 20, 40, or 60 μM adriamycin (Doxorubicin-HCL, Selleckchem, Houston, Texas, USA). The medium was refreshed at 8 dpf to remove feeding debris. After 48 h adriamycin was washed out three times and larvae were either fixed for histological studies or homogenized in TRI-Reagent (Sigma-Aldrich) for mRNA analysis.

Filtration assay

DBP larvae expressing eGFP as a fusion protein with the vitamin D-binding protein (~68kDa) were anesthetized with tricaine (0.1–0.5%) at 7 dpf before treatment and the caudal artery was focused with a Leica TCS SP5 10x air objective (Wetzlar, Germany). After treatment with ADR, larvae were again anesthetized and imaged. For each concentration and each round of treatment (4) 10 corresponding larvae were imaged before and after treatment, resulting in 40 larvae per concentration. The vascular eGFP intensity was measured with ImageJ (National Institutes of Health, Bethesda, MD, USA) and the intensity after treatment was normalized to the fluorescence intensity before treatment.

Histology

Hematoxylin and eosin (HE) staining was performed on plastic sections. Larvae were fixed overnight in 2% PFA at 4˚C and dehydrated in an ascending series of ethanol on the next day. Following dehydration, larvae were treated with infiltration medium, embedded in Technovit® 7100 (Kulzer, Hanau, Germany) and hardened overnight. Plastic sections (4 μm) were cut with a rotational microtome (Jung RM2055, Leica Biosystems, Wetzlar, Germany). Sections were stained with Gill´s hematoxylin, alcoholic eosin and mounted with Eukitt® (Sigma-Aldrich). Images were taken with an Olympus BX50 microscope (Tokio, Japan).

Immunofluorescence

Cryosections (6 μm) were cut on a Microm HM 560 microtome (Thermo Fisher Scientific, Waltham, Massachusetts, USA) and immunofluorescence staining was performed as previously described [21]. Nephrin staining was carried out overnight at 4˚C with 1:2000 rabbit anti-zebrafish nephrin (gift of Dr. A. Majumdar, Uppsala, Sweden) and Alexa-Fluor-647 anti-rabbit antibody (Invitrogen, Carlsbad, California, USA). An antigen retrieval step was necessary for podocin staining. Briefly, cryosections were boiled in Tris-HCL pH 9.0 for 10 min. After antigen retrieval and blocking, cryosections were incubated with a rabbit anti-podocin antibody (Proteintech, Rosemont, Illinois, USA; 1:200) o.n. at 4˚C followed by an incubation with Alexa-Fluor-647-labeled anti-rabbit antibody (Invitrogen). Nuclei were stained with Hoechst 33342 (Sigma-Aldrich) and sections were finally mounted with Mowiol (Carl Roth, Karlsruhe, Germany). Confocal microscopy of cryosections was carried out on a Leica TCS SP5 with a 40x and a 63x oil immersion objective.

RNA isolation and cDNA synthesis

RNA of 8–12 larvae was isolated with TRI-Reagent according to manufacturer´s protocol. The QuantiTect reverse transcription kit (Qiagen, Hilden, Germany) was used for cDNA synthesis out of 1 μg RNA.

RT-PCR and RT-qPCR

PCRs were performed as previously described [21]. In brief, DreamTaq DNA Polymerase (Thermo Fisher Scientific) was used for RT-PCR and RT-qPCR was carried out with iQ SYBR green Supermix (BioRad, Hercules, California, USA) on an iCycler Thermal Cycler (BioRad). Primer sequences were the following: *nphs1*-FOR: CAATGTCCCTAACCCGCACT, *nphs1*-REV: ACGCCTCACATTGCAGAGAA, *nphs2*-FOR: GAAGCAAGACGTCAGGCACA, *nphs2*-REV: GGTATGTTGAGGACCACGGC, *eef1a1l1*-FOR: AAGGAGGGTAATGCTAGCGG, *eef1a1l1*-REV: GGGCGAAGGTCACAACCATA. Controls without cDNA template, without RNA and samples without reverse transcriptase (RT) in the RT reaction were included in every run. Melting curves for each primer were also checked.

Ultrastructural analysis

Larvae were fixed with 4% glutaraldehyde, 1% PFA and 1% sucrose in 0.1 M HEPES at 4˚C overnight. Dehydration in an ascending ethanol series was performed after post-fixation in 2% osmium tetroxide. The larvae were embedded in EPON 812 (Serva, Heidelberg, Germany) and cut with an Ultracut UCT ultramicrotome (Leica, Wetzlar, Germany). Ultrathin sections (70 μm) were drawn on a copper grip and contrasted with Sato´s lead stain and 5% uranyl acetate for 5 min. Images were acquired with a LIBRA 120 transmission electron microscope (Zeiss, Oberkochen, Germany).

In vivo imaging by 2-photon microscopy

ET larvae were embedded, positioned in 0.6% low melting agarose and anesthetized as described earlier [22]. Before treatment and 48 h post treatment with 0, 20, 40 and 60 μM ADR automated z-stacks over a distance of up to 90 μm with 1 μm distance between frames were acquired with a LSM710MP (Carl Zeiss Microimaging, Jena, Germany) and a Chameleon Ti-Sapphire Laser (Chameleon, Coherent, Santa Clara, CA, USA). A 20x (1.0 NA) water immersion objective was used with an excitation wavelength of 890 nm for eGFP. Movies were generated with ImageJ.

Statistics

Mann-Whitney *U* test was used for analysis in which p values <0.05 were considered statistically significant. Error bars represent ±SD. All experiments were repeated four times with 18 to 58 larvae per treatment group in each round. A total of 784 larvae were used for this study.

Results

ADR treatment did not induce edema formation

Zebrafish larvae were treated with three different concentrations of ADR (20, 40 and 60 μM) in tank water for 48 h. Theses doses were chosen on the basis of Zennaro at al. [16] and preliminary experiments. The mortality of zebrafish larvae increased after the treatment with 60 μM ADR but no evident edema formation was observed. However, ADR in lower concentrations did not lead to any edema formation (periocular, pericardial or yolk sac). In contrast to the zebrafish larvae treated with 60 μM ADR, low dose treated larvae survived similar to the larvae of the control group (Fig 1).

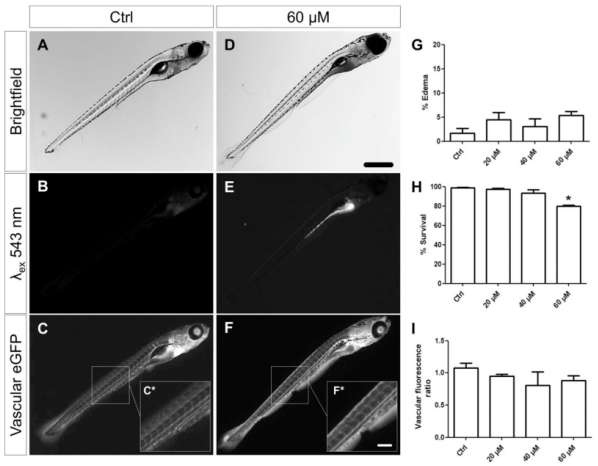

Fig 1. Evaluation of phenotype, autofluorescence, vascular eGFP fluorescence, survival and edema rate of larvae after treatment. Treated larvae did not develop periocular or pericardial edemas at a significant rate (**A, D, G**). However, high concentrations of ADR caused an increase in mortality of the larvae (**H**). All doses of ADR led to a strong accumulation of ADR in the intestinal tract which caused a remarkable autofluorescence over a wide spectrum (**B, E**). Quantification of the vascular eGFP fluorescence of DBP larvae (Tg(-3.5fabp10a:gc-eGFP) after ADR treatment did not reveal a significant vascular reduction of the eGFP-DBP fusion protein (~68 kDa) **(C, F, I)**. Scale bar in **D** represents to 200 µm, in **F*** to 50 µm. $^{*}P = 0{,}03$.

https://doi.org/10.1371/journal.pone.0242436.g001

The filtration barrier remains intact during ADR treatment

To study the function of the filtration barrier, a screening zebrafish strain expressing the 68 kDa eGFP-vitamin D-binding protein (Tg(-3.5fabp10a:gc-eGFP)) in the blood was used [20]. Under healthy conditions, all vessels of the larvae show a strong fluorescence of eGFP in contrast to a loss of the fluorescence if the filtration barrier becomes leaky which results in the excretion of the eGFP-vitamin D-binding protein [10].

After the treatment of the zebrafish larvae (7 dpf) with different concentrations of ADR, the fluorescence of the vasculature remained unchanged (Fig 1), indicating an intact filtration barrier. Beside the eGFP fluorescence, a strong red fluorescence in the intestine was observed when exposed to an excitation wavelength of 543 nm which was caused by the uptake of ADR by the larvae (Fig 1).

ADR did not affect the morphology of the glomeruli

In order to examine the glomerular morphology in ADR-treated zebrafish larvae at 9 dpf, histological sections were cut and were stained with hematoxylin and eosin (HE). We have found that ADR treatment at different concentrations did not change the morphology and the size of the glomerulus, respectively. Furthermore, neither a loss of podocytes nor areas of naked glomerular basement membrane (GBM) were observed suggesting that ADR has no effect on the glomerular structure (Fig 2).

ADR did not influence the expression of slit membrane proteins

In order to assess the integrity of the pronephric filtration barrier of zebrafish larvae, the *ET* strain was used which expresses eGFP in podocytes under the control of the wt1a promotor.

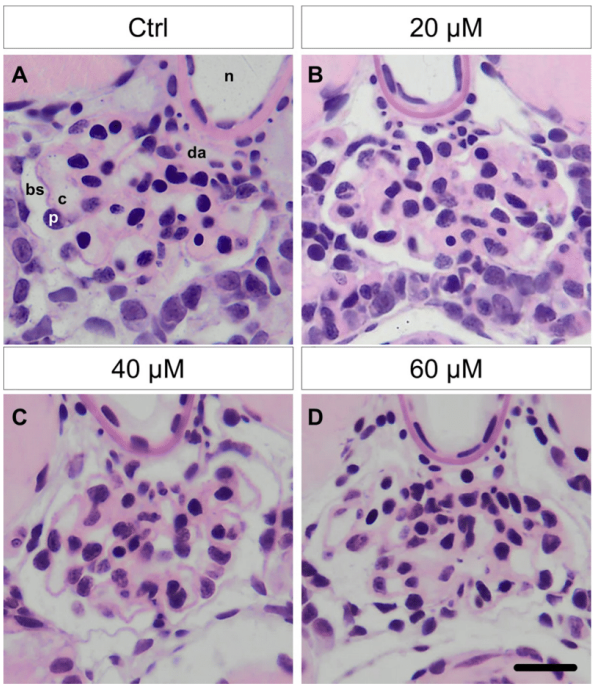

Fig 2. Glomeruli of ADR-treated larvae did not show morphological alterations demonstrated by HE staining on histological sections. A loss of podocytes or a Bowman's space edema could not be observed (**A-D**). **n**: notochord, **da**: dorsal aorta, **c**: capillary, **p**:podocyte, **bs**: Bowman's space. Scale bar represents 10 µm.

https://doi.org/10.1371/journal.pone.0242436.g002

Cryosections of ADR-treated larvae revealed that endogenous eGFP fluorescence was not diminished in the presence of ADR (Fig 3). In accordance with this, immunostainings of the slit membrane proteins nephrin and podocin showed a well-organized, meandering pattern in the pronephric glomerulus in each group. Furthermore, we have not found a significant regulation of podocin and nephrin mRNA due to ADR treatment quantified by RT-(q)PCR (Fig 3 and S1 Fig). These results hint towards an insusceptibility of larval zebrafish podocytes to ADR.

ADR had no impact on glomeruli *in vivo*

Living larvae (9 dpf) were imaged and the glomerular integrity was assessed before and after ADR treatment by 2-PM. *In vivo* z-stacks of treated larvae did not show impaired glomeruli and were indistinguishable from controls (Fig 3A and S2-S6 Movies in S1 File).

ADR has no impact on the ultrastructure of the glomerular filtration barrier

The filtration barrier of larval zebrafish is remarkably similar to the mammalian counterpart, especially in terms of morphology. Podocyte foot processes (FP) are basolaterally connected by

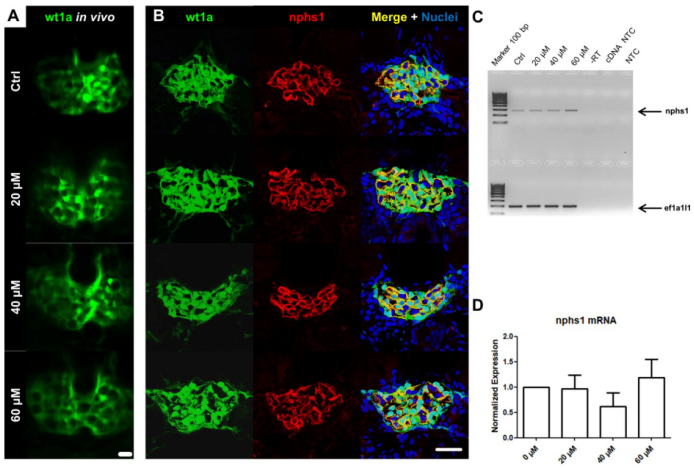

Fig 3. Evaluation of wt1a expression *in vivo* and immunostaining of cryosections for the slit membrane protein nephrin in ADR-treated larvae. 2-PM *in vivo* imaging revealed no morphological changes or glomerular abnormalities in treated larvae **(A)**. Immunostainings showed that ADR treatment neither reduces the expression of the pronephric transcription factor wt1a nor changes the expression pattern of nephrin **(B)**. RT-PCR **(C)** and RT-qPCR **(D)** confirmed that nephrin mRNA expression was not altered in ADR-treated larvae at 9 dpf. Scale bars represent 10 µm.

https://doi.org/10.1371/journal.pone.0242436.g003

slit-membrane and adhere to the three-layered GBM on top of a fenestrated endothelium. In many pathologic conditions, the slit-membrane perishes and foot processes flatten and merge. This condition is called effacement. To find out whether FP morphology is affected by ADR administration, ultrathin sections were examined with a transmission electron microscope (TEM). Ctrl- and ADR-treated (60 µM) larvae both showed highly organized and interdigitating foot processes which are connected by the slit membrane. Podocyte foot process effacement was not observed in ADR-treated larvae. Furthermore, the morphology of the glomerular endothelium was unchanged as well as the thickness of the GBM was similar to the Ctrl larvae (Fig 4).

Discussion

The zebrafish larva is a well-established model organism to investigate pronephric development, morphology and function. Due to the low maintenance costs and rapid maturation of even highly specialized cells like functional podocytes within 3.5 dpf [6], it offers considerable advantages over mammalian organisms. The enormous reproduction rate of several hundred eggs per week makes it an ideal model for high throughput screening of drugs. Since kidney diseases and especially the ones affecting the glomerulus are on an alarming rise, it is of crucial importance to find causative medical treatments. The first step to establish a drug screening assay in zebrafish larvae is induction of a reliable and reproducible glomerular injury that mimics diseases like FSGS.

An induction of glomerular injury in zebrafish larvae has been achieved successfully by several approaches in the past. The injection of morpholinos at early developmental stages which repress mRNA translation of essential proteins for the pronephric development or ones that target podocyte specific mRNAs directly have shown convincing results [18, 23, 24]. Although

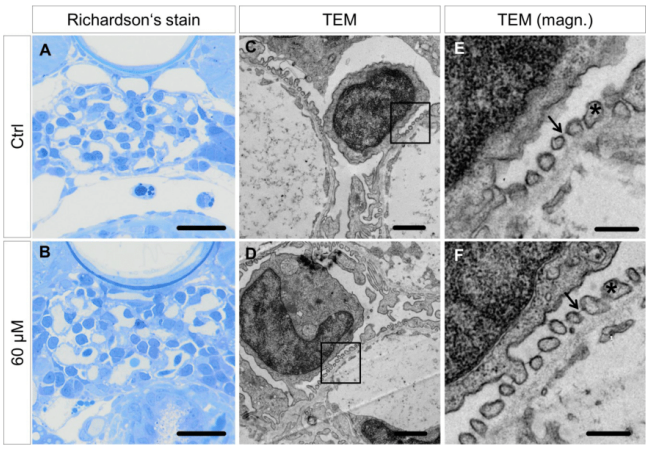

Fig 4. Morphology and ultrastructure of larval glomeruli. Morphological investigations by Richardson's staining of semithin sections (500 nm) did not show abnormalities of the glomerular morphology due to ADR treatment (**A, B**). Ultrastructural analysis of the pronephric filtration barrier confirmed the abscence of a glomerular phenotype (**C**-**F**). The interdigitating pattern of podocyte foot processes (asterisk in **E** and **F**) is present in both control was well as 60 μM ADR-treated larvae. The slit membrane as a highly organized structure connecting foot processes was not affected by ADR (arrows in **E** and **F**). Scale bars in **A** and **B** represent 10 μm, in **C** and **D** 1 μm, in **E** and **F** 200 nm.

https://doi.org/10.1371/journal.pone.0242436.g004

this technique provides robust results, it is limited to represent developmental defects of the pronephros and no direct damage to fully functional podocytes.

In order to target mRNA translation in the pronephric glomerulus in later developmental stages, Vivo-morpholinos have successfully been used by our group [25]. This technique offers induction of injury at stages in which podocytes are fully functional but is not suitable for high-throughput experiments because of the time-consuming manner in which intravenous injections in zebrafish larvae have to be performed. An excellent method to specifically induce damage to podocytes in zebrafish larvae has been carried out with the nitroreductase-metronidazole system [10, 26]. Podocyte apoptosis, formation of pseudocysts, podocyte detachment and proteinuria can be induced by adding metronidazole to the medium without injection [21, 27]. Although this model is very robust and provides easily reproducible results, it is limited to one zebrafish strain.

Since ADR is commonly used in rodent models to induce glomerular injury, we tested the effect of this compound on glomeruli of zebrafish larvae. It was reported that the application of ADR at early larval stages affects their proper development and the formation of the filtration barrier [16, 28]. Since injections of ADR into the cardiac sinus venosus in zebrafish larvae at 3 dpf causes off-target cardiovascular effects, ADR was being considered unsuitable for induction of an pronephric injury via injection [17].

In the present study, we found that application of ADR to the tank water of zebrafish larvae with a fully functional pronephric filtration barrier caused a significant increase in mortality at 60 μM but did not cause an occurrence of hallmarks for nephrotic syndromes such as pericardial or periorbital edema. In accordance with this, a renal loss of eGFP of DBP larvae could not be observed in treated larvae indicating an intact and size-selective filtration barrier. Interestingly, ADR accumulated in the intestinal tract of treated larvae which led to a strong fluorescence when excited with a wavelength of 543 nm. According to Motlagh and colleagues, ADR

has its peak of fluorescence at ~591 nm with an emissive bandwidth of 150 nm [29]. Therefore, zebrafish strains that express endogenous fluorophores in this bandwidth (e.g. mCherry with λ_{Em} ~ 610 nm, RFP with λ_{Em} ~ 588 nm) as well as conjugated antibodies that emit in this bandwidth (e.g. Cy3 with λ_{Em} ~ 570 nm) cannot be used in ADR treatments.

In order to identify possible pre-nephrotic pathohistological alterations of the glomerular filtration barrier, HE staining and immunofluorescence staining for nephrin and podocin of *ET* larval glomeruli were performed. Treated larvae did not show histologic hallmarks of glomerular injury such as podocyte loss, dilated capillaries or Bowman´s space edema. Immunofluorescence staining did not reveal a changed protein expression of nephrin or podocin. RT-(q)PCR results undermined the unaltered expression of these two important podocyte proteins upon ADR treatment.

Since transparent zebrafish larvae are ideal for *in vivo* observations, imaging of living ADR-treated larvae was performed by 2-PM. Z-stacks of glomeruli displayed no injury in living larvae after treatment which strongly corroborates the results of a missing nephrotic phenotype.

Ultrastructural analysis of treated larvae further revealed that ADR did not have any impact on the glomerular filtration barrier. Even larvae that were treated with 60 μM still showed a fenestrated endothelium, a normal GBM and interdigitating foot processed connected by a slit membrane. Foot process effacement or a thickening of the GBM was not induced, which are further hallmarks of glomerular injury.

Most rat strains but only a few mouse strains are susceptible to ADR nephropathy [14]. Zheng and colleagues found that ADR susceptibility in mice is a Mendelian trait. A decreased expression of the Prmt7 protein of the *DOXNPH* locus is responsible for susceptibility to ADR nephropathy in mice [30]. It was shown that zebrafish larvae express prmt7 at early developmental stages [31, 32] but little is known about the expression of prmt7 at later stages.

In conclusion, zebrafish larvae are an excellent animal model to study kidney function *in vivo*. However, ADR is not a suitable drug to induce acute podocyte or glomerular injury in zebrafish larvae. Further substances have to be tested in order to find a drug that induces glomerular injury and mimics FSGS in zebrafish larvae.

Supporting information

S1 Fig. Effects of ADR treatment on the expression of podocin. Similar to nephrin, podocin showed a meandering expression along the slit membrane in glomeruli throughout all ADR concentrations (A). These results were corroborated by podocin mRNA analysis of treated larvae via RT-PCR and RT-qPCR (B, C). Scale bar represents 10 μm.
(TIF)

S1 File. S2-S6 Movies. Representative 2-photon microscopy *in vivo* z-stacks of ET larvae before treatment at 7 dpf and after treatment at 9 dpf. No signs of glomerular injury such as podocyte loss or bowman's space edema were seen after ADR treatment. Treated larvae displayed an intact glomerular cytoarchitecture, primary processes of podocytes could be resolved in all groups.
(ZIP)

S1 Raw images.
(PDF)

Acknowledgments

The authors thank Mandy Weise and Oliver Zabel for their excellent technical assistance.

Author Contributions

Conceptualization: Maximilian Schindler, Karlhans Endlich, Nicole Endlich.

Formal analysis: Maximilian Schindler.

Funding acquisition: Nicole Endlich.

Investigation: Maximilian Schindler.

Methodology: Maximilian Schindler, Antje Blumenthal.

Project administration: Nicole Endlich.

Resources: Marcus Johannes Moeller, Karlhans Endlich, Nicole Endlich.

Software: Maximilian Schindler.

Supervision: Karlhans Endlich, Nicole Endlich.

Visualization: Maximilian Schindler.

Writing – original draft: Maximilian Schindler.

Writing – review & editing: Antje Blumenthal, Marcus Johannes Moeller, Nicole Endlich.

References

1. Cockwell P, Fisher L-A. The global burden of chronic kidney disease. The Lancet. 2020; 395: 662–664. https://doi.org/10.1016/S0140-6736(19)32977-0
2. Ponticelli C, Glassock RJ, editors. Treatment of Primary Glomerulonephritis: Oxford University Press; 2019.
3. Bose B, Cattran D. Glomerular diseases. FSGS. Clin J Am Soc Nephrol. 2014; 9: 626–632. https://doi.org/10.2215/CJN.05810513 PMID: 23990165
4. Floege J, Amann K. Primary glomerulonephritides. The Lancet. 2016; 387: 2036–2048. https://doi.org/10.1016/S0140-6736(16)00272-5 PMID: 26921911
5. Lazareth H, Lenoir O, Tharaux P-L. Parietal epithelial cells role in repair versus scarring after glomerular injury. Current opinion in nephrology and hypertension. 2020; 29: 293–301. https://doi.org/10.1097/MNH.0000000000000600 PMID: 32235272
6. Drummond IA, Davidson AJ. Zebrafish kidney development. Methods Cell Biol. 2010; 100: 233–260. https://doi.org/10.1016/B978-0-12-384892-5.00009-8 PMID: 21111220
7. Poureetezadi SJ, Wingert RA. Little fish, big catch. Zebrafish as a model for kidney disease. Kidney Int. 2016; 89: 1204–1210. https://doi.org/10.1016/j.kint.2016.01.031 PMID: 27165832
8. Drummond IA, Majumdar A, Hentschel H, Elger M, Solnica-Krezel L, Schier AF, et al. Early development of the zebrafish pronephros and analysis of mutations affecting pronephric function. Development. 1998; 125: 4655–4667. PMID: 9806915
9. Kramer-Zucker AG, Wiessner S, Jensen AM, Drummond IA. Organization of the pronephric filtration apparatus in zebrafish requires Nephrin, Podocin and the FERM domain protein Mosaic eyes. Dev Biol. 2005; 285: 316–329. https://doi.org/10.1016/j.ydbio.2005.06.038 PMID: 16102746
10. Zhou W, Hildebrandt F. Inducible podocyte injury and proteinuria in transgenic zebrafish. J Am Soc Nephrol. 2012; 23: 1039–1047. https://doi.org/10.1681/ASN.2011080776 PMID: 22440901
11. Fogo AB. Animal models of FSGS. Lessons for pathogenesis and treatment. Semin Nephrol. 2003; 23: 161–171. https://doi.org/10.1053/snep.2003.50015 PMID: 12704576
12. Yang JW, Dettmar AK, Kronbichler A, Gee HY, Saleem M, Kim SH, et al. Recent advances of animal model of focal segmental glomerulosclerosis. Clin Exp Nephrol. 2018; 22: 752–763. https://doi.org/10.1007/s10157-018-1552-8 PMID: 29556761
13. Wang Y, Wang YP, Tay YC, Harris DC. Progressive adriamycin nephropathy in mice. Sequence of histologic and immunohistochemical events. Kidney Int. 2000; 58: 1797–1804. https://doi.org/10.1046/j.1523-1755.2000.00342.x PMID: 11012915
14. Lee VWS, Harris DCH. Adriamycin nephropathy. A model of focal segmental glomerulosclerosis. Nephrology (Carlton). 2011; 16: 30–38. https://doi.org/10.1111/j.1440-1797.2010.01383.x PMID: 21175974

15. Pereira WdF Brito-Melo GEA, Almeida CAS de Moreira LL, Cordeiro CW Carvalho TGR, et al. The experimental model of nephrotic syndrome induced by Doxorubicin in rodents. An update. Inflamm Res. 2015; 64: 287–301. https://doi.org/10.1007/s00011-015-0813-1 PMID: 25788426

16. Zennaro C, Mariotti M, Carraro M, Pasqualetti S, Corbelli A, Armelloni S, et al. Podocyte developmental defects caused by adriamycin in zebrafish embryos and larvae. A novel model of glomerular damage. PLoS ONE. 2014; 9: e98131. https://doi.org/10.1371/journal.pone.0098131 PMID: 24845233

17. Rider SA, Bruton FA, Collins RG, Conway BR, Mullins JJ. The Efficacy of Puromycin and Adriamycin for Induction of Glomerular Failure in Larval Zebrafish Validated by an Assay of Glomerular Permeability Dynamics. Zebrafish. 2018; 15: 234–242. https://doi.org/10.1089/zeb.2017.1527 PMID: 29480793

18. Müller T, Rumpel E, Hradetzky S, Bollig F, Wegner H, Blumenthal A, et al. Non-muscle myosin IIA is required for the development of the zebrafish glomerulus. Kidney Int. 2011; 80: 1055–1063. https://doi.org/10.1038/ki.2011.256 PMID: 21849970

19. Bollig F, Perner B, Besenbeck B, Köthe S, Ebert C, Taudien S, et al. A highly conserved retinoic acid responsive element controls wt1a expression in the zebrafish pronephros. Development. 2009; 136: 2883–2892. https://doi.org/10.1242/dev.031773 PMID: 19666820

20. Xie J, Farage E, Sugimoto M, Anand-Apte B. A novel transgenic zebrafish model for blood-brain and blood-retinal barrier development. BMC Dev Biol. 2010; 10: 76. https://doi.org/10.1186/1471-213X-10-76 PMID: 20653957

21. Siegerist F, Blumenthal A, Zhou W, Endlich K, Endlich N. Acute podocyte injury is not a stimulus for podocytes to migrate along the glomerular basement membrane in zebrafish larvae. Sci Rep. 2017; 7: 43655. https://doi.org/10.1038/srep43655 PMID: 28252672

22. Endlich N, Simon O, Göpferich A, Wegner H, Moeller MJ, Rumpel E, et al. Two-Photon Microscopy Reveals Stationary Podocytes in Living Zebrafish Larvae. J Am Soc Nephrol. 2014; 25: 681–686. https://doi.org/10.1681/ASN.2013020178 PMID: 24309184

23. Perner B, Englert C, Bollig F. The Wilms tumor genes wt1a and wt1b control different steps during formation of the zebrafish pronephros. Dev Biol. 2007; 309: 87–96. https://doi.org/10.1016/j.ydbio.2007.06.022 PMID: 17651719

24. Kroeger PT, Drummond BE, Miceli R, McKernan M, Gerlach GF, Marra AN, et al. The zebrafish kidney mutant zeppelin reveals that brca2/fancd1 is essential for pronephros development. Dev Biol. 2017; 428: 148–163. https://doi.org/10.1016/j.ydbio.2017.05.025 PMID: 28579318

25. Endlich N, Kliewe F, Kindt F, Schmidt K, Kotb AM, Artelt N, et al. The transcription factor Dach1 is essential for podocyte function. J Cell Mol Med. 2018; 22: 2656–2669. https://doi.org/10.1111/jcmm.13544 PMID: 29498212

26. Huang J, McKee M, Huang HD, Xiang A, Davidson AJ, Lu HAJ. A zebrafish model of conditional targeted podocyte ablation and regeneration. Kidney Int. 2013; 83: 1193–1200. https://doi.org/10.1038/ki.2013.6 PMID: 23466998

27. Siegerist F, Zhou W, Endlich K, Endlich N. 4D in vivo imaging of glomerular barrier function in a zebrafish podocyte injury model. Acta Physiol (Oxf). 2017; 220: 167–173. https://doi.org/10.1111/apha.12754 PMID: 27414464

28. Akthar IST, Pichiah PBT, Arunachalam S, Raja S. Adriamycin inhibits embryonic development in zebrafish through downregulation of Kruppel-like factor4. J Biochem Mol Toxicol. 2018: e22235. https://doi.org/10.1002/jbt.22235 PMID: 30286259

29. Motlagh NSH, Parvin P, Ghasemi F, Atyabi F. Fluorescence properties of several chemotherapy drugs. Doxorubicin, paclitaxel and bleomycin. Biomed Opt Express. 2016; 7: 2400–2406. https://doi.org/10.1364/BOE.7.002400 PMID: 27375954

30. Zheng Z, Schmidt-Ott KM, Chua S, Foster KA, Frankel RZ, Pavlidis P, et al. A Mendelian locus on chromosome 16 determines susceptibility to doxorubicin nephropathy in the mouse. Proc Natl Acad Sci U S A. 2005; 102: 2502–2507. https://doi.org/10.1073/pnas.0409786102 PMID: 15699352

31. Zhang W-W, Zhang Y-B, Zhao X-X, Hua Y, Wu Z-L, Yan Y-C, et al. Prmt7 regulates epiboly by facilitating 2-OST and modulating actin cytoskeleton. J Mol Cell Biol. 2015; 7: 489–491. https://doi.org/10.1093/jmcb/mjv040 PMID: 26186943

32. Zhang W, Zhang Y, Li S, Wu Z, Yan Y, Li Y. Prmt7 regulates epiboly and gastrulation cell movements by facilitating syntenin. Acta Biochim Biophys Sin (Shanghai). 2018; 50: 1280–1287. https://doi.org/10.1093/abbs/gmy136 PMID: 30383201

Publication II

Prolonged podocyte depletion in larval zebrafish resembles mammalian focal and segmental glomerulosclerosis

Published in The FASEB Journal, peer-reviewed journal

Kerrin Ursula Ingeborg Hansen, Florian Siegerist, Sophie Daniel, **Maximilian Schindler**, Anna Lervolino, Antje Blumenthal, Christoph Daniel, Kerstin Amann, Weibin Zhou, Karlhans Endlich, Nicole Endlich

DOI: 10.1096/fj.202000724R

Received: 27 March 2020 | Revised: 15 September 2020 | Accepted: 21 September 2020

DOI: 10.1096/fj.202000724R

RESEARCH ARTICLE

THE FASEB JOURNAL

Prolonged podocyte depletion in larval zebrafish resembles mammalian focal and segmental glomerulosclerosis

Kerrin Ursula Ingeborg Hansen[1] | **Florian Siegerist**[1] | **Sophie Daniel**[1] | **Maximilian Schindler**[1] | **Anna Iervolino**[1,2] | **Antje Blumenthal**[1] | **Christoph Daniel**[3] | **Kerstin Amann**[3] | **Weibin Zhou**[4] | **Karlhans Endlich**[1] | **Nicole Endlich**[1]

[1]Institute for Anatomy and Cell Biology, University Medicine Greifswald, Greifswald, Germany

[2]Biogem Research Institute Gaetano Salvatore, Ariano Irpino, Italy

[3]Department of Nephropathology, Institute of Pathology, University of Erlangen-Nürnberg, Erlangen, Germany

[4]Division of Nephrology, Department of Medicine, Icahn School of Medicine at Mount Sinai, New York City, NY, USA

Correspondence
Nicole Endlich, Institute for Anatomy and Cell Biology, University Medicine Greifswald, Friedrich-Loeffler Str. 23c, Greifswald 17487, Germany.
Email: nicole.endlich@uni-greifswald.de

Funding information
Bundesministerium für Bildung und Forschung (BMBF), Grant/Award Number: 01GM1518B

Abstract

Focal and segmental glomerulosclerosis (FSGS) is a histological pattern frequently found in patients with nephrotic syndrome that often progress to end-stage kidney disease. The initial step in development of this histologically defined entity is injury and ultimately depletion of podocytes, highly arborized interdigitating cells on the glomerular capillaries with important function for the glomerular filtration barrier. Since there are still no causal therapeutic options, animal models are needed to develop new treatment strategies. Here, we present an FSGS-like model in zebrafish larvae, an eligible vertebrate model for kidney research. In a transgenic zebrafish strain, podocytes were depleted, and the glomerular response was investigated by histological and morphometrical analysis combined with immunofluorescence staining and ultrastructural analysis by transmission electron microscopy. By intravenous injection of fluorescent high-molecular weight dextran, we confirmed leakage of the size selective filtration barrier. Additionally, we observed severe podocyte foot process effacement of remaining podocytes, activation of proximal tubule-like parietal epithelial cells identified by ultrastructural cytomorphology, and expression of proximal tubule markers. These activated cells deposited extracellular matrix on the glomerular tuft which are all hallmarks of FSGS. Our findings indicate that glomerular response to podocyte depletion in larval zebrafish resembles human FSGS in several important characteristics. Therefore, this model will help to investigate the disease development and the effects of potential drugs in a living organism.

KEYWORDS

FSGS, glomerulus, podocyte injury, zebrafish model organism

Abbreviations: DMSO, dimethyl sulfoxide; dpf, days post fertilization; FFPE, formalin fixed paraffin embedded; FITC, fluorescein isothiocyanate; FSGS, focal and segmental glomerulosclerosis; GBM, glomerular basement membrane; Hpf, hours post fertilization; MTZ, metronidazole; NTR, nitroreductase; PAM, periodic acid methenamine; PAN, puromycin aminonucleoside; PBS, phosphate buffered saline; pcna, proliferating cell nuclear antigen; PEC, parietal epithelial cell; TEM, transmission electron microscopy; ZFIN, Zebrafish Information Network.

1 | INTRODUCTION

Focal segmental glomerulosclerosis (FSGS) is a life-threatening progressive disease with limited therapeutic options often resulting in end stage kidney disease. It is well known that podocyte damage and subsequent depletion are the first steps in the development of FSGS[1] followed by an activation of parietal epithelial cells (PECs). This activation leads to the formation of cellular lesions on the glomerular tuft.[2] Recently, Kuppe and colleagues have shown that upon activation, PECs develop a cuboidal phenotype and are the main cell type in sclerotic lesions.[3] Simultaneously, remaining podocytes lose their complex 3-D morphology, interdigitating podocyte foot processes become broadened as well as flattened which is named foot process effacement.

Since experimental procedures in rodents are not suitable for high-throughput drug screenings, we and others use zebrafish larvae as a simple vertebrate model[4] to study glomerular morphology[5] as well as the permselectivity of the glomerular filtration barrier.[6] Starting at 48 hours past fertilization (dpf), zebrafish larvae develop a single already filtering glomerulus which is connected to a pair of tubules.[4] Analogous to mammals, the glomerular filtration barrier consists of a fenestrated endothelium, the glomerular basement membrane (GBM), and interdigitating podocyte foot processes, which are bridged by an electron-dense slit diaphragm that is formed by homodimerization of the transmembrane protein nephrin.[4] Due to the translucency of the early larvae, the rapid development of the filtration barrier of its simple kidney, its morphology and genetics homologous to mammals, the zebrafish model is ideally suitable for high-throughput drug screenings.[7] As the zebrafish model is easily accessible to fast genetic methods like morpholino-oligonucleotide-mediated knockdowns of genes, the model has been used in a number of studies investigating genetic causes of primary FSGS by generating knockdowns of *nphs1/nphs2*,[8] *cd2ap*,[9] *wt1*,[10] or *inf2*.[11]

To generate a podocyte injury comparable to FSGS, we applied the transgenic nitroreductase/metronidazole (NTR/MTZ) model for cell-specific tissue ablation, first established in zebrafish by Davidson and collegues.[12] In our model of podocyte depletion, the prodrug MTZ is activated exclusively in podocytes expressing the NTR under control of the *nphs2* promotor via the Gal4/UAS-system.[13] Activated MTZ functions as a DNA cross linking agent, which induces selective cell death of podocytes. This leads to rapid onset of proteinuria and edema resembling human nephrotic syndrome.[5,6,14] The aim of this study was to examine the glomerular response upon partial podocyte depletion and to investigate the applicability of this model for human FSGS.

2 | MATERIALS AND METHODS

2.1 | Zebrafish husbandry and MTZ treatment

Zebrafish (Danio rerio) were bred, maintained, and staged as described before.[6] We used the double transgenic strain Tg (*nphs2*:GAL4); Tg (UAS:*Eco.nfsb*-mCherry), ZFIN: ZDB-FISH-160601-2 backcrossed to transparent mitfa$^{w2/w2}$ for at least two generations to generate homozygous double transgenic larvae for all experiments. Larvae express the bacterial enzyme nitroreductase and the fluorescent protein mCherry exclusively in podocytes. Prior to all experiments, larvae were selected for homogenous mCherry expression in the group within the glomerulus. From this selected groups, larvae were randomly assigned to the treatment and control groups. All experiments were performed according to German animal protection law overseen by the "Landesamt für Landwirtschaft, Lebensmittelsicherheit und Fischerei, Rostock" of the federal state of Mecklenburg—Western Pomerania. For drug treatment, 0.1% DMSO was freshly diluted in E3-embryo medium. MTZ (Sigma-Aldrich, St. Louis, MO, USA) was added at a concentration of 80 µmol L^{-1} for all experiments. Controls were treated with 0.1% DMSO-solution only. Treatment was started at 4 dpf and a treatment period of 48 hours was held for all experiments.

2.2 | Histology

Larvae for histological analysis were fixed at 6 dpf and at 9 dpf in 4% paraformaldehyde at 4°C overnight. Glycol methacrylate plastic resin embedding was performed with Technovit 7100 (Kulzer GmbH, Hanau, Germany) as per the manufacturer's instructions. 4 µm transversal sections were made with a Jung RM 2055 rotational microtome (Leica Microsystems, Wetzlar, Germany). H&E and PAM silver staining according to Jones were performed adhering to Technovit 7100 routine staining protocols.

2.3 | Immunofluorescence staining

For *podocin*, *collagen I alpha 1* and *atp1a1* staining, larvae were fixed in 4% paraformaldehyde at 4°C overnight and embedded in paraffin according to the standard protocols. 5 µm sections were made on a Leica SM 200R microtome. After heat-mediated antigen retrieval, sections were incubated with primary antibodies 1:500 polyclonal rabbit anti-podocin (Proteintech, IL, USA) or 1:500 polyclonal rabbit anti-col1a1 (GeneTex, CA, USA) or 1:200 monoclonal mouse anti-*atp1a1* (a6F clone, Developmental

Studies Hybridoma Bank, University of Iowa, deposited by DM Fambrough, Johns Hopkins School of Medicine) at 4°C overnight. For *pcna*, *pax2a* and *laminin* staining, larvae were fixed in 2% paraformaldehyde at 4°C overnight. 30% sucrose in PBS was mixed 1:1 with TissueTek (Sakura Finetek Europe, AV, Netherlands) and used for infiltration for 3 hours at room temperature. Samples were snap-frozen in liquid nitrogen. Between 4-5 µm sections were made on a Microm HM 560 microtome (Thermo Fisher Scientific, MA, USA). After permeabilization with 0.3% Triton X-100 and five washes with PBS, slides were incubated with 1:50 polyclonal rabbit anti-*pcna* (sc-56, Santa Cruz Biotechnology, TX, USA), 1:500 rabbit anti-pax2a (ab229318, abcam), or 1:35 polyclonal rabbit anti-*laminin* (L9393, Sigma-Aldrich) at 4°C overnight. Slides were washed five times in PBS. For all stainings except staining for *atp1a1*, Alexa Fluor 488-, or 647-conjugated goat anti-rabbit IgG F(ab) 2 antibody fragment (Dianova, Hamburg, Germany) were used at 1:300 dilution. For *atp1a1* staining, Cy3-conjugated goat anti-mouse IgG (Jackson ImmunoResearch, PA, USA) was used at a 1:300 dilution. For the staining of human FSGS and control tissue biopsies, anonymized excess tissue of kidney biopsies that was diagnosed by experienced nephropathologists of the Dept. of Nephropathology, University Erlangen-Nürnberg, was used. The use of kidney biopsies from Erlangen has been approved by the Ethics Committee of the Friedrich Alexander University of Erlangen-Nürnberg, waiving the need for retrospective consent for the use of archived excess material (Ref. No. 4415). Briefly, 5 µm sections of FFPE-material was collected on super frost slides, deparaffinized in xylene, and hydrated in an ascending ethanol series. After heat-mediated epitope retrieval in 10 mM citric acid buffer pH6 in a pressure cooker, sections were incubated with the aforementioned *atp1a1* antibody (1:200) and a guinea pig anti *nephrin* antiserum (1:300, gpN2, Progen, Heidelberg, Germany) at 4°C overnight. After five washes in PBS the primary antibodies were detected using 1:800 Cy3-conjugated donkey anti guinea pig and 1:800 Alexa Fluor 488-conjugated goat anti mouse antibodies Dianova, Hamburg, Germany). In all stainings, cell nuclei were counterstained with 0.1 mg/mL DAPI (4′,6-Diamidine-2′-phenylindole dihydrochloride, Sigma, MO, USA) for 20 minutes. After one wash with PBS, and with A. dest, slides were mounted with Mowiol for microscopy (Roth, Karlsruhe, Germany). Immunofluorescence micrographs were acquired with a TCS SP5 confocal laser scanning microscope (C-LSM) using the 63x, 1.4 NA oil immersion objective (Leica Microsystems, Wetzlar, Germany). Brightfield images were acquired with an Olympus BX50 light microscope using the 40x, 0.6 NA objective (Olympus, Hamburg, Germany). ImageJ V1.51f (Wayne Rasband, National Institutes of Health, USA) was used for all morphometric measurements, the cell counter plugin was used to count pax2a^{+} cells on the glomerular tuft.

2.4 | Transmission electron microscopy

Larvae collected at early 9 dpf were fixed in 4% glutaraldehyde, 1% paraformaldehyde, and 1% sucrose in 0.1 M HEPES at 4°C overnight and embedded in EPON 812 (Serva, Heidelberg, Germany) as per the manufacturer's instructions. Semithin (500 nm) and ultrathin sections (70 nm) were made on an Ultracut UCT microtome (Leica Microsystems, Heidelberg, Germany). Semithin sections were stained with methylene blue. UItrathin sections were placed on copper grids, contrasted with 5% uranyl acetate for 5 minutes and with Sato's lead stain for 5 minutes. Images were acquired with a LIBRA 120 TEM (Carl Zeiss GmbH, Oberkochen, Germany) with an anode voltage of 80 kV.

2.5 | Statistical analysis

GraphPad prism V5.01 (GraphPad Software, CA, USA) was used for all statistical analyses. Gaussian distribution was checked by Kolmogorov-Smirnov testing. If passed, Student's t test was used for significance testing and mean was given in the results. For statistical testing of nonparametric data, Mann-Whitney U test was applied, and median was used. P-values lower 0.05 were considered statistically significant.

3 | RESULTS

We used the transgenic zebrafish strain *Cherry* (Tg(*nphs2*:GAL4); Tg(UAS:Eco.nfsb-mCherry); mitfa$^{w2/w2}$ on AB-Tü background) for all experiments. *Cherry* larvae express the bacterial NTR together with the red fluorescent protein mCherry under control of a podocyte-specific GAL4-driver (Figure 1A). After administration of the prodrug MTZ to the medium, MTZ is taken up by the cells and converted into a cytotoxic agent uniquely in NTR-expressing cells, in this case podocytes (Figure 1A′). MTZ induces interstrand DNA crosslinking and subsequent apoptosis in a concentration dependent manner,[14,15] resulting in areas with denuded GBM due to the detachment of affected podocytes. To generate conditions comparable to the situation found at the onset of FSGS in mammals, we used a low dose of MTZ to deplete only a subset of podocytes. Cherry larvae were treated with low-dose MTZ (80 µmol L^{-1} in 0.1% DMSO) or with 0.1% DMSO as a control beginning at 4 dpf. MTZ and DMSO was washed out after 48 hours of treatment.

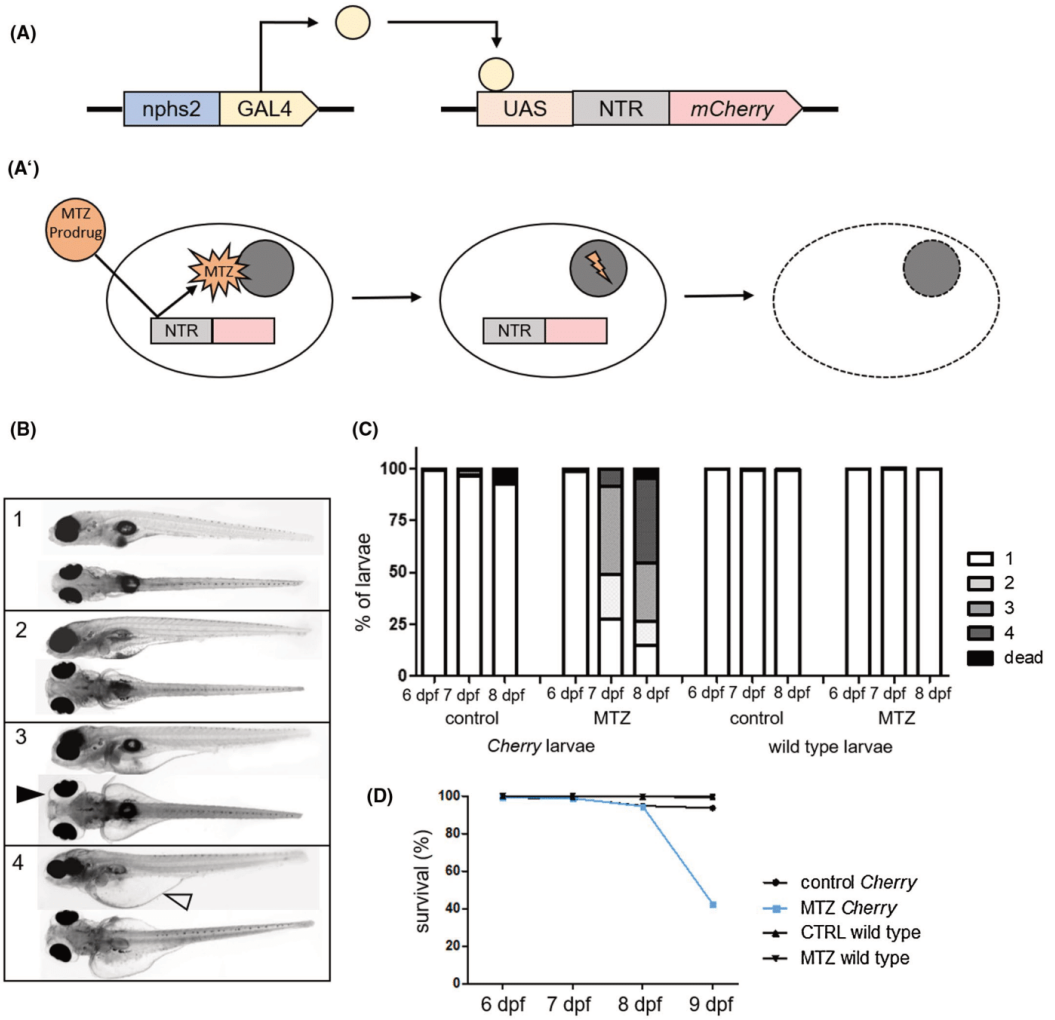

FIGURE 1 A, Schematically shows gene expression in the used transgenic zebrafish line. Gal4 is expressed under the *nphs2* promotor. After binding to its specific recognition sequence UAS (upstream activation sequence), it activates the expression of a bacterial nitroreductase (NTR) and the red fluorescence protein *mCherry*. A′ shows a scheme of how MTZ is activated by NTR and subsequently induces DNA damage, which leads to apoptosis. B shows representative micrographs of 8 dpf zebrafish larvae to demonstrate the grading of developing edema after podocyte depletion. (1) no edema, (2) mild edema, (3) medium edema, and (4) severe edema. The black arrowhead exemplary indicates periocular edema, the blank arrowhead indicates abdominal edema. The graph in C shows relative distributions of phenotypes in n = 251 control-treated and n = 275 MTZ-treated *Cherry* larvae in four individual experiments and in n = 250 control-treated and n = 250 MTZ-treated wild-type larvae. As visualized in the diagram in D, survival rates of podocyte-depleted *Cherry* larvae are similar to controls until an abrupt decrease at 9 dpf

We observed edema of different severity in larvae treated with low-dose MTZ which was graded into four categories starting from 1 (no edema) to 4 (severe whole body edema with bent body axis) as shown in representative images of 8 dpf zebrafish larvae in Figure 1B. We found that MTZ-treated *Cherry* larvae developed edema 1 day after MTZ-washout (7 dpf). At 8 dpf, 69% (of total n = 275) of living MTZ-treated *Cherry* larvae showed medium to severe edema formation (Figure 1C) and 51% of MTZ-treated *Cherry* larvae finally died at 9 dpf (Figure 1D). In contrast to that, only 10% (of n = 251) of the control-treated *Cherry* larvae showed edema of any severity or died during the observation time

(Figure 1C,D). In contrast to that, nitroreductase-negative non-transgenic wild-type larvae (AB-Tü strain) treated with either 80 μmol L^{-1} MTZ in 0.1% DMSO or 0.1% DMSO vehicle control did not show significant edema or decreases viability (Figure 1C,D).

To indirectly quantify proteinuria and to determine the integrity of the glomerular filtration barrier, we intravenously injected far-red fluorescent low molecular weight dextran (10 kDa conjugated to Alexa Fluor-647) together with green fluorescent high molecular weight dextran (500 kDa, FITC), directly after MTZ-washout. 0.5 and 19 hours after the injection of the dextrans, we determined the intravascular fluorescence in the caudal vein by in vivo confocal laser scanning microscopy (C-LSM), shown in Figure 2A. The fluorescence of FITC decreased by 59% in MTZ-treated larvae after 19 hours ($P = .0002$ compared to the controls; n = 31), whereas the fluorescence of FITC in controls did only decline slightly (Figure 2B). Moreover, immunofluorescence staining with a polyclonal *podocin* antibody showed a significant reduction in MTZ-treated larvae in comparison to controls, which displayed a regular and strong linear staining pattern along the glomerular capillaries (Figure 2C,D).

Transmission electron microscopy (TEM) of MTZ-treated larvae at 9 dpf revealed disintegrated cells along the GBM localized close to podocytes (Figure 2E). The foot processes of remaining podocytes of MTZ-treated larvae were severely effaced, whereas controls the exhibited intact podocytes with regular foot processes that were bridged by an electron dense slit membrane (magnifications in Figure 2E).

Furthermore, histologic analysis of formalin-fixed and plastic-embedded larvae showed a reduced glomerular cell density in MTZ-treated larvae compared to controls (median: 0.014 nuclei per μm^2 in MTZ-treated larvae vs 0.022 nuclei per μm^2; $P = .0011$; n = 24) (Figure S1A,B). It remained still reduced after 3 days of regeneration (0.0161 nuclei per μm^2 vs 0.0325 nuclei per μm^2 in controls at 9 dpf; $P = .0003$; n = 24), although the absolute cell numbers at the capillaries of MTZ-treated larvae increased to a level similar to controls (Figure S1B,C). Numbers of podocytes per glomerular cross-section determined by TEM remained significantly reduced (mean: 9.0 vs 13.25 at 9 dpf; $P = .0043$; n = 17) (Figure S1D). Moreover, we found that the Bowman's capsules were enlarged after MTZ-treatment, which was determined as the area of the largest of the consecutive glomerular serial cross-sections for each larva. At 6 dpf, the mean was 1043 μm^2 after MTZ treatment compared to 538 μm^2 in controls (Figure S1E, $P = .0008$, n = 24). The difference was even higher at 9 dpf (1085 μm^2 in MTZ-treated larvae vs 374 μm^2, $P = .0019$, n = 24).

In podocyte-depleted larvae, distinct severities of podocyte impairment could be discriminated by TEM: In 45% (5 of n = 11) of MTZ-treated larvae, glomeruli showed a uniform electron dense GBM, well fenestrated endothelial cells similar to controls, but a severe foot process effacement (Figure 3A). Only a few capillaries showed normal foot processes. Moreover, dilatations of the sub-podocyte space were frequently found (asterisk in Figure 3A). In 36% (4/11) of MTZ-treated larvae, no typical foot processes of podocytes were visible. As shown in Figure 3B, visceral epithelial cells were instead showing tight junctions and microvillous transformation. 18% (2/11) of MTZ-treated larvae showed a phenotype of intermediate severity that showed characteristics of both previously described. Total numbers of local electron-dense contacts to neighboring cells per visceral epithelial cell were increased from 0.29 in controls to 2.2 tight junctions per cell in MTZ-treated larvae ($P = .0002$, n = 20) (Figure 3B,C).

Histomorphologic analysis showed a thickening of the PEC-layer that progressed between 6 to 9 dpf (Figure 4A). After MTZ washout (6 dpf), mean thickness of PECs was 0.9 μm in controls and 1.11 μm in podocyte-depleted larvae ($P = .0043$; n = 24). At 9 dpf, it was 0.78 μm in controls and 3.96 μm after MTZ treatment ($P = .0001$; n = 24) (Figure 4B). Under baseline conditions, PECs show very little proliferation but become more replicative after injury-induced activation. Immunostaining for *proliferating cell nuclear antigen* (*pcna*), an antigen only present during S-phase in cellular replication, revealed proliferating PECs only in podocyte-depleted larvae (Figure 4C).

To investigate whether these cuboidal cells on the glomerular tuft were of PEC/tubular-origin, we immunostained with a polyclonal antibody for the transcription factor *pax2a* which is a marker of the proximal tubular neck segment and parietal epithelial cells in the zebrafish pronephros.[16] As shown in the C-LSM micrograph in Figure 4D, proximal tubule cells and PECs where strongly *pax2a*-positive under baseline conditions. Upon podocyte-depletion we found an increase of the *pax2a* protein abundance on the parietal leaf of Bowman's space. Additionally, the de-novo appearing cuboidal cells on the glomerular tuft also expressed strongly *pax2a,* whereas podocytes were *pax2a* negative. Figure 4E shows counts of *pax2a*-positive cells on the glomerular tuft in MTZ-treated larvae and in controls. After podocyte depletion, a statistically significant number of $pax2a^+$ cells were recruited to the glomerular tuft.

To further discriminate the origin of these cuboidal $pax2a^+$ cells on the glomerular tuft, we additionally stained for the Na^+-K^+-ATPase subunit alpha 1 (*atp1a1*) using a monoclonal antibody which in mammalian kidneys is a tubular marker and under baseline conditions not expressed in the glomerulus or PECs as shown in the immunohistochemistry micrographs of the protein atlas database (http://proteinatlas.org) in Figure S2. To verify that *atp1a1* is expressed in the proximal tubules and not in healthy PECs in zebrafish as well, we stained sections of MTZ-treated and control zebrafish larvae for *pax2a* and *atp1a1* simultaneously. A co-expression

of both markers was found, as shown in Figure 5A. Similar to mammals, proximal tubule cells where strongly expressing *atp1a1* under control and diseased conditions in the basolateral cell membrane. Only after podocyte-depletion, activated prismatic PECs were also found *atp1a1*-positive. Additionally, we frequently found double positive cuboidal *atp1a1* and *pax2a* positive cells on the glomerular tuft (Figure 5B).

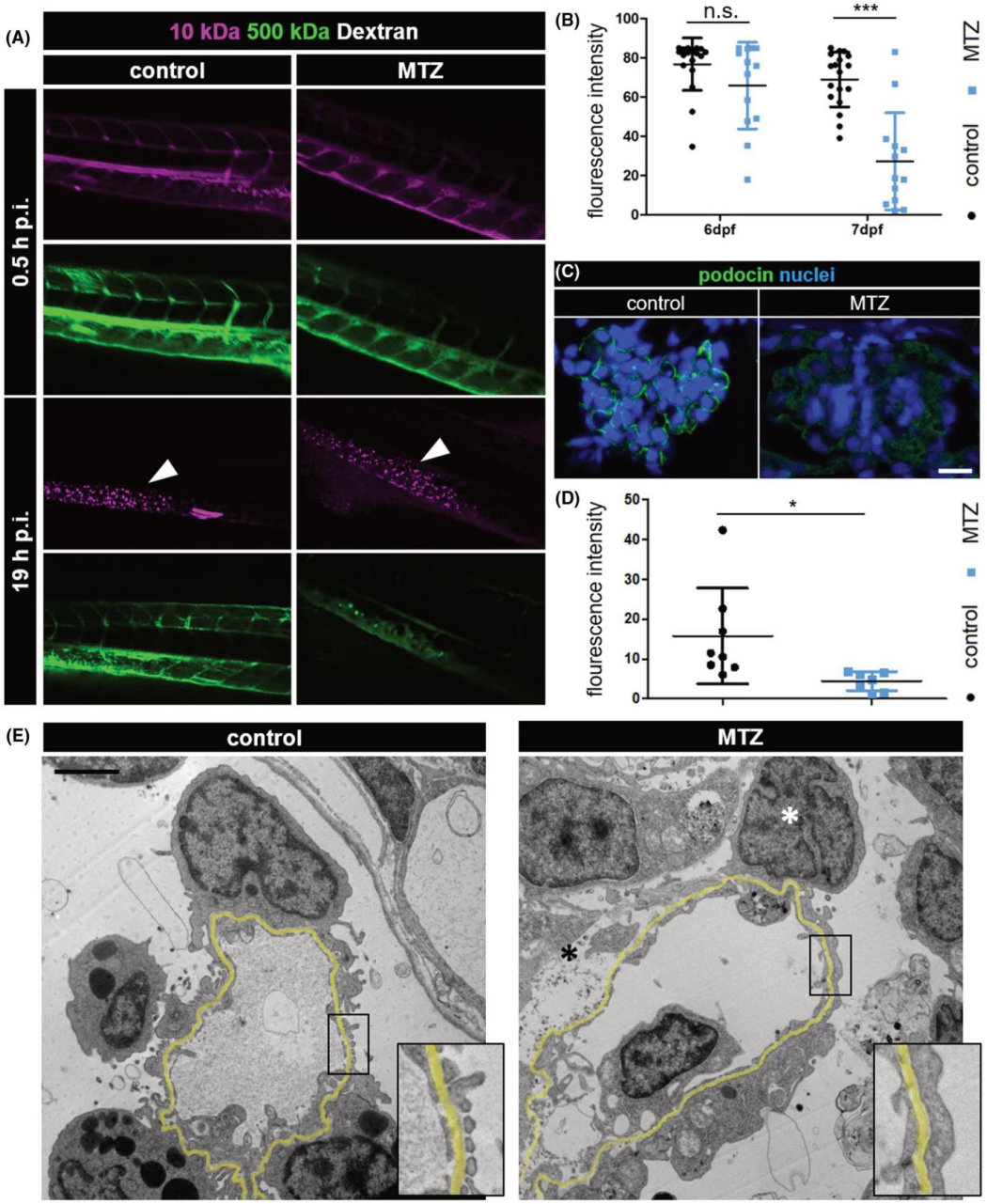

FIGURE 2 A, Confocal laser scanning micrographs of podocyte-depleted and control larvae 0.5 and 19 hours after injection with a mixture of FITC-conjugated 500 kDa and Alexa Fluor647-conjugated 10 kDa dextran directly after metronidazole washout. Notice the decrease of 500 kDa dextran in podocyte-depleted larvae, whereas 10 kDa dextran accumulates in the tissue as shown in the caudal fin (white arrowheads). As shown in graph B, fluorescence intensity of FITC measured in the caudal vein was significantly lower in podocyte-depleted larvae 19 hours after dextran injection. C, The linear staining pattern of podocin 3 days after vehicle treatment in controls while the signal is greatly reduced in podocyte-depleted larvae. The scale bar represents 10 µm. D, Quantification of these differences by fluorescence intensity. Transmission electron micrographs of 9 dpf control larvae in panel E reveal a normal morphology with fine foot processes connected by a slit diaphragm, whereas podocyte foot processes in MTZ-treated larvae are broadly effaced, as shown in detail in the magnifications at the bottom right corner of each image. The white asterisk labels the nucleus of a remaining podocyte after MTZ treatment. Remnants of an apoptotic podocyte are marked by the black asterisk. The GBM is highlighted in yellow. Scale bar represents 2 µm

To find out whether this finding was restricted to the zebrafish model only or rather a conserved mechanism, we stained FFPE sections of kidney biopsies of n = 4 patients with biopsy-proven FSGS and of n = 4 controls (tumor-free excess tissue of tumor nephrectomies with healthy appearing histology) for *atp1a1* and the podocyte-marker *nephrin*. As expected, in the healthy controls, *atp1a1* expression was absent in cells of the glomerular tuft and PECs and began right at the PEC-proximal tubular interface (arrowhead in Figure 5C). In contrast to that, activated PECs in the FSGS biopsies showed *atp1a1* positivity (arrow in Figure 5C). This phenomenon could be seen in at least one glomerulus in three out of four of the examined biopsies (Figure S3).

Another feature of human FSGS is the presence of adhesions of the parietal and visceral epithelial layer that are formed by activated PECs to the denuded areas of the GBM. In line with the previous findings, we found that in glomeruli of podocyte-depleted larvae, adhesions between the activated parietal and visceral glomerular cell layer were visible in H&E sections (Figure 6A) and TEM micrographs (Figure 6B). Since podocyte loss in humans is followed by progressive scarring of the glomerulus, we investigated extracellular matrix deposition in podocyte-depleted zebrafish larvae. While Jone's stain showed slight accumulation of silver-positive material on the glomerular tuft at 9 dpf (Figure 4A), a strong accumulation of laminin was seen (Figure 6C) with significant GBM-thickening (Figure 6D). However, we could not detect the accumulation of *collagen I* at 9 dpf (Figure S4).

Following podocyte injury and using classic histology and TEM, we identified immigrating neutrophils and macrophages within Bowman's capsule only in podocyte-depleted larvae and not in healthy control animals (Figure S5).

4 | DISCUSSION

It has been shown previously that the main reason leading to the histologic pattern of FSGS is injury and subsequent loss of podocytes. Regardless of the initial cause of podocyte injury, may it be genetic, by endogenous circulating podocytotoxic factors or directly exogenously toxic, the relationship between podocyte depletion and glomerulosclerosis has been shown in humans,[17-19] as well as in animal models such as transgenic mouse models of podocyte ablation,[20,21] puromycin aminonucleoside (PAN)-treated rats[22] and podocyte ablation by diphtheria toxin injection in transgenic rats expressing the human diphtheria toxin receptor exclusively in podocytes.[23] Unfortunately, these model organisms are not easily usable in high-throughput assays and even in the era of CRISPR/Cas9 genetic manipulation is rather difficult and time-consuming. In the zebrafish model, the small larval size and conserved morphology of the pronephros offers a general applicability for high-throughput assays as larvae can easily be treated and screened in the 96-well format as it has been shown before for modulators of polycystic kidney disease using a morpholino-based genetic zebrafish model[24] or a developmental drug nephrotoxicity assay[25] which both used pronephric morphometry as the primary readout.

To analyze the glomerular response to podocyte depletion in zebrafish and investigate the suitability of larval zebrafish as a model for human FSGS, a targeted model of podocyte depletion was needed. PAN has been shown to induce podocyte injury in larval zebrafish, but since it has to be intravenously injected, it is not directly eligible for high-throughput screenings in which minimal hands-on time is a prerequisite for scalability.[9] Another available method of podocyte depletion is laser-induced injury, but spatial specificity of the damage requires ablation of single cells, so treatment of higher counts of larvae at the same time would not be possible.[26] Non-transgenic attempts to induce podocyte injury by adding reagents to the water have not been successful for the effect was either minimal or not limited to podocytes.[27]

To date the only inducible model of podocyte depletion that combines the ease of adding a reagent to the medium with the advantage of cell-specific ablation is the NTR/MTZ model.[5,14] In this study, we chose a short treatment with low-dose MTZ to deplete a subset of podocytes so that larvae survived long enough to investigate glomerular response and adaption to injury.

As described before, MTZ-treated larvae developed periocular edema, which is a hallmark for hypoproteinemic proteinuria.[14] Wild-type larvae did not develop significant

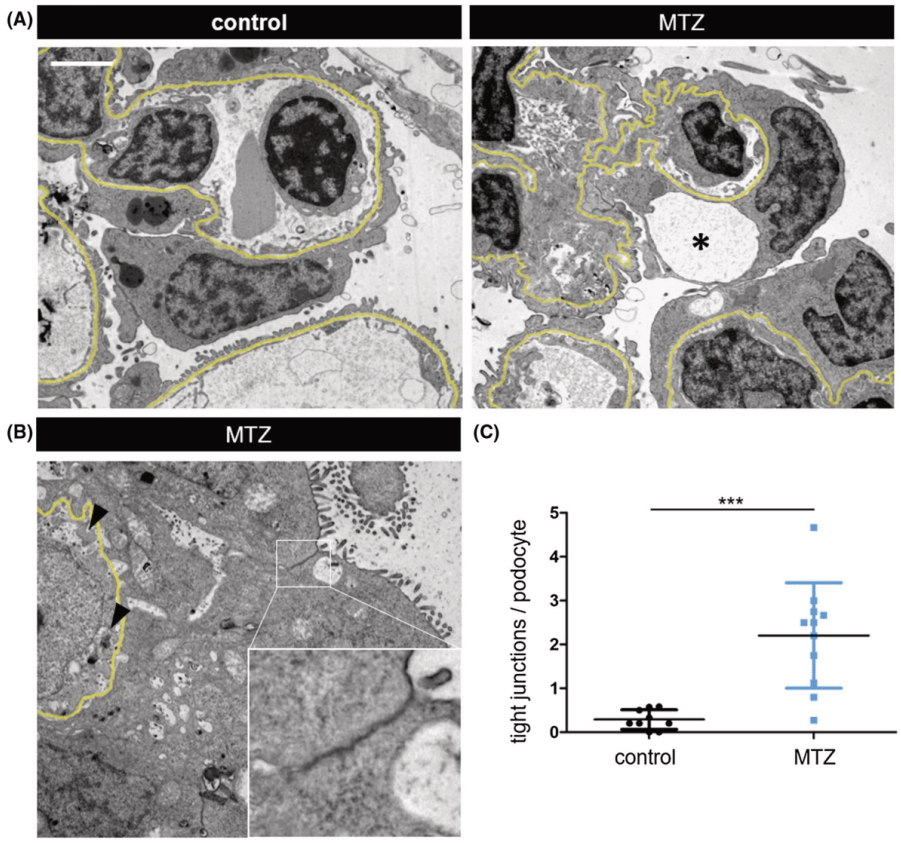

FIGURE 3 Contrasting intact podocyte foot processes in control larvae, podocyte-depleted glomeruli displayed signs of podocyte impairment as shown in the representative micrographs in A. Adjacent to a capillary displaying almost normal morphology; podocyte foot process effacement and subpodocyte space, pseudocysts (asterisk) can be seen. Scale bar represents 2 µm. MTZ-treated larvae showed markedly increased tight junctions between remaining podocytes in n = 20 larvae (B, C). An electron-dense tight junction is shown in detail in the bottom right corner of the picture in B. Black arrowheads accentuate loss of fenestration and cellular integrity of the capillary endothelium

numbers of edema, indicating NTR-dependency and specificity of the phenotype. Furthermore, we verified the loss of permselectivity of the glomerular filtration barrier using clearance of fluorescent-labeled high molecular weight dextran from the vasculature which under healthy conditions is retained in the blood plasma by the GFB. Three days after MTZ washout, some non-detached podocytes were found on the glomerular capillaries that showed severe foot process effacement and reduction of the expression of the slit membrane protein *podocin* as a sign of persistent podocyte injury. An increase of tight junctions between neighboring podocytes can be interpreted as a mechanism to prevent detachment from the GBM under increased mechanical forces and filtration which has been described extensively in human patients and mammalian models.[28,29]

Although the size of the glomerular tuft significantly increased, the total number of podocytes per glomerular cross section remained significantly lower than in controls, indicating cellular hypertrophy of remaining podocytes. Previous work has shown that insufficient podocyte-hypertrophy and subsequent mechanical stress leads to the development of sub-podocyte space pseudocysts preceding podocyte detachment.[30] Furthermore, increased filtration in the sub-podocyte space has been suggested to play an important role in the regulation of glomerular permeability.[31]

Another key feature of mammalian FSGS is the activation of PECs which contribute to fibrotic lesions, as it has nicely been shown by Smeets and colleagues,[32] and thickening of Bowman's capsule.[33] By analyzing the *pax2* expression, Ohtaka et al and Dijkman et al furthermore showed that cells

on the parietal-visceral interface contribute to cellular lesions in human FSGS.[34,35]

In our model, PECs started to proliferate and changed their morphology toward a cuboidal, microvillous phenotype following activation due to podocyte detachment. These findings strongly support the hypothesis that upon podocyte-depletion, flat PECs transform to cuboidal PECs, as it has recently been shown by Kuppe et al.[3] Together with the

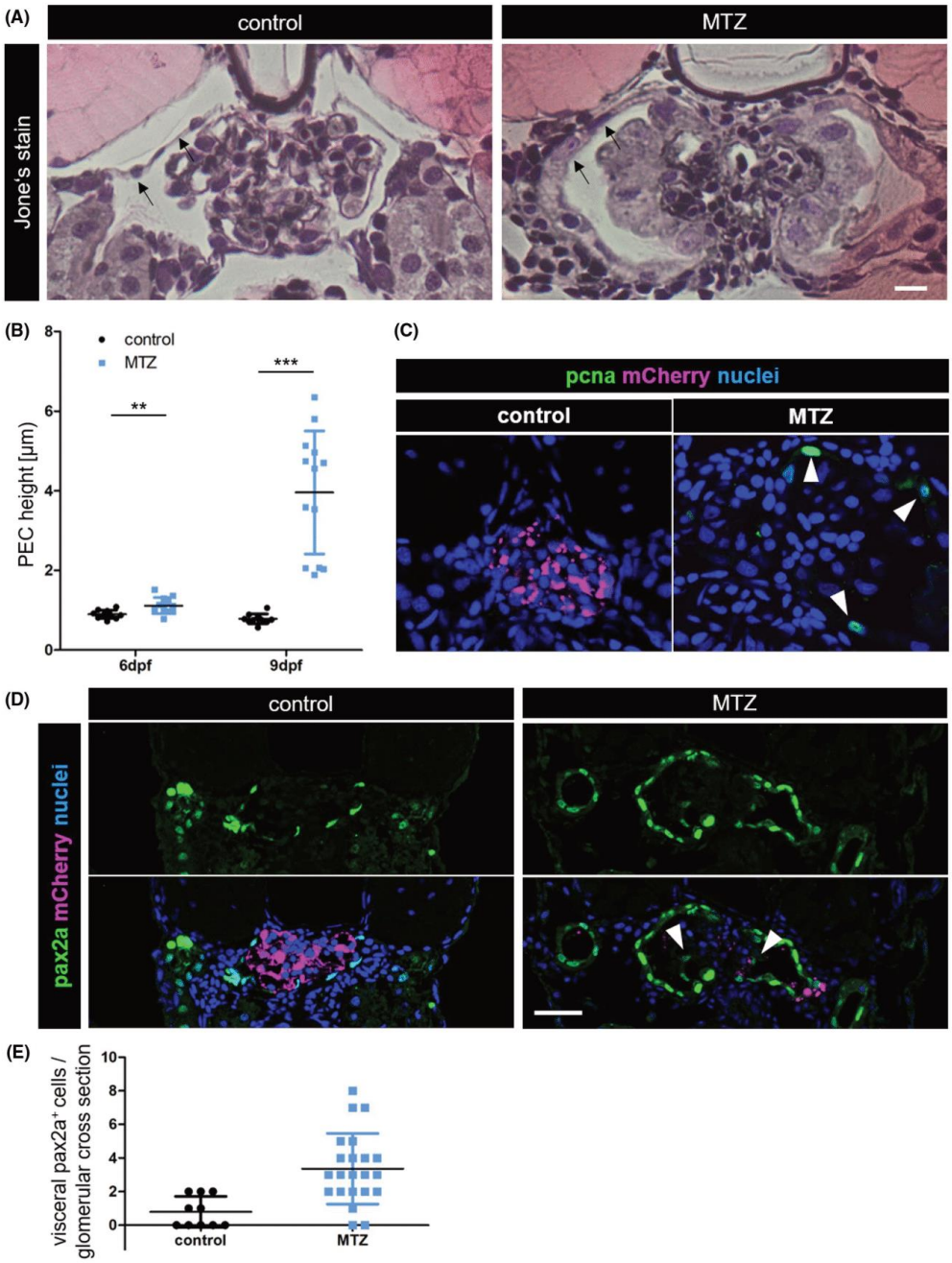

FIGURE 4 Panel A representative micrographs of Jone's-stained plastic sections of podocyte-depleted and control larvae. Black arrows point at the PEC layer. The scale bar represents 10 µm. The graph in B shows the result of PEC height measurements in H&E-stained plastic sections of n = 25 podocyte-depleted and n = 23 control larvae. A statistically significant increase is visible in podocyte-depleted larvae directly after, and 3 days after treatment. The micrographs in panel C show *pcna*-staining of larvae collected at 9 dpf. Expression of *mCherry* labels podocytes. Podocyte-depleted larvae show *pcna*-positivity of PECs (white arrowheads). Panel D demonstrates *pax2a*-positive PEC-nuclei under baseline conditions with increased expression of *pax2a* in cuboidal PECs and cuboidal cells on the glomerular tuft 3 days after podocyte depletion (white arrowheads). The scale bar represents 25 µm. The graph in E shows quantification of these differences

typical cytomorphology and the expression of *pax2a, atp1a1,* and not *podocin* (no podocin protein in immunofluorescence and no podocin promotor activity as shown by missing transgene expression), we characterized them as cuboidal proximal-tubule like PECs that covered the denuded areas of the GBM in the most severely injured 36% of MTZ-treated larvae, which fits previous findings in a murine model of collapsing FSGS.[36] Furthermore, using immunofluorescence in FSGS biopsies, we could show that the presence of *atp1a1* was not restricted to the model we used but a general and conserved mechanism as the pattern of *atp1a1* expression in MTZ-treated zebrafish larvae strongly resembled the situation found in human FSGS patients.

In contrast to that, other groups have suggested that PECs are recruited to the glomerular tuft and replace podocytes.[37,38] Another work additionally mentions attachment of PECs to the apical sides of podocytes after activation and both propose extracellular matrix conglomerates in FSGS to be synthesized by PECs as we have demonstrated in our model.[36,39] Still, the pathways involved in PEC activation following podocyte injury remain incompletely understood. Romoli et al recently proposed *cxcl12* derived by podocytes into Bowman's Space as a quiescence signal to PECs.[40] A study performed by Kuppe et al in 2015 focused on the role of PECs in secondary FSGS in humans. It revealed that cells expressing the marker *anxa3* for all PECs and the PEC matrix marker *lkiv69* were involved in all stages of secondary FSGS, whereas the PEC activation markers *cd44* and *krt19* were expressed in cellular lesions, but only rarely in sclerotic lesions. The findings where independent of the underlying glomerular disease, indicating a common cellular pathway in the development of sclerotic lesions.[41]

Although zebrafish larvae have the general ability to develop sclerosis,[42] they seem to develop remarkably little fibrosis and instead regenerate tissue as shown for cardiomyocytes.[43] Expression analysis of the prevalent extracellular matrix component collagen 1, which is expressed in tissues of the musculoskeletal system of healthy individuals, does not seem to detect sclerotic lesions sensitively, for we could not detect it in the glomerulus despite clear accumulation of laminin. Since accumulation of laminin, in combination with other extracellular matrix components, directly causes a thickening of the GBM, GBM width is equal to quantification of laminin staining as a readout.

As a potential readout for potential positive influence of screened drugs on the disease cause two different approaches can be chosen: First, an aim of analysis could be the impact of potential drugs on the number of *atp1a1*- or *pax2a*-positive cells on the glomerular tuft as an indicator of involvement of cuboidal PECs contribute to sclerotic lesions. At least for *pax2a*, a number of fluorescent reporter strains are available which can be readily used to automate detection of intraglomerular *pax2a* expression and, therefore, quantification of recruitment of disease-accelerating proximal-tubule like cuboidal PECs.

Second, as a more direct marker for disease progression, effects on proteinuria using transgene reporter lines like the eGFP-labeled vitamin D binding protein line could be used. In this model strains, 78 kDa eGFP-labeled vitamin D-binding protein is synthesized in hepatocytes and secreted to the blood plasma. As in healthy conditions, the eGFP-fusion cannot pass the GFB freely, its intravascular fluorescence intensity directly reflects the function of the GFB as we have shown for the NTR-MTZ model before.[6] Therefore, the slope of the intravascular eGFP-intensity decrease directly correlates with progression of proteinuria and is ideal as a primary screening readout. In 2020, Steenbergen et al presented a similar approach with easier imaging but more complicated iv injections where they used intravascular FITC-inulin clearance as a readout in a high-content zebrafish drug screening pipeline for automated imaging in the 96 well format.[44]

Taken together, here we have shown that podocyte depletion in zebrafish larvae is a versatile model that resembles the clinical and histological appearance of human FSGS in important characteristics such as proteinuria, development of edema, formation of viscero-parietal adhesions, PEC activation and -proliferation as well as deposition of extracellular matrix. Our results establish a basis not only for the use of the FSGS-like disease in zebrafish as a model for further studies investigating the pathogenesis of FSGS, but also for assessing the effects of potential drugs on disease development in a vertebrate model suitable for high-throughput experiments.

Additionally, we have found strong evidence, that the development of glomerular sclerotic lesions by the activation of proximal tubulus-like PECs is a conserved process that is present across vertebrate species.

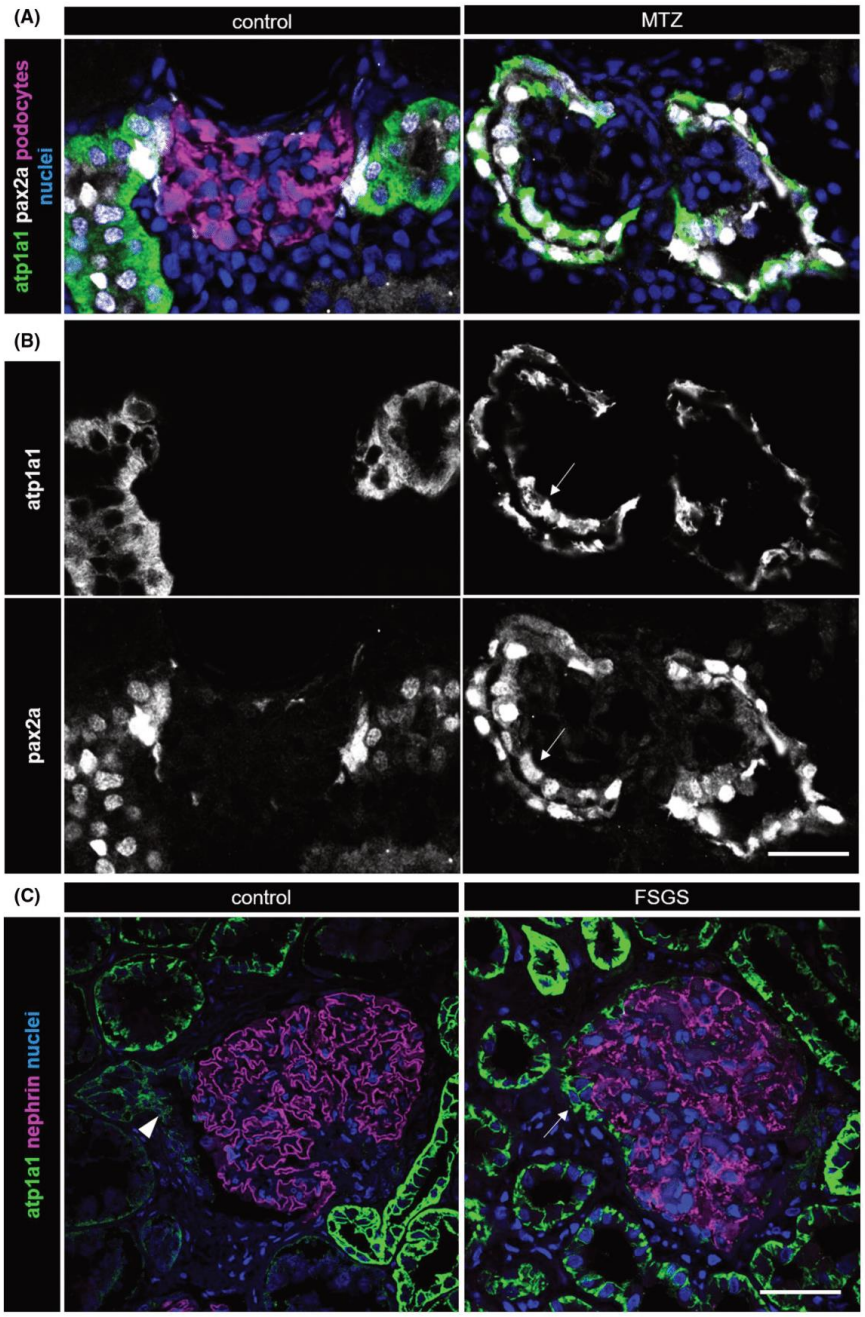

FIGURE 5 Co-expression of *atp1a1* and *pax2a* in proximal tubule cells of 9 dpf zebrafish larvae is shown in A. Panel B shows *atp1a1* expression and *pax2a* expression separately. It is limited to the proximal tubule in control larvae; whereas in podocyte-depleted larvae, it is also found in activated parietal epithelial cells and on the glomerular tuft (white arrows). The scale bar represents 20 µm. The micrographs in C exemplary show *atp1a1* expression in a human glomerulus under healthy conditions, where it is limited to the tubule (white arrowhead), and in a patient with FSGS. Notice *atp1a1* positivity of cells on the glomerular capillaries in FSGS, highlighted by the white arrow. *Nephrin* expression marks podocytes. The scale bar represents 50 µm

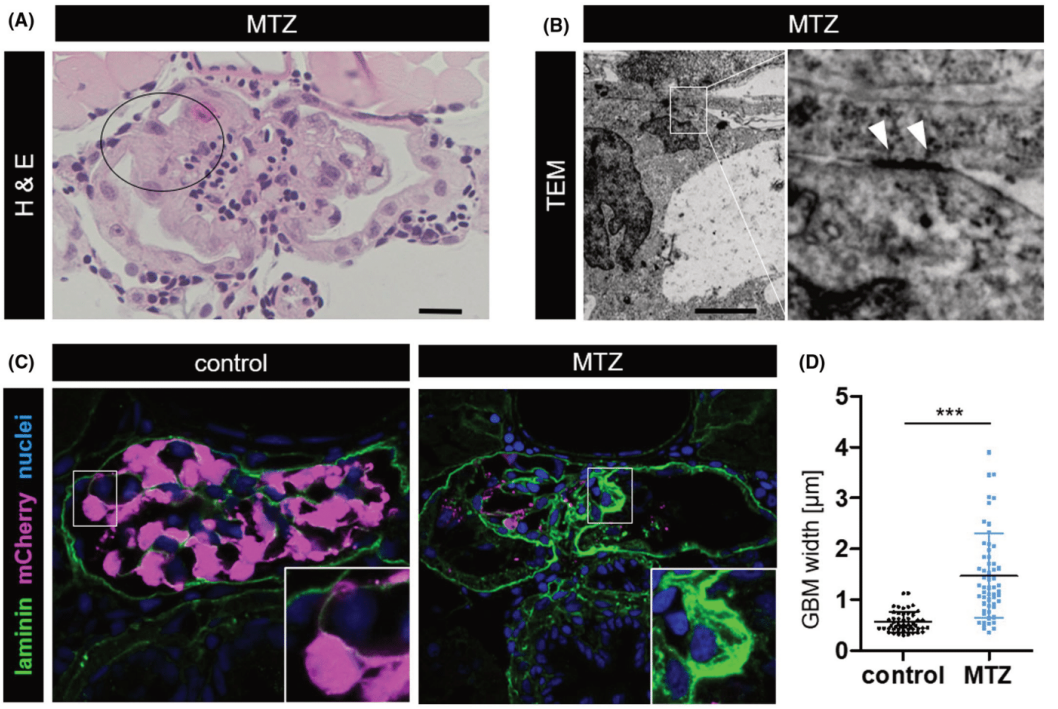

FIGURE 6 A, Parieto-visceral adhesion in an H&E-stained plastic section. Scale bar represents 10 µm. The transmission electron micrograph shown in picture B further characterizes one adhesion. Scale bar represents 2 µm. White arrowheads highlight local electron-dense parieto-visceral contacts in the magnification of B. C, Immunostaining for laminin in podocyte-depleted and control larvae at 9 dpf. A significant deposition of laminin on the glomerular tuft can be noticed as shown in the inserts. *mCherry* expression labels podocytes. The graph in D quantifies the thickness of the laminin-layer within the GBM measured orthogonally as the full width at half maximum. Podocyte-depleted larvae showed statistically significant increased laminin-deposition as measured in five randomly picked capillaries in each three consecutive glomerular cross-sections of n = 5 podocyte-depleted and n = 6 control larvae

ACKNOWLEDGMENTS

This work was supported by three scholarships of the Gerhard Domagk program of the University Medicine Greifswald to KH, FS, and SD and by a grant of the Federal Ministry of Education and Research (BMBF, grant 01GM1518B, STOP-FSGS) to NE This work was generously supported by the Südmeyer fund for kidney and vascular research ("Südmeyer-Stiftung für Nieren- und Gefäßforschung") and the Dr Gerhard Büchtemann fund, Hamburg, Germany. The authors thank Mandy Weise and Oliver Zabel for excellent technical assistance. Open access funding enabled and organized by Projekt DEAL. All authors declare no conflicts of interest.

AUTHOR CONTRIBUTIONS

K. Ursula Ingeborg Hansen, F. Siegerist, S. Daniel, M. Schindler, A. Iervolino, and A. Blumenthal established methods and performed experiments; K. Ursula Ingeborg Hansen, F. Siegerist, K. Endlich, and N. Endlich planned experiments, analyzed and interpreted data; W. Zhou established the transgenic lines used in the study; C. Daniel and K. Amann contributed selected human kidney biopsies of FSGS and control cases. All authors reviewed and approved the final version of the manuscript.

REFERENCES

1. Kriz W. Progressive renal failure—inability of podocytes to replicate and the consequences for development of glomerulosclerosis. *Nephrol Dial Transplant*. 1996;11:1738-1742.
2. D'Agati VD, Fogo AB, Bruijn JA, Jennette JC. Pathologic classification of focal segmental glomerulosclerosis. A working proposal. *Am J Kidney Dis*. 2004;43:368-382.
3. Kuppe C, Leuchtle K, Wagner A, et al. Novel parietal epithelial cell subpopulations contribute to focal segmental glomerulosclerosis and glomerular tip lesions. *Kidney Internat*. 2019;96:80-93.
4. Drummond IA. Kidney development and disease in the zebrafish. *J Amer Soc Nephrol*. 2005;16:299-304.
5. Siegerist F, Blumenthal A, Zhou W, Endlich K, Endlich N. Acute podocyte injury is not a stimulus for podocytes to migrate along

the glomerular basement membrane in zebrafish larvae. *Sci Rep*. 2017;7:43655. Accessed May 2017. https://www.nature.com/articles/srep43655.
6. Siegerist F, Zhou W, Endlich K, Endlich N. 4D in vivo imaging of glomerular barrier function in a zebrafish podocyte injury model. *Acta Physiol*. 220 2016;(1):167–173.
7. MacRae CA, Peterson RT. Zebrafish as tools for drug discovery. *Nat Rev Drug Discovery*. 2015;14:721-731.
8. Kramer-Zucker AG, Wiessner S, Jensen AM, Drummond IA. Organization of the pronephric filtration apparatus in zebrafish requires Nephrin, Podocin and the FERM domain protein Mosaic eyes. *Dev Biol*. 2005;285:316-329.
9. Hentschel DM, Mengel M, Boehme L, et al. Rapid screening of glomerular slit diaphragm integrity in larval zebrafish. *Am J Physiol Renal Physiol*. 2007;293:F1746-F1750.
10. Perner B, Englert C, Bollig F. The Wilms tumor genes wt1a and wt1b control different steps during formation of the zebrafish pronephros. *Dev Biol*. 2007;309:87-96.
11. Sun H, Al-Romaih KI, MacRae CA, Pollak MR. Human kidney disease-causing inf2 mutations perturb rho/dia signaling in the glomerulus. *EBioMedicine*. 2014;1:107-115.
12. Davison JM, Akitake CM, Goll MG, et al. Transactivation from Gal4-VP16 transgenic insertions for tissue-specific cell labeling and ablation in zebrafish. *Dev Biol*. 2007;304:811-824.
13. Asakawa K, Kawakami K. Targeted gene expression by the Gal4-UAS system in zebrafish. *Dev Growth Differ*. 2008;50:391-399.
14. Zhou W, Hildebrandt F. Inducible podocyte injury and proteinuria in transgenic zebrafish. *J Amer Soc Nephrol*. 2012;23:1039-1047.
15. Knox RJ, Friedlos F, Jarman M, Roberts JJ. A new cytotoxic, DNA interstrand crosslinking agent, 5-(aziridin-1-yl)-4-hydroxylamino-2-nitrobenzamide, is formed from 5-(aziridin-1-yl)-2,4-dinitrobenzamide (CB 1954) by a nitroreductase enzyme in Walker carcinoma cells. *Biochem Pharmacol*. 1988;37:4661-4669.
16. Miceli R, Kroeger P, Wingert R. Molecular mechanisms of podocyte development revealed by zebrafish kidney research. *Cell Develop Biol*. 2014;3:1–7.
17. Kriz W, Lemley KV. The role of the podocyte in glomerulosclerosis. *Curr Opin Nephrol Hypertens*. 1999;8:489-497.
18. Bertram JF, Douglas-Denton RN, Diouf B, Hughson MD, Hoy WE. Human nephron number. Implications for health and disease. *Pediatr Nephrol*. 2011;26:1529-1533.
19. Shankland SJ. The podocyte's response to injury. Role in proteinuria and glomerulosclerosis. *Kidney Int*. 2006;69:2131-2147.
20. Matsusaka T, Xin J, Niwa S, et al. Genetic engineering of glomerular sclerosis in the mouse via control of onset and severity of podocyte-specific injury. *J Amer Soc Nephrol*. 2005;16:1013-1023.
21. Macary G, Rossert J, Bruneval P, et al. Transgenic mice expressing nitroreductase gene under the control of the podocin promoter. A new murine model of inductible glomerular injury. *Virchows Archiv*. 2010;456:325-337.
22. Kim YH, Goyal M, Kurnit D, et al. Podocyte depletion and glomerulosclerosis have a direct relationship in the PAN-treated rat. *Kidney Int*. 2001;60:957-968.
23. Wharram BL, Goyal M, Wiggins JE, et al. Podocyte depletion causes glomerulosclerosis. Diphtheria toxin-induced podocyte depletion in rats expressing human diphtheria toxin receptor transgene. *J Amer Soc Nephrol*. 2005;16:2941-2952.
24. Pandey G, Westhoff JH, Schaefer F, Gehrig J. A smart imaging workflow for organ-specific screening in a cystic kidney zebrafish disease model. *Internat J Mol Sci*. 2019;20:1290.
25. Westhoff JH, Steenbergen PJ, Thomas LSV, Heigwer J, Bruckner T, Cooper L, Tönshoff B, Hoffmann GF, Gehrig J In vivo High-Content Screening in Zebrafish for Developmental Nephrotoxicity of Approved Drugs, *Frontiers in Cell and Developmental Biology*. (2020; 8: 1–15. http://dx.doi.org/10.3389/fcell.2020.00583.
26. McKee RA, Wingert RA. Zebrafish renal pathology. Emerging models of acute kidney injury. *Curr Pathobiol Rep*. 2015;3:171-181.
27. Kato Y, Tonomura Y, Hanafusa H, Nishimura K, Fukushima T, Ueno M. Adult zebrafish model for screening drug-induced kidney injury. *Toxicol Sci*. 2020;174:241-253.
28. Kriz W, Lemley KV. A potential role for mechanical forces in the detachment of podocytes and the progression of CKD. *J Amer Soc Nephrol*. 2015;26:258-269.
29. Endlich K, Kliewe F, Endlich N. Stressed podocytes-mechanical forces, sensors, signaling and response. *Pflugers Arch*. 2017;469:937-949.
30. Kriz W, Hähnel B, Hosser H, Rösener S, Waldherr R. Structural analysis of how podocytes detach from the glomerular basement membrane under hypertrophic stress. *Front Endocrinol*. 2014;5:207.
31. Neal CR, Crook H, Bell E, Harper SJ, Bates DO. Three-dimensional reconstruction of glomeruli by electron microscopy reveals a distinct restrictive urinary subpodocyte space. *J Amer Soc Nephrol*. 2005;16:1223-1235.
32. Smeets B, Te Loeke NAJM, Dijkman HBPM, et al. The parietal epithelial cell. A key player in the pathogenesis of focal segmental glomerulosclerosis in Thy-1.1 transgenic mice. *J Amer Soc Nephrol*. 2004;15:928-939.
33. Holderied A, Romoli S, Eberhard J, et al. Glomerular parietal epithelial cell activation induces collagen secretion and thickening of Bowman's capsule in diabetes. *Lab Invest*. 2015;95:273-282.
34. Ohtaka A, Ootaka T, Sato H, et al. Significance of early phenotypic change of glomerular podocytes detected by Pax2 in primary focal segmental glomerulosclerosis. *Am J Kidney Dis*. 2002;39:475-485.
35. Dijkman H, Smeets B, van der Laak J, Steenbergen E, Wetzels J. The parietal epithelial cell is crucially involved in human idiopathic focal segmental glomerulosclerosis. *Kidney Int*. 2005;68:1562-1572.
36. Suzuki T, Matsusaka T, Nakayama M, et al. Genetic podocyte lineage reveals progressive podocytopenia with parietal cell hyperplasia in a murine model of cellular/collapsing focal segmental glomerulosclerosis. *Amer J Pathol*. 2009;174:1675-1682.
37. Appel D, Kershaw DB, Smeets B, et al. Recruitment of podocytes from glomerular parietal epithelial cells. *J Amer Soc Nephrol*. 2009;20:333-343.
38. Eng DG, Sunseri MW, Kaverina NV, Roeder SS, Pippin JW, Shankland SJ. Glomerular parietal epithelial cells contribute to adult podocyte regeneration in experimental focal segmental glomerulosclerosis. *Kidney Int*. 2015;88:999-1012.
39. Nagata M. Podocyte injury and its consequences. *Kidney Int*. 2016;89:1221-1230.
40. Romoli S, Angelotti ML, Antonelli G, et al. CXCL12 blockade preferentially regenerates lost podocytes in cortical nephrons by targeting an intrinsic podocyte-progenitor feedback mechanism. *Kidney Int*. 2018;94:1111-1126.

41. Kuppe C, Gröne H-J, Ostendorf T, et al. Common histological patterns in glomerular epithelial cells in secondary focal segmental glomerulosclerosis. *Kidney Int*. 2015;88:990-998.
42. Yin C, Evason KJ, Maher JJ, Stainier DYR. The basic helix-loop-helix transcription factor, heart and neural crest derivatives expressed transcript 2, marks hepatic stellate cells in zebrafish. Analysis of stellate cell entry into the developing liver. *Hepatology*. 2012;56:1958-1970.
43. Poss KD, Wilson LG, Keating MT. Heart regeneration in zebrafish. *Science*. 2002;298:2188-2190.
44. Steenbergen PJ, Heigwer J, Pandey G, Tönshoff B, Gehrig J, Westhoff JH. A multiparametric assay platform for simultaneous in vivo assessment of pronephric morphology, renal function and heart rate in larval zebrafish. *Cells*. 2020;9:1269.

SUPPORTING INFORMATION

Additional supporting information may be found online in the Supporting Information section.

How to cite this article: Ursula Ingeborg Hansen K, Siegerist F, Daniel S, et al. Prolonged podocyte depletion in larval zebrafish resembles mammalian focal and segmental glomerulosclerosis. *The FASEB Journal*. 2020;34:15961–15974. https://doi.org/10.1096/fj.202000724R

Publication III

A novel high-content screening assay identified belinostat to be protective in a FSGS-like zebrafish model

Manuscript submitted to the Journal of the American Society of Nephrology for peer-review

Maximilian Schindler, Florian Siegerist, Tim Lange, Sophia-Marie Bach, Jochen Gehrig, Sheraz Gul, Nicole Endlich

JASN® Journal of the American Society of Nephrology

A novel high-content screening assay identified belinostat to be protective in a FSGS-like zebrafish model

Journal:	*Journal of the American Society of Nephrology*
Manuscript ID	JASN-2022-07-0760
Manuscript Type:	Original Article - Basic Research
Date Submitted by the Author:	05-Jul-2022
Complete List of Authors:	Schindler, Maximilian; University Medicine Greifswald, Anatomy and Cell Biology Siegerist, Florian; University Medicine Greifswald, Anatomy and Cell Biology Lange, Tim; University Medicine Greifswald, Anatomy and Cell Biology Bach, Sophia-Marie; University Medicine Greifswald, Anatomy and Cell Biology Gehrig, Jochen; Acquifer Imaging GmbH Gul, Sheraz; Fraunhofer Institute for Translational Medicine and Pharmacology ITMP Endlich, Nicole; University of Greifswald, Department of Anatomy and Cell Biology
Keywords:	cell ablation, chronic kidney disease, drug metabolism, focal segmental glomerulosclerosis, glomerular disease, glomerulosclerosis, podocyte, proteinuria
Note: The following files were submitted by the author for peer review, but cannot be converted to PDF. You must view these files (e.g. movies) online.	
Movie 1 - Segmentation Process Vasculature.mp4 Movie 2 - DMSO 24 h.mp4 Movie 3 - MTZ 24 h.mp4	

Authors: Schindler, Maximilian; Siegerist, Florian; Lange, Tim; Bach, Sophia-Marie; Gehrig, Jochen; Gul, Sheraz; Endlich, Nicole

Title: A novel high-content screening assay identified belinostat to be protective in a FSGS-like zebrafish model

Running title: High-content FSGS drug screening

Manuscript Type: Original Article - Basic Research

Manuscript Category: CUST_BASIC_RESEARCH_CATEGORY :No data available.

Funders: Bundesministerium fÃ¼r Bildung und Forschung, (Grant / Award Number: '01GM1518B, STOPâ€FSGS')
Bundesministerium fÃ¼r Wirtschaft und Energie, (Grant / Award Number: '16KN077229')

Financial Disclosure: CUST_FINANCIAL_DISCLOSURE :No data available. The authors have nothing to disclose.

Study Group/Organization Name: CUST_STUDY_GROUP/ORGANIZATION_NAME :No data available.

Study Group Members' Names: CUST_STUDY_GROUP_MEMBERS :No data available.

Total number of words: 3344

Abstract: Focal and segmental glomerulosclerosis (FSGS) often leads to end-stage kidney disease. Herein, the complex 3D morphology of podocytes is affected resulting in loss of the size selectivity of the filtration barrier and development of irreversible sclerotic lesions. Until today, therapeutic options are limited and podocyte-specific drugs are missing. Therefore, identification of compounds and drugs, especially FDA-approved ones that can delay or stop the progression of FSGS is of great importance. To achieve this, we established a high-content screening assay by using a FSGS-like zebrafish model. In order to combine a high-throughput with an in vivo model, a specific zebrafish screening strain (â€œScreeFiâ€) was used in this study. The ScreeFi strain expresses the nitroreductase and mCherry exclusively in podocytes. Additional expression of a circulating 78 kDa vitamin-D-binding eGFP fusion protein provides a readout for proteinuria. Addition of 80 ÂµM metronidazole for 24 hours into the fish water resulted in FSGS-like lesions. A specific screening microscope was used together with custom written analysis codes to quantify fluorescence intensities on a large scale. A 138 compound drug library was screened for podocyte-protective effects and candidates were validated by follow-up experiments (n=280 larvae per hit). Using this novel in vivo high-content drug screening, we identified 7 hits that were potentially protective in our FSGS-like model. Validation of these candidates identified the FDA-approved drug belinostat as a protective drug against podocyte injury, proteinuria and edema formation. Belinostat was identified in this novel high-content screening as a promising drug for the treatment of FSGS.

Significance statement

This work presents a novel *in vivo* high-content assay for the screening of protective, mainly FDA-approved drugs/compounds in a specific zebrafish larval FSGS model which uses an automated analysis to obtain a high number of candidates. With this screening system, we identified the FDA-approved drug belinostat as a potential candidate to prevent disease progression of FSGS. As a repurposed drug, belinostat has a short road to a clinical translation.

A novel high-content screening assay identified belinostat to be protective in a FSGS-like zebrafish model

Maximilian Schindler[1], Florian Siegerist[1], Tim Lange[1], Sophia-Marie Bach[1], Jochen Gehrig[2], Sheraz Gul[3, 4], Nicole Endlich[1]

[1]Department of Anatomy and Cell Biology, University Medicine Greifswald, Greifswald, Germany

[2]Acquifer Imaging GmbH, Heidelberg, Germany

[3]Fraunhofer Institute for Translational Medicine and Pharmacology ITMP, Hamburg, Germany

[4]Fraunhofer Cluster of Excellence for Immune-Mediated Diseases CIMD, 22525 Hamburg, Germany

Running title: High-content FSGS drug screening

Word count abstract: 248

Word count text: 3344

*Corresponding author: nicole.endlich@uni-greifswald.de

Orcid-ID: 0000-0001-6817-4099

Keywords: podocyte, FSGS, proteinuria, drug screening, FDA-approved, zebrafish

Significance statement

This work presents a novel *in vivo* high-content assay for the screening of protective, mainly FDA-approved drugs/compounds in a specific zebrafish larval FSGS model which uses an automated analysis to obtain a high number of candidates. With this screening system, we identified the FDA-approved drug belinostat as a potential candidate to prevent disease progression of FSGS. As a repurposed drug, belinostat has a short road to a clinical translation.

Abstract

Background: Focal and segmental glomerulosclerosis (FSGS) often leads to end-stage kidney disease. Herein, the complex 3D morphology of podocytes is affected resulting in loss of the size selectivity of the filtration barrier and development of irreversible sclerotic lesions. Until today, therapeutic options are limited and podocyte-specific drugs are missing. Therefore, identification of compounds and drugs, especially FDA-approved ones that can delay or stop the progression of FSGS is of great importance. To achieve this, we established a high-content screening assay by using a FSGS-like zebrafish model.

Methods: In order to combine a high-throughput with an *in vivo* model, a specific zebrafish screening strain ("*ScreeFi*") was used in this study. The *ScreeFi* strain expresses the nitroreductase and mCherry exclusively in podocytes. Additional expression of a circulating 78 kDa vitamin-D-binding eGFP fusion protein provides a readout for proteinuria. Addition of 80 µM metronidazole for 24 hours into the fish water resulted in FSGS-like lesions. A specific screening microscope was used together with custom written analysis codes to quantify fluorescence intensities on a large scale. A 138 compound drug library was screened for podocyte-protective effects and candidates were validated by follow-up experiments (n=280 larvae per hit).

Results: Using this novel *in vivo* high-content drug screening, we identified 7 hits that were potentially protective in our FSGS-like model. Validation of these candidates identified the FDA-approved drug belinostat as a protective drug against podocyte injury, proteinuria and edema formation.

Conclusion: Belinostat was identified in this novel high-content screening as a promising drug for the treatment of FSGS.

Introduction

In more than 75% of kidney patients, podocytes are damaged and lost.[1] Podocytes as a postmitotic cell type, are attached to the outer aspect of the glomerular capillaries with their interdigitating foot processes. Their complex morphology together with the slit membrane between these interdigitating foot processes are essential for the size-selectivity of the glomerular filtration barrier.[2,3] Any changes of the foot process morphology are directly linked with a change of function.

Focal and segmental glomerulosclerosis (FSGS) is defined by foot process effacement, a loss of podocytes, a development of sclerotic lesions as well as glomerular matrix accumulation.[4–6] Until now, therapeutic options for patients suffering from FSGS are very limited and often progressive loss of kidney function cannot be prevented.[7,8] This lack leads to a high demand for drugs that stop or delay FSGS progression.

A promising approach to identify compounds or drugs that achieve this goal are large scale drug screenings. Unfortunately, on the one hand, cell culture-based systems cannot fully provide physiologically relevant conditions such as blood pressure and cellular crosstalk. On the other hand, reproduction time and ethical concerns of mammalian models are limiting factors in high-throughput screening. Therefore, we focused our attention to a simple vertebrate model, the zebrafish larva (*Danio rerio*).

The zebrafish larva is a widely used vertebrate model to study kidney development, function and disease.[9–11] The remarkable homology of the pronephric glomerulus to mammalian glomeruli with a fenestrated endothelium, a glomerular basement

membrane and podocytes with interdigitating foot processes makes this model suitable especially for glomerular research.[12–15] Moreover, optical transparency, a high fecundity and a rapid *ex utero* development provide decisive advantages in contrast to mammalian models in terms of microscopic access and experimental throughput. Zebrafish larvae represent an elegant bridge between cell culture, *C. elegans*, *Drosophila melanogaster* and mammals.[16–19]

Drug screening that target a specific cell type or aim to prevent a certain disease are heavily dependent on a reliable injury or disease model. Induction of FSGS-like lesions in mammals can be carried out by several approaches which mostly include injection e.g. puromycin aminonucleoside (PAN).[20,21] However, injection-based approaches are not suitable for high-content screening. To overcome this, we have focused on the cell specific ablation using the nitroreductase/metronidazole (NTR/MTZ) system which is an elegant way to avoid side effects.[22,23] Our group recently established a protocol to induce FSGS-like lesions in zebrafish larvae using this method.[24] Moreover, crossbreeding of the podocyte-specific MTZ-sensitive zebrafish strain with a strain that expresses a circulating vitamin-D-binding eGFP fusion protein (VDP-eGFP, 78 kDa) generates a “screening fish” (*ScreeFi*) that is perfectly equipped for an imaging-based, high-throughput drug screening on a reliable FSGS model.[25] Podocyte specific injury in this *ScreeFi* induces podocyte depletion and results in a loss of glomerular mCherry fluorescence as well as a subsequent glomerular leakage of VDP-eGFP, causing a decrease in vascular eGFP fluorescence.[24,26]

Automated data analysis is crucial for high-content, imaging-based screening. The assessment of vascular eGFP fluorescence requires a reliable, automated

segmentation of blood vessels in order to measure the fluorescence exclusively in the vasculature. The same is true for an automated measurement of the mCherry fluorescence exclusively in podocytes. The open source image processing software FIJI provides outstanding possibilities for such a task.[27] Since stable and vibration-free imaging is an essential prerequisite for exact fluorescence intensity measurements, we used a specific imaging machine (IM) which was developed for *in vivo* screening in the multiwell format equipped with a static microscopic stage and moving objectives.[28,29]

In the past, epigenetic changes have been shown to play an important role in kidney cell biology and disease.[30,31] It is notable that histone deacetylases (HDACs) seem to play a pivotal role in kidney injury and are an interesting pharmacological target in podocytes.[32,33] Although HDACs regulate inflammatory processes and autophagy in podocytes,[34] little is known about the effects of epigenetic drugs in FSGS. Therefore, we used a drug/compound library including epigenetic drugs/compounds in this screening exercise. To accelerate the translation of an identified drug into the clinic and treatment of patients, our library included FDA-approved drugs.

To summarize, our group developed a rapid and semi-automated *in vivo* high-content drug screening assay that quantifies podocyte fluorescence and integrity of the glomerular filtration barrier in a FSGS-like zebrafish model. Using a 138 drug/ compound library and a subsequent validation of candidates, the FDA-approved drug belinostat was identified as a potential drug for the treatment of FSGS. Belinostat is already used for treatment of patients with T-cell lymphoma and therefore a translation of belinostat into renal therapy could be substantially accelerated.

Methods

Zebrafish strains and husbandry

Zebrafish stocks were maintained as previously described.[17] Several groups of two males and two females were permanently put together as mating pairs for the screening experiments. These groups were always composed of two individuals of the following zebrafish strains: Tg(*-3.5fabp10a:gc-eGFP*); *mitfa*$^{w2/w2}$; *mpv17*$^{a9/a9}$, Tg(*-3.5fabp10a:gc-eGFP*);Tg(*nphs2:GAL4-VP16*); Tg(*UAS:Eco.nfsB-mCherry*); *mitfa*$^{w2/w2}$; *mpv17*$^{a9/a9}$, further termed *ScreeFi.*[22,25,26] Larvae from these groups were raised under standard conditions until 4 days post fertilization (dpf) and transgene expression was checked with a fluorescence stereomicroscope (SMZ 18 Nikon, Düsseldorf, Germany) exposed to 0.1 mg/ml tricaine anesthesia (MS-222, #E10521, Merck, Darmstadt, Germany). All experiments are according to the German animal protection law and were overseen and approved (file #7221.3-1-06/21) by the "Landesamt für Landwirtschaft, Lebensmittelsicherheit und Fischerei, Rostock" (LALLF M-V) of the federal state of Mecklenburg-Western Pomerania.

Induction of podocyte injury and drug treatment

Groups of 12 larvae from one breeding were distributed into a 24-well plate (#662160 Greiner, Frickenhausen, Germany). For each clutch of eggs, 12 larvae were treated with 0.2% v/v DMSO (Sigma-Aldrich, Taufkirchen, Germany) dissolved in E3 as negative control and 12 larvae were treated with 80 µM metronidazole (MTZ; Sigma-Aldrich) dissolved in DMSO as our injury control and reference group. A custom drug library

including epigenetic and FDA-approved drugs was designed and purchased from Enzo Life Sciences, Inc. (Lausen, Switzerland) and was used for the screening experiments. The compounds were structurally diverse and reported to possess epigenetic modifying properties in biochemical and cell-based assays with the strongest link with HDAC and Sirtuin enzyme target class. Larvae were co-treated with 80 µM MTZ and 100 µM compounds each in 0.2% v/v DMSO. The total volume was 400 µl for each well with 12 larvae and the wells were sealed with Adhesive Clear PCR Seal (#600208, Biozym Scientific, Hessisch-Oldendorf) to prevent evaporation. The plates were incubated at 28.5°C and protected from light. After 24 hours, the compounds were washed three times with 0.5x E3.

Preparation for imaging

After washout at 5 dpf, E3 in the 12-well plate was replaced with E3-containing 0.4 mg/ml tricaine solution. Larvae were individually transferred into the wells of a 96-well plate (#644101, Greiner) which was prepared with custom agarose molds. For the molds, 45 µl of 0.7% agarose (Biozym LE agarose) were transferred into each well and a custom 3D-printed orientation tool was inserted into the agarose.[35] Each larva was transferred into the single wells of the 96-well plate and oriented laterally in the molds.

Image acquisition for the screening was performed with an Acquifer Imaging Machine (IM; ACQUIFER Imaging, Heidelberg, Germany). This high-content screening device is equipped with a sCMOS (2048 x 2048 pixels) camera and a temperature-controlled incubation chamber (set to 28.5 °C). Overview images of each laterally oriented larva were obtained with a 2x objective. For each larva, a region of interest (ROI) at the tail region caudal of the cloaca was selected with a 10x objective in order to image the

blood flow and vasculature. After creating custom modified imaging scripts via FIJI,[27] 10 consecutive brightfield frames at a framerate of 13 Hz were acquired (10x objective), followed by one frame at 470 nm. The ROI of each larva was dragged to the glomerular region and one frame of each glomerulus was acquired at 555 nm using a 10x objective. The focal plane for both acquisitions was detected with a built-in two-step software autofocus.

Following image acquisition, tricaine-containing E3 was washed out two times and replaced by 150 µl E3. The 96-well plate was again sealed and incubated for another 24 hours at 28.5°C. At 6 dpf, larvae were anesthetized with 0.4 mg tricaine, oriented laterally and imaged in the same way as described before. Two values for the vascular eGFP fluorescence and two values for the glomerular mCherry fluorescence were taken for each individual larva.

Data storage and processing

Since acquisition and subsequent automated analysis of >70000 images of zebrafish larvae requires large storage and random access memory, a HIVE (ACQUIFER Imaging) was used for storage and processing. Custom written FIJI macros were written in the IJ1 language and used for image analysis. The macros were written in such a way that a full folder of raw image data of one 96-well plate could be dragged into and directly processed by FIJI.

Measurement of the vascular fluorescence, an indicator for proteinuria

Vascular eGFP fluorescence was segmented and measured fully automatic via a custom FIJI macro, similar to Steenbergen and colleagues.[36] For each larva, 10

brightfield slices and one slice at 470 nm were acquired at the caudal region. The macro fuses the brightfield slices to a short movie in which the blood flow is clearly observable due to the movement of erythrocytes. After blurring and background subtraction, the standard deviation of this movie is created. This standard deviation shows all areas in which pixel changes occur which are circulating erythrocytes. Subsequent thresholding and size restriction allow the creation of ROIs which distinctively detect areas of blood flow. These ROIs are then used as segmentation masks for the 470 nm image in which the mean fluorescence is measured exclusively in the blood vessels due to prior blood flow detection.

Glomerular fluorescence determines the degree of podocyte depletion

Fluorescence of the *nphs2*-driven podocyte mCherry was detected and measured fully automatically via FIJI. For each larva and each image obtained with 555 nm channel, the center of mass (x and y coordinate of the brightness-weighted average of all pixel) is determined which is in this case the center of the pronephric glomerulus. A circular custom ROI is created and gets automatically drawn to the center. The ROI for the mCherry signal is always of the same size (70688 pixels with 0.65 µm/pixel ratio) and the mean fluorescence intensity in this ROI is measured for each larva and both timepoints.

Generation of time-lapse movies

For Movie 1 and 2, *ScreeFi* larvae were treated with either 0.1% DMSO v/v or 80 µM MTZ for 24 hours from 4 to 5 dpf. After washout, larvae were dorsally oriented and embedded in 20 µl 0.6% agarose in the mold with E3 medium containing 0.1 mg/ml

tricaine. After acquisition of overview images in the 555 nm with the 2x objective, ROIs were placed at the glomerular mCherry signal with the 4x objective in the IM. The eGFP and the mCherry signal were imaged once in an hour from 5 to 6 dpf and the focus plane detection was determined in the 555 nm channel. Processing of two-channel multi page TIFs and movie creation was conducted with FIJI.

Data analysis and statistics

Both macros create excel files with all necessary data. The macro for the vascular fluorescence additionally creates a subfolder with images of the segmentation masks to check the segmentation process. By a build-in exclusion algorithm, larvae in which no vascular blood flow is detected, are not analyzed and values of these larvae will not appear in the excel files but in a text file. Values from these larvae were then also excluded from the excel files of the glomerular measurement.

For both readouts and each larva, one mean fluorescence value is determined at 5 dpf after the treatment and at 6 dpf. The ratio of vascular fluorescence to glomerular fluorescence was calculated for each larva and Gaussian distribution was checked with a Kolmogorov-Smirnov test for each readout and each plate. Ratios of treatment groups were subsequently analyzed by either one-way ANOVA followed by a Dunnet´s multiple comparison test or by a Kruskal-Wallis test followed by Dunn's multiple comparison. The MTZ group on every plate served as a control group, $p < 0.05$ was considered as statistically significant. Data analysis and graphs were created with GraphPad Prism 9.1.2 (GraphPad Software, San Diego, California USA). Volcano plots were created using VolcaNoseR (DOI: 10.1101/2020.05.07.082263).

Results

Establishment of larval imaging and signal analysis

In order to cover two central aspects for the integrity of the larval glomerular filtration barrier, we used the Tg(*-3.5fabp10a:gc-eGFP*); Tg(*nphs2:GAL4-VP16*); Tg(*UAS:Eco.nfsB-mCherry*); *mitfa*$^{w2/w2}$; *mpv17*$^{a9/a9}$ – the *ScreeFi* strain for all screening experiments. This strain expresses a circulating fusion protein of the vitamin D-binding protein with eGFP (VDP-eGFP) which has a size of 78 kDa and is unable to pass the glomerular filtration barrier under healthy conditions. Impairment of the glomerular filtration barrier directly results in clearance of VDP-eGFP from the vasculature and can be used as a surrogate parameter for proteinuria. Additionally, podocyte-specific expression of mCherry and the bacterial NTR allows direct *in vivo* microscopic assessment of the presence of healthy or injured podocytes.[26]

We found that lateral orientation of the larvae provides a suitable field of view for the IM for both readouts, the vascular eGFP fluorescence as an indicator for proteinuria at the tail region and the podocyte mCherry signal as an ideal indicator for podocyte depletion. Custom agarose molds were used for this purpose, allowing rapid lateral orientation of 96 larvae per plate.

To determine the vascular eGFP fluorescence, a ROI for each larva in the 96-well plate was selected on an overview image (Fig. 1A, B). We were able to reliably and automatically segment the vasculature in zebrafish larvae via FIJI by using the standard deviation of the pixel change (highest in vasculature with moving blood cells, Fig. 1C,

Movie 1). Moreover, the custom written FIJI script also excludes larvae from analysis which showed no blood flow in the caudal vasculature (Fig. S1). This ensures that only viable larvae are included in the evaluation.

For automated detection of the mCherry signal in podocytes, a different approach was developed. Since segmentation in the brightfield channel was not possible due to a lack of contrast or pixel value change in the target structure, we directly used the mCherry fluorescence image as detection template. This enables an automatic and reliable detection of the podocytes and the measurement of the mean fluorescence intensity in a defined area (Fig. 1D).

Generation of an experimental screening and imaging pipeline

As expression levels of transgenic reporters may vary between clutches of embryos from different founders, heterogeneity may increase in datasets obtained over several weeks. To circumvent this, the workflow of this new assay obtains two measurements of the two readouts for each larva, one at 5 dpf and one at 6 dpf. This generated robust fluorescence ratios for the degree of proteinuria and podocyte condition (Fig. 2).

Titration of the podocyte specific injury for the screening

After the addition of MTZ to the larval medium, the podocyte-specific NTR converts the prodrug MTZ into a toxin which exclusively damages podocytes. The degree of injury is dependent on the concentration and exposure time of MTZ.[22] Since our previous work has shown that a treatment of transgenic larvae at 4 dpf with 80 µM MTZ for 48 hours resulted in a phenotype that resembles FSGS,[24] we had to recalibrate the MTZ concentration in the *ScreeFi* to avoid feeding of the larvae in the multiwell plates.

Zebrafish larvae start feeding at 6 dpf[37] and our aim was to avoid treatment with MTZ and compounds in the agarose cavities of the 96-well plates to exclude the influence of agarose on MTZ and compounds. For his reason, 6 dpf had to be the endpoint and the time of the second measurement.

Therefore, larvae were treated with different concentrations of MTZ (80 µM, 160 µM and 320 µM) for 24 hours. After washout at 5 dpf, no difference of the mCherry fluorescence intensity was found between the control (0.1% v/v DMSO) and the 80 µM group in contrast to the treatment with 160 µM and 320 µM MTZ which resulted in a strong podocyte depletion (Fig. 3A). Imaging of the same larvae after further 24 hours revealed a loss of mCherry fluorescence in the 80 µM MTZ group. MTZ-induced glomerular injury in the 160 µM and 320 µM group lead to a further reduction of mCherry signal intensities, close to a complete loss of podocytes (Fig. 3A).

Podocyte injury or loss leads to proteinuria, in the case of our *ScreeFi* to a quantifiable leakage of the VDP-eGFP. After washout of MTZ at 5 dpf, the eGFP signal was not reduced in the 80 µM MTZ group. In contrast, a treatment with 160 µM and 320 µM MTZ for 24 hours caused a reduction of the vascular eGFP signal and a visible uptake of eGFP in the proximal convoluted tubules indicating a leakage of the filtration barrier (Fig. 3B).

At 6 dpf, a clear vascular loss and tubular uptake of the VDP-eGFP was detected in 80 µM MTZ treated larvae compared to the DMSO control. Glomerular leakage in the 160 µM MTZ and 320 µM MTZ group progressed to a state in which a clear vascular signal could not be detected anymore (Fig. 3B).

Edema formation is a hallmark of a disrupted filtration barrier in zebrafish (Huang et al. 2013). Exposure of larvae to 80 µM MTZ for 24 hours from 4-5 dpf induced no edema formation at 5 dpf, but a slight edema formation at 6 dpf. Slight edema was visible after treatment with 160 µM at 5 dpf which progressed to severe edema at 6 dpf. Larvae treated with 320 µM MTZ developed severe edema at 5 dpf which progressed until 6 dpf (Fig. 3C).

A significant loss of glomerular mCherry and vascular eGFP was detected in all three MTZ treatment groups by our assay from 5 to 6 dpf. Treatment with 80 µM MTZ for 24 hours resulted in a quantifiable proteinuric phenotype and podocyte depletion in the time frame of our screening setup and will therefore be used for all further experiments (Fig. 3D).

Screening of a drug library

After establishing a workflow and degree of injury, a drug library of 138 mainly epigenetic drugs/compounds was used to identify drugs that potentially impede or prevent podocyte damage and the resulting proteinuria. Out of 138 compounds, 5 compounds were able to significantly attenuate the loss of vascular eGFP compared to the corresponding MTZ control (Fig. 4).

Two compounds induced an elevated loss of eGFP together with MTZ in comparison to MTZ only. A significant reduction of podocyte depletion was observed with 4 compounds. A total of 36 compounds had a lethal effect on zebrafish larvae within the 24 hours treatment (from 4 to 5 dpf; Table 1).

Follow-up experiments of primary screening hits

The two compounds santacruzamate A and cambinol showed a protective effect in both readouts, a reduction of proteinuria and a deceleration of podocyte depletion. These were the most promising candidates for further verification experiments with a higher larvae count. As a follow-up, three additional 96-well plates were analyzed with each 12 larvae DMSO, 12 larvae compound only, 36 larvae MTZ only and 36 larvae with compound santacruzamate A or cambinol plus MTZ. These results showed that the protective effect of santacruzamate A on podocytes could not be confirmed (Fig. 5A, B). The initial protective effect of cambinol was also excluded in the verification experiments (Fig. 5C, D).

Follow-up experiments of secondary screening hits

Verification experiments were also performed on compounds that had a protective effect only in one of the two readouts, meaning either a decrease of proteinuria or a reduction of podocyte depletion. Of the total 7 substances, belinostat showed a significant reduction of proteinuria and podocyte depletion in the follow-up experiments (Fig. 6A, B).

Verification of belinostat as a protective agent

To further confirm these results, a serial dilution of belinostat was started. We observed that the treatment of larvae for 48 hours with MTZ induced edema formation of four different severity levels, scaling from type 1 = no edema to type 4 = severe edema formation (Fig. 6C). We categorized the severity level of the DMSO group, MTZ and MTZ plus 1 µM, 10 µM or 100 µM belinostat at 6, 7 and 8 dpf. After washout at 6 dpf, all

three treatment groups with MTZ + belinostat showed a reduced number of larvae with type 3 and 4 edema in a dose-dependent manner. Co-treatment with MTZ and 100 μM belinostat induced edema formation in 15% of larvae with 0% type 4 edema in contrast to 60% edema with 31% type 4 edema in the MTZ group at 6 dpf. At 7 dpf, progression of edema formation was decelerated in all three groups for all three types of edema that received belinostat, again in a dose-dependent manner. The delay in edema formation in the belinostat groups stayed consistent at 8 dpf. 83.6% of larvae treated with MTZ developed edema with 58.2% showing type 4 edema. Co-treatment of MTZ with 100 μM belinostat caused edema formation in 64.2% of larvae with 28.3% type 4 edema (Fig. 6D). These results clearly confirmed the protective effect of belinostat in a dose-dependent manner on larval podocytes in this injury model.

Discussion

FSGS is a podocyte-related disease characterized by effacement and detachment of podocytes, activated PECs as well as glomerular matrix accumulation.[38] Since there are no curative drugs available until today, it is very important to identify appropriate small molecules and drugs that have the capacity to inhibit or reverse podocyte injury in FSGS patients.

For efficient identification of potential drugs, high-content screenings are an important tool. For this purpose, genetically modified zebrafish larvae are an ideal model to establish an appropriate screening platform, similar to what has recently been shown for therapeutics against neurodegenerative disorders such as Parkinson's disease.[39] Here, we present for the first time a high-content screening method using a podocyte-specific ablation system which was established by our group as a model for FSGS.[24] After implementing automated segmentation and measurement algorithms to quantify fluorescence in vessels and of podocytes, it was possible to quantify whether podocytes and the filtration barrier were healthy or affected on a large scale. An important requirement of an automated zebrafish larvae screening is that the position of the larvae remains stable during the image acquisition procedure. Otherwise changes of the fluorescence intensities or segmentation problems could be due to a different position of the larvae. To avoid this, a specific screening microscope was used with moving optics in contrast to a mobile stage to ensure that the multiwell plate did not move during imaging. This was recently demonstrated by Westhoff and colleagues in a morphometric screen for developmental nephrotoxicity.[28]

One important aim of our current work was to shorten the treatment period established for the FSGS-like zebrafish model in our high-content screening from 48 hours to 24 hours to avoid feeding of hundreds of isolated larvae in 96-well plates beyond 6 dpf.[37] For this reason, we started experiments with different MTZ concentrations for a shorter duration to find a concentration that induces podocyte depletion and proteinuria. We found that treatment with 80 µM MTZ for 24 hours successfully depleted podocytes and significantly reduced vascular and podocyte fluorescence. Doses beyond 80 µM induced a very strong phenotype within 24 hours including a complete loss of podocytes which barely resembles mammalian FSGS. For this reason, we used 80 µM MTZ for all following experiments.

In our experiments, we used a library including epigenetic drugs/compounds for the screening. There is strong evidence that epigenetic modifications in podocytes might contribute to injury susceptibility or resilience.[40–43] Majumder and colleagues reported that an elevated level of histone H3 lysine 27 trimethylation protects against glomerular and specifically podocyte injury.[44] First results in our screening suggested that santacruzamate A, a HDAC 2 inhibitor and cambinol, a class III histone deacetylase inhibitor, are protective in our FSGS-like zebrafish model. However, the subsequent validation in following experiments did not confirm the initial results and therefore these drugs were excluded.

A third candidate which was suggested to be protective for podocytes was the FDA-approved drug belinostat. Belinostat is described to be a broad-acting histone deacetylase inhibitor that promotes apoptosis and inhibits proliferation of cancer cells.[45–47] Validation experiments with 280 larvae confirmed the protective effect of belinostat in

this assay. Moreover, we could show that the effect of belinostat on larval podocytes that were treated with MTZ over 48 hours instead of 24 hours is protective in a dose-dependent manner. Interestingly, Belinostat is FDA-approved and is currently used to treat patients suffering from peripheral T-cell lymphoma. It is reported to promote differentiation of rhabdomyosarcoma cells which contributes to its tumor suppressive effect.[48] However, there is no evidence in the literature indicating a protective effect of belinostat or its metabolites on podocyte-related diseases or kidney diseases in general.

The next step is to unravel the pathway that could be responsible for the protective effect of belinostat. Nephroprotective effects of HDAC inhibitiors in general have also been reported earlier, especially in the case of acute kidney injury. [32,33] It is also published that the Hippo- and the GSK3 pathways, respectively, are regulated by belinostat.[49,50] Another possibility for the protective effect of belinostat might be that this pan-HDAC inhibition affects non-histone targets and modifies immune responses.[51,52] A pro-differentiating effect in combination with a modified immune response could explain the protective effect in this FSGS-like model. Further experiments in the future will provide more insight into the signaling cascade, specifically in podocytes.

In summary, our group established a novel high-content *in vivo* drug screening assay in zebrafish larvae using a reliable podocyte injury model. State-of-the-art screening microscopy, automated segmentation and measurements allow the assessment of podocyte injury and proteinuria on a large scale. This work identified a FDA-approved drug as protective for larval podocytes. These results open up the possibility of belinostat being a novel therapeutic option for patients suffering from FSGS.

Author contributions

Conceptualization: MS; NE, Methodology: MS; FS; SMB; NE, Software: MS; FS; JG, Validation: MS; FS; TL; NE, Formal analysis: MS; TL; Investigation: MS; SMB, Resources: JG; SG; NE, Data curation: MS; TL; JG; SG, Writing – original draft preparation: MS; NE, Writing – review and editing: FS; TL; JG; SG, Visualization: MS, NE; Supervision: NE, Project administration: NE, Funding acquisition: NE.

All authors reviewed and accepted the final form of the manuscript.

Acknowledgements

The experimental support of Marianne Klawitter, Thor-Magnus Koppe and Juan Saydou Dikou is highly appreciated. The authors are very grateful for the excellent zebrafish husbandry by Oliver Zabel and Steffen Prellwitz. The European Patent Office issued a patent (Application number: EP22179045.4) that is related to this study.

Disclosures

NE is CEO of the NIPOKA GmbH, Greifswald, Germany.

JG is an employee of ACQUIFER Imaging GmbH, Heidelberg, Germany.

Funding

This work was funded by the federal Ministry of Education and Research (BMBF grant 01GM1518B, STOP-FSGS) to NE. Additionally, the Bundesamt für Wirtschaft und Kilmaschutz (BMWi) funded this project (grant 16KN077229, title: Alterna Tier-vivoPod). Furthermore, this work was generously supported by the Dr. Gerhard Büchtemann fund, Hamburg, Germany and the Südmeyer fund for kidney and vascular research ('Südmeyer Stiftung für Nieren- und Gefäßforschung').

Data sharing statement

The FIJI macro code is available at https://github.com/MaximilianSchindler.

References

1. Wiggins RC: The spectrum of podocytopathies: a unifying view of glomerular diseases. *Kidney international* 71(12): 1205–14, 2007
2. Pavenstädt H, Kriz W, Kretzler M: Cell biology of the glomerular podocyte. *Physiological reviews* 83(1): 253–307, 2003
3. Garg P: A Review of Podocyte Biology. *American journal of nephrology* 47 Suppl 1: 3–13, 2018
4. Kriz W, Lemley KV: A potential role for mechanical forces in the detachment of podocytes and the progression of CKD. *Journal of the American Society of Nephrology JASN* 26(2): 258–69, 2015
5. Bose B, Cattran D: Glomerular diseases: FSGS. *Clinical journal of the American Society of Nephrology CJASN* 9(3): 626–32, 2014
6. Kriz W, Hosser H, Hähnel B, Gretz N, Provoost AP: From segmental glomerulosclerosis to total nephron degeneration and interstitial fibrosis: a histopathological study in rat models and human glomerulopathies. *Nephrology, dialysis, transplantation official publication of the European Dialysis and Transplant Association - European Renal Association* 13(11): 2781–98, 1998
7. Vriese AS de, Sethi S, Nath KA, Glassock RJ, Fervenza FC: Differentiating Primary, Genetic, and Secondary FSGS in Adults: A Clinicopathologic Approach. *Journal of the American Society of Nephrology JASN* 29(3): 759–74, 2018
8. Rosenberg AZ, Kopp JB: Focal Segmental Glomerulosclerosis. *Clinical journal of the American Society of Nephrology CJASN* 12(3): 502–17, 2017

9. Poureetezadi SJ, Wingert RA: Little fish, big catch: zebrafish as a model for kidney disease. *Kidney international* 89(6): 1204–10, 2016

10. Drummond IA, Davidson AJ: Zebrafish kidney development. *Methods in cell biology* 100: 233–60, 2010

11. Drummond IA, Majumdar A, Hentschel H, Elger M, Solnica-Krezel L, Schier AF, Neuhauss SC, Stemple DL, Zwartkruis F, Rangini Z, Driever W, Fishman MC: Early development of the zebrafish pronephros and analysis of mutations affecting pronephric function. *Development (Cambridge, England)* 125(23): 4655–67, 1998

12. Siegerist F, Lange T, Iervolino A, Koppe TM, Zhou W, Capasso G, Endlich K, Endlich N: Evaluation of endogenous miRNA reference genes across different zebrafish strains, developmental stages and kidney disease models. *Scientific reports* 11(1): 22894, 2021

13. Kroeger PT, Wingert RA: Using zebrafish to study podocyte genesis during kidney development and regeneration. *Genesis (New York, N.Y. 2000)* 52(9): 771–92, 2014

14. Müller T, Rumpel E, Hradetzky S, Bollig F, Wegner H, Blumenthal A, Greinacher A, Endlich K, Endlich N: Non-muscle myosin IIA is required for the development of the zebrafish glomerulus. *Kidney international* 80(10): 1055–63, 2011

15. Kramer-Zucker AG, Wiessner S, Jensen AM, Drummond IA: Organization of the pronephric filtration apparatus in zebrafish requires Nephrin, Podocin and the FERM domain protein Mosaic eyes. *Developmental biology* 285(2): 316–29, 2005

16. Bolten JS, Pratsinis A, Alter CL, Fricker G, Huwyler J: Zebrafish (Danio rerio) larva as an in vivo vertebrate model to study renal function. *American journal of physiology. Renal physiology* 322(3): F280-F294, 2022

17. Schindler M, Blumenthal A, Moeller MJ, Endlich K, Endlich N: Adriamycin does not damage podocytes of zebrafish larvae. *PloS one* 15(11): e0242436, 2020

18. Siegerist F, Blumenthal A, Zhou W, Endlich K, Endlich N: Acute podocyte injury is not a stimulus for podocytes to migrate along the glomerular basement membrane in zebrafish larvae. *Scientific reports* 7: 43655, 2017

19. Endlich N, Siegerist F, Endlich K: Are podocytes motile? *Pflugers Archiv European journal of physiology* 469(7-8): 951–7, 2017

20. Yang JW, Dettmar AK, Kronbichler A, Gee HY, Saleem M, Kim SH, Shin JI: Recent advances of animal model of focal segmental glomerulosclerosis. *Clinical and experimental nephrology* 22(4): 752–63, 2018

21. Fogo AB: Animal models of FSGS: lessons for pathogenesis and treatment. *Seminars in nephrology* 23(2): 161–71, 2003

22. Zhou W, Hildebrandt F: Inducible podocyte injury and proteinuria in transgenic zebrafish. *Journal of the American Society of Nephrology JASN* 23(6): 1039–47, 2012

23. Davison JM, Akitake CM, Goll MG, Rhee JM, Gosse N, Baier H, Halpern ME, Leach SD, Parsons MJ: Transactivation from Gal4-VP16 transgenic insertions for tissue-specific cell labeling and ablation in zebrafish. *Developmental biology* 304(2): 811–24, 2007

24. Hansen KUI, Siegerist F, Daniel S, Schindler M, Iervolino A, Blumenthal A, Daniel C, Amann K, Zhou W, Endlich K, Endlich N: Prolonged podocyte depletion in larval zebrafish resembles mammalian focal and segmental glomerulosclerosis. *FASEB*

journal official publication of the Federation of American Societies for Experimental Biology 34(12): 15961–74, 2020

25. Xie J, Farage E, Sugimoto M, Anand-Apte B: A novel transgenic zebrafish model for blood-brain and blood-retinal barrier development. *BMC developmental biology* 10: 76, 2010

26. Siegerist F, Zhou W, Endlich K, Endlich N: 4D in vivo imaging of glomerular barrier function in a zebrafish podocyte injury model. *Acta physiologica (Oxford, England)* 220(1): 167–73, 2017

27. Schindelin J, Arganda-Carreras I, Frise E, Kaynig V, Longair M, Pietzsch T, Preibisch S, Rueden C, Saalfeld S, Schmid B, Tinevez J-Y, White DJ, Hartenstein V, Eliceiri K, Tomancak P, Cardona A: Fiji: an open-source platform for biological-image analysis. *Nature methods* 9(7): 676–82, 2012

28. Westhoff JH, Steenbergen PJ, Thomas LSV, Heigwer J, Bruckner T, Cooper L, Tönshoff B, Hoffmann GF, Gehrig J: In vivo High-Content Screening in Zebrafish for Developmental Nephrotoxicity of Approved Drugs. *Frontiers in cell and developmental biology* 8: 583, 2020

29. Pandey G, Westhoff JH, Schaefer F, Gehrig J: A Smart Imaging Workflow for Organ-Specific Screening in a Cystic Kidney Zebrafish Disease Model. *International journal of molecular sciences* 20(6), 2019

30. Li LX, Agborbesong E, Zhang L, Li X: Investigation of epigenetics in kidney cell biology. *Methods in cell biology* 153: 255–78, 2019

31. Wanner N, Vornweg J, Combes A, Wilson S, Plappert J, Rafflenbeul G, Puelles VG, Rahman R-U, Liwinski T, Lindner S, Grahammer F, Kretz O, Wlodek ME, Romano T,

Moritz KM, Boerries M, Busch H, Bonn S, Little MH, Bechtel-Walz W, Huber TB: DNA Methyltransferase 1 Controls Nephron Progenitor Cell Renewal and Differentiation. *Journal of the American Society of Nephrology JASN* 30(1): 63–78, 2019

32. Zhang L, Cao W: Histone deacetylase 3 (HDAC3) as an important epigenetic regulator of kidney diseases. *Journal of molecular medicine (Berlin, Germany)* 100(1): 43–51, 2022
33. Hyndman KA, Kasztan M, Mendoza LD, Monteiro-Pai S: Dynamic changes in histone deacetylases following kidney ischemia-reperfusion injury are critical for promoting proximal tubule proliferation. *American journal of physiology. Renal physiology* 316(5): F875-F888, 2019
34. Liu S, Gao X, Fan Z, Wang Q: SIRT2 Affects Cell Proliferation and Apoptosis by Suppressing the Level of Autophagy in Renal Podocytes. *Disease markers* 2022: 4586198, 2022
35. Wittbrodt JN, Liebel U, Gehrig J: Generation of orientation tools for automated zebrafish screening assays using desktop 3D printing. *BMC biotechnology* 14: 36, 2014
36. Steenbergen PJ, Heigwer J, Pandey G, Tönshoff B, Gehrig J, Westhoff JH: A Multiparametric Assay Platform for Simultaneous In Vivo Assessment of Pronephric Morphology, Renal Function and Heart Rate in Larval Zebrafish. *Cells* 9(5), 2020
37. Lucore EC, Connaughton VP: Observational learning and irreversible starvation in first-feeding zebrafish larvae: is it okay to copy from your friends? *Zoology (Jena, Germany)* 145: 125896, 2021

38. D'Agati VD: Podocyte Growing Pains in Adaptive FSGS. *Journal of the American Society of Nephrology JASN* 28(10): 2825–7, 2017

39. Kim G-HJ, Mo H, Liu H, Wu Z, Chen S, Zheng J, Zhao X, Nucum D, Shortland J, Peng L, Elepano M, Tang B, Olson S, Paras N, Li H, Renslo AR, Arkin MR, Huang B, Lu B, Sirota M, Guo S: A zebrafish screen reveals Renin-angiotensin system inhibitors as neuroprotective via mitochondrial restoration in dopamine neurons. *eLife* 10, 2021

40. Kuo F-C, Chao C-T, Lin S-H: The Dynamics and Plasticity of Epigenetics in Diabetic Kidney Disease: Therapeutic Applications Vis-à-Vis. *International journal of molecular sciences* 23(2), 2022

41. Lange T, Artelt N, Kindt F, Stracke S, Rettig R, Lendeckel U, Chadjichristos CE, Kavvadas P, Chatziantoniou C, Endlich K, Endlich N: MiR-21 is up-regulated in urinary exosomes of chronic kidney disease patients and after glomerular injury. *Journal of cellular and molecular medicine* 23(7): 4839–43, 2019

42. Allison SJ: Epigenetics: H3K27me3 in glomerular disease. *Nature reviews. Nephrology* 14(3): 143, 2018

43. Liu M, Liang K, Zhen J, Zhou M, Wang X, Wang Z, Wei X, Zhang Y, Sun Y, Zhou Z, Su H, Zhang C, Li N, Gao C, Peng J, Yi F: Sirt6 deficiency exacerbates podocyte injury and proteinuria through targeting Notch signaling. *Nature communications* 8(1): 413, 2017

44. Majumder S, Thieme K, Batchu SN, Alghamdi TA, Bowskill BB, Kabir MG, Liu Y, Advani SL, White KE, Geldenhuys L, Tennankore KK, Poyah P, Siddiqi FS, Advani

A: Shifts in podocyte histone H3K27me3 regulate mouse and human glomerular disease. *The Journal of clinical investigation* 128(1): 483–99, 2018

45. Lee H-Z, Kwitkowski VE, Del Valle PL, Ricci MS, Saber H, Habtemariam BA, Bullock J, Bloomquist E, Li Shen Y, Chen X-H, Brown J, Mehrotra N, Dorff S, Charlab R, Kane RC, Kaminskas E, Justice R, Farrell AT, Pazdur R: FDA Approval: Belinostat for the Treatment of Patients with Relapsed or Refractory Peripheral T-cell Lymphoma. *Clinical cancer research an official journal of the American Association for Cancer Research* 21(12): 2666–70, 2015
46. Foss F, Advani R, Duvic M, Hymes KB, Intragumtornchai T, Lekhakula A, Shpilberg O, Lerner A, Belt RJ, Jacobsen ED, Laurent G, Ben-Yehuda D, Beylot-Barry M, Hillen U, Knoblauch P, Bhat G, Chawla S, Allen LF, Pohlman B: A Phase II trial of Belinostat (PXD101) in patients with relapsed or refractory peripheral or cutaneous T-cell lymphoma. *British journal of haematology* 168(6): 811–9, 2015
47. Emanuele S, Lauricella M, Tesoriere G: Histone deacetylase inhibitors: apoptotic effects and clinical implications (Review). *International journal of oncology* 33(4): 637–46, 2008
48. Marampon F, Di Nisio V, Pietrantoni I, Petragnano F, Fasciani I, Scicchitano BM, Ciccarelli C, Gravina GL, Festuccia C, Del Fattore A, Tombolini M, Felice F de, Musio D, Cecconi S, Tini P, Maddalo M, Codenotti S, Fanzani A, Polimeni A, Maggio R, Tombolini V: Pro-differentiating and radiosensitizing effects of inhibiting HDACs by PXD-101 (Belinostat) in in vitro and in vivo models of human rhabdomyosarcoma cell lines. *Cancer letters* 461: 90–101, 2019

49. Wennmann DO, Vollenbröker B, Eckart AK, Bonse J, Erdmann F, Wolters DA, Schenk LK, Schulze U, Kremerskothen J, Weide T, Pavenstädt H: The Hippo pathway is controlled by Angiotensin II signaling and its reactivation induces apoptosis in podocytes. *Cell death & disease* 5: e1519, 2014

50. Basu D, Reyes-Múgica M, Rebbaa A: Histone acetylation-mediated regulation of the Hippo pathway. *PloS one* 8(5): e62478, 2013

51. Jeong Y, Du R, Zhu X, Yin S, Wang J, Cui H, Cao W, Lowenstein CJ: Histone deacetylase isoforms regulate innate immune responses by deacetylating mitogen-activated protein kinase phosphatase-1. *Journal of leukocyte biology* 95(4): 651–9, 2014

52. Choudhary C, Kumar C, Gnad F, Nielsen ML, Rehman M, Walther TC, Olsen JV, Mann M: Lysine acetylation targets protein complexes and co-regulates major cellular functions. *Science (New York, N.Y.)* 325(5942): 834–40, 2009

Supplemental table of contents

Tables

Table 1: List of toxic compounds. All compounds in this list had a lethal effect on all 12 larvae in conjunction with 80 µM MTZ.

Toxic compounds			
SW-100	3-TYP	Remetinostat	Scopolin
Tenovin-6	UF010	Ophiopogonin D'	Sinapinic acid
Droxinostat	HDAC8-IN-1	BRD 4354	Valproic acid (sodium salt)
Trichostatin A	Selisistat R-enantiomer	SRT2183	Scriptaid
PCI-34051	UBCS039	Quisinostat	J22352
Sirtuin modulator 1	BG45	Splitomicin	SRT 1720 (Hydrochloride)
Selisistat S-enantiomer	AK-1	SR-4370	OPC 95%
TMP195	Sirtinol	Fimepinostat	Huperzine A
Inauhzin	Panobinostat	Tenovin-6 (Hydrochloride)	R-Alpha lipoic acid

Figures and figure legends

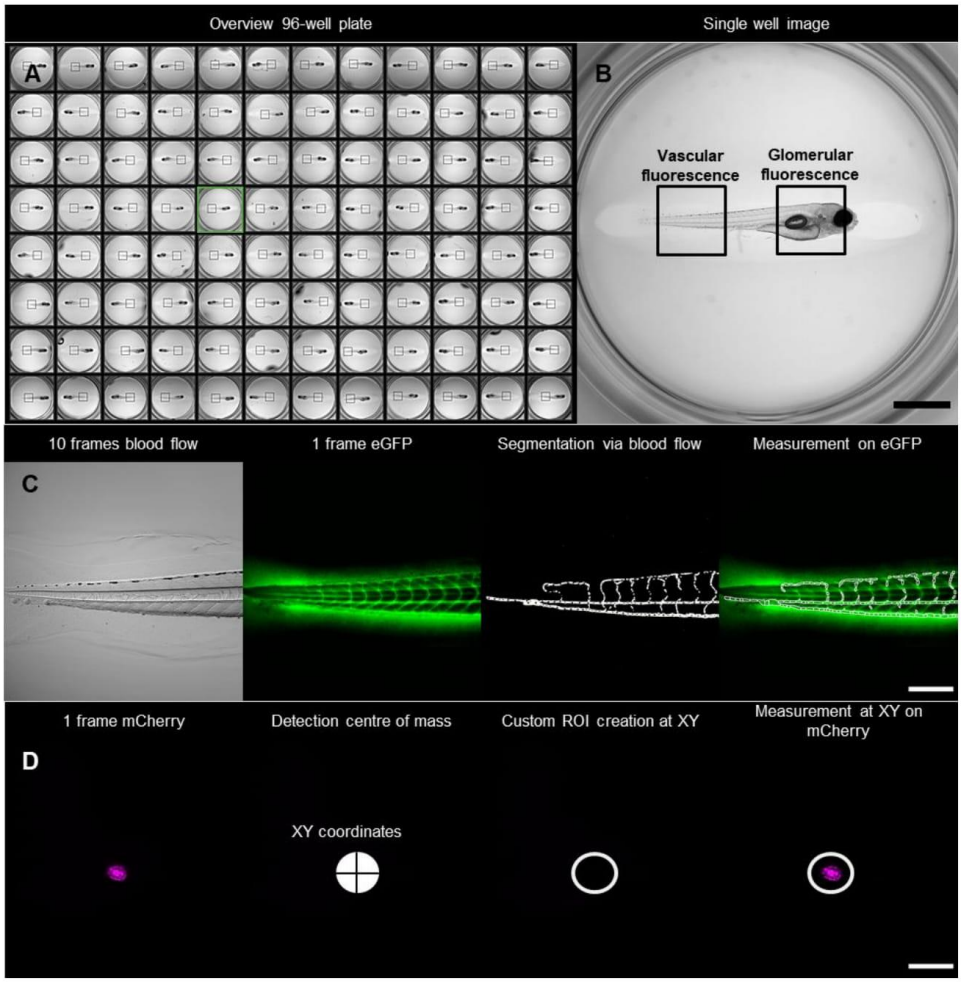

Figure 1: Imaging setup of vascular and glomerular fluorescence with the imaging machine. At first, an overview image of all wells of the 96-well plate is acquired with a 2x objective (**A**). A region of interest (ROI) at the larval tail is manually selected for the vascular fluorescence (**B**). At this region, a 10x objective acquires 10 consecutive frames in the brightfield channel and 1 frame at 470 nm (eGFP) of

each larva. A custom FIJI code automatically segments vessels on the basis of moving erythrocytes and measures the fluorescence intensity exclusively in the vasculature (**C**). For podocyte presence, another ROI at the glomerular region is manually selected (**B**). For each larva, one frame at 555 nm (mCherry) is acquired. The FIJI code automatically detects podocytes and creates a defined ROI. Afterwards the mCherry fluorescence intensity is measured within this ROI (**D**). Scale bar in (**B**) 1 mm, in (**C**) and (**D**) 250 µm.

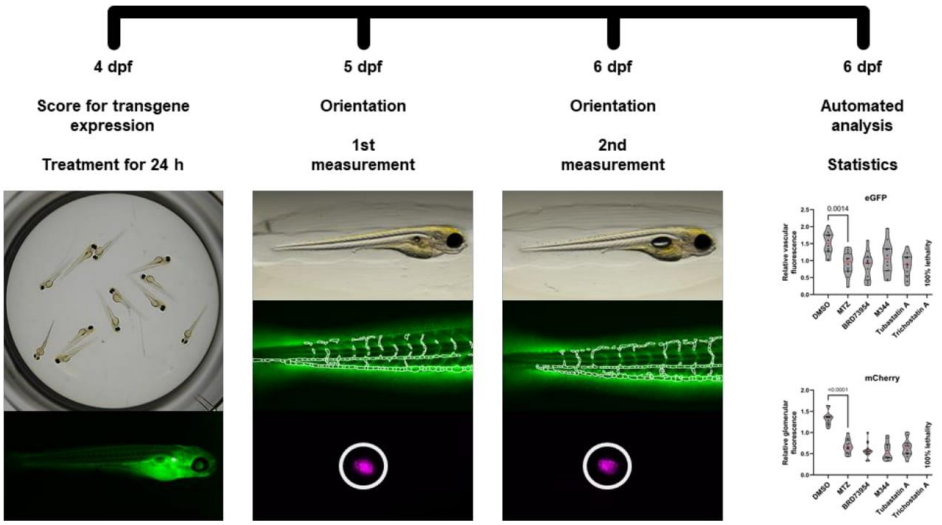

Figure 2: Workflow of the high throughput *in vivo* drug screening assay. Transgene expression of *nphs2:ntr-mCherry* in podocytes and the VDP-eGFP in the vasculature is checked with a stereomicroscope at 4 days post fertilization (dpf). Larvae from one clutch are distributed in groups of n=12 in 24-well plates for treatments. After 24 hours, all compounds are washed out and the larvae are placed individually into a 96-well plate. Following lateral orientation, images of vascular and glomerular fluorescence are acquired at 5 dpf. After another 24 hours, the vascular and glomerular fluorescence is acquired again of the exact same larvae. The fluorescence ratios of both readouts for each individual larva serve as input for the statistics.

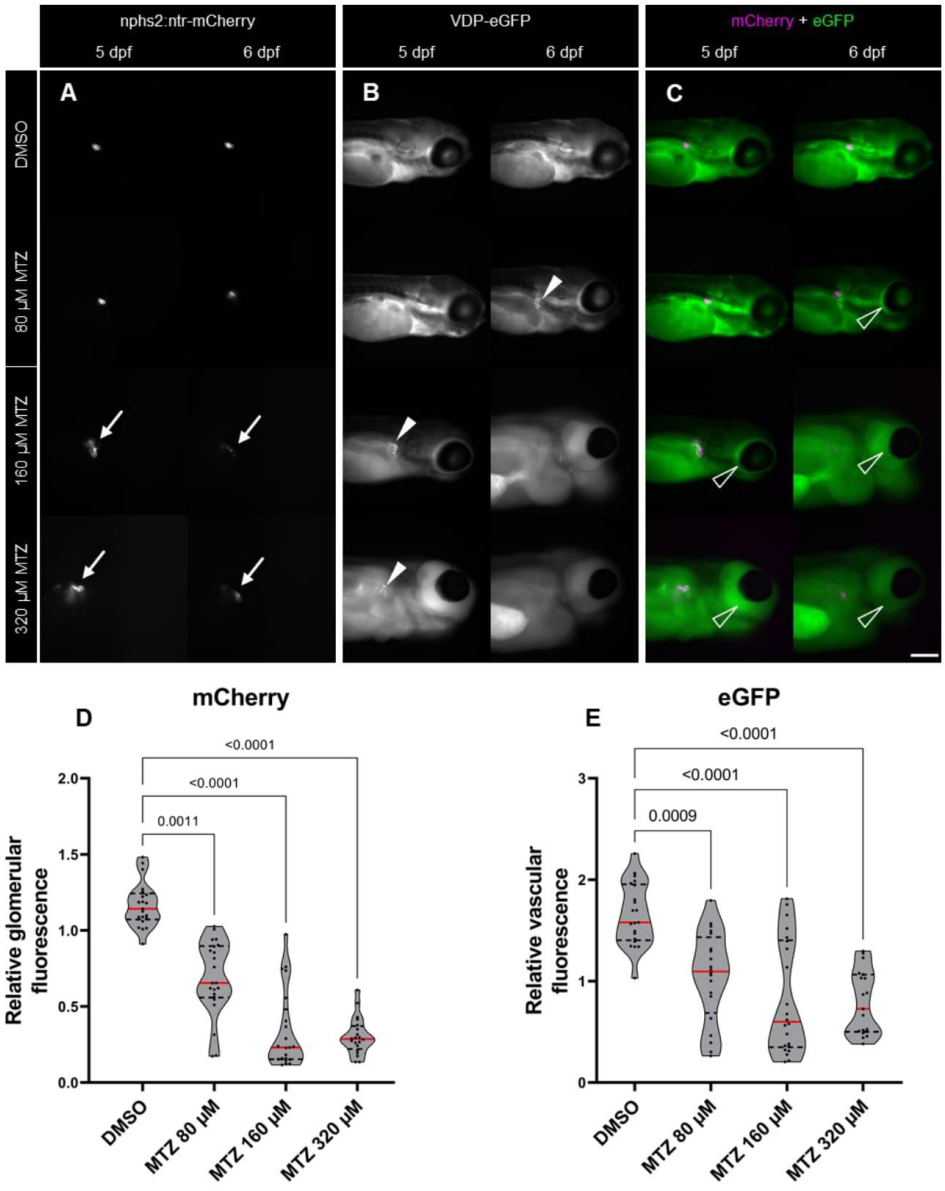

Figure 3: Different Metronidazole (MTZ) concentrations cause an acute or chronic larval podocyte injury accompanied by proteinuria. After 24 hours treatment, the mCherry signal of the DMSO control

and the 80 µM MTZ group did not differ at 5 dpf. 160 µM and 320 µM MTZ caused a loss of mCherry fluorescence and a distribution of the mCherry signal into the proximal convoluted tubules at 5 dpf (arrows in A). At 6 dpf, the 80 µM MTZ group showed a loss of mCherry fluorescence. The glomerular injury in the 160 µM and 320 µM group did progress to a state in which podocytes are barely present on the glomerular tuft (A). 160 µM and 320 µM MTZ caused a strong glomerular leakage and a tubular reabsorption of the 78 kDa VDP-eGFP at 5 dpf (arrowheads in B). Disruption of the glomerular filtration barrier was observable in the 80 µM group not at 5, but at 6 dpf (B). Podocyte specific injury and proteinuria is accompanied by periocular edema formation. After 24 hours treatment with 320 µM MTZ, larvae developed severe edema at 5 dpf (arrowheads in C). Treatment with 160 µM caused slight edema formation at 5 dpf and severe edema formation at 6 dpf. 80 µM MTZ caused no visible edema at 5 dpf and slight edema at 6 dpf. The DMSO control group did not show edema at all (C). All three MTZ groups developed a statistical significant loss of the podocyte mCherry fluorescence in the screening setup (D). Accordingly, a significant loss of vascular eGFP (proteinuria) could be detected (DMSO n=21, 80 µM MTZ n=20, 160 µM MTZ n=22, 320 µM MTZ n=19). Data distribution was checked via Kolmogorov-Smirnov test and significance was determined by Kruskal-Wallis test, followed by Dunns´s multiple comparison, the DMSO group served as control and $p \leq 0.05$ was considered statistically significant. Scale bar in (C) represents 250 µm.

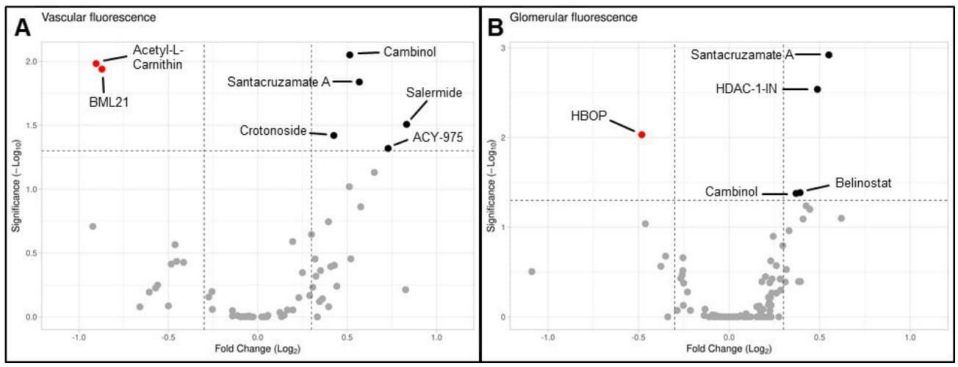

Figure 4: Overview of protective and potential harmful effects on larval podocytes. Out of 138 compounds of the drug library, 5 caused a significant decrease of proteinuria depicted by a reduced glomerular leakage in comparison to their corresponding MTZ Groups (black dots in **A**). Two substances induced an elevated loss of vascular fluorescence together with MTZ compared to MTZ only (red dots in **A**). 4 compounds prevented podocyte injury shown by a significantly reduced loss of glomerular mCherry fluorescence (black dots in **B**). One compound caused an elevated loss of podocyte mCherry fluorescence in conjunction with MTZ (red dot in **B**). The y-axis depicts the negative $\log_{10}$ logarithm of p=0.05 and the cut-off for the fold change on the x-axis is 0.3.

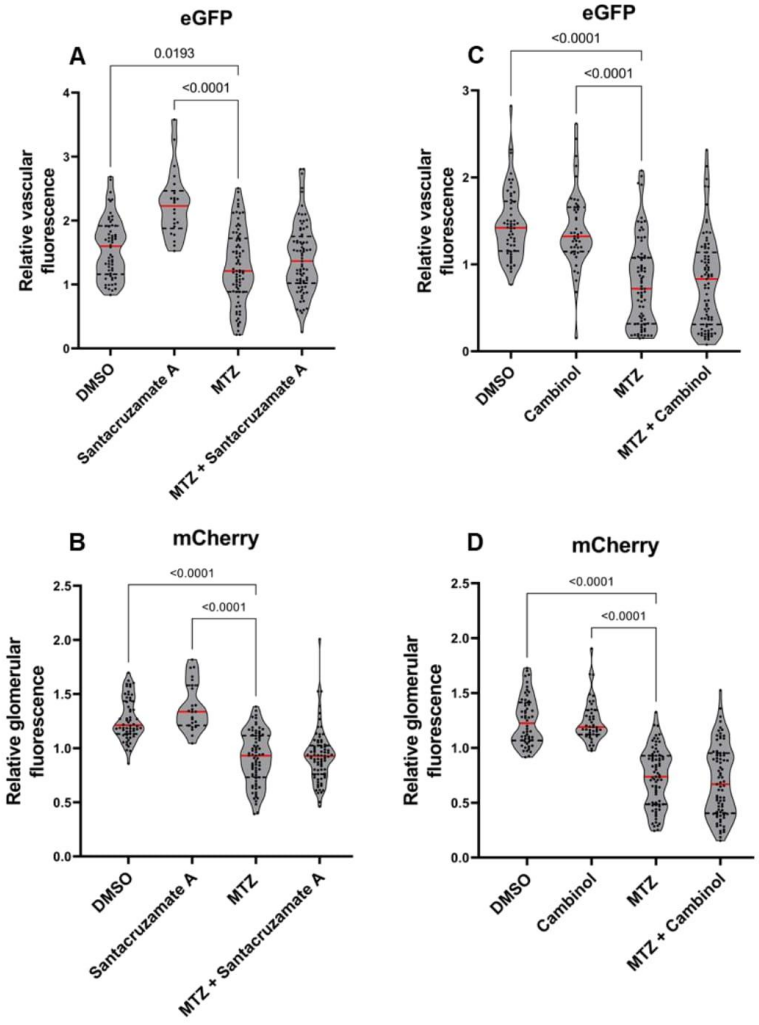

Figure 5: Follow-up experiments of top 2 candidates. Treatment with santacruzamate A at 10 µM alone had no deteriorating effect in terms of vascular or glomerular fluorescence depicted by significantly higher fluorescence ratios compared to MTZ. 80 µM MTZ caused a significant loss of vascular and glomerular fluorescence. Santacruzamate A was not able to decelerate or prevent MTZ injury in our co-treatment setup (DMSO n=58, santacruzamate A n=22, MTZ n=75, MTZ+santacruzamate A n=75, **A, B**).

Follow-up experiments with cambinol showed similar effects. 10 µM cambinol had no harmful effect on podocytes or the glomerular filtration barrier by itself. MTZ induced a significant loss of both fluorescences and cambinol was not able to protect the larval podocytes from MTZ injury (DMSO n=54, cambinol n=43, MTZ n=75, MTZ+cambinol n=79, **C, D**). Data distribution was tested with Kolmogorov-Smirnov test, significance was checked by Kruskal-Wallis test, followed by Dunns´s multiple comparison, the MTZ group served as control, $p \leq 0.05$ was considered statistically significant.

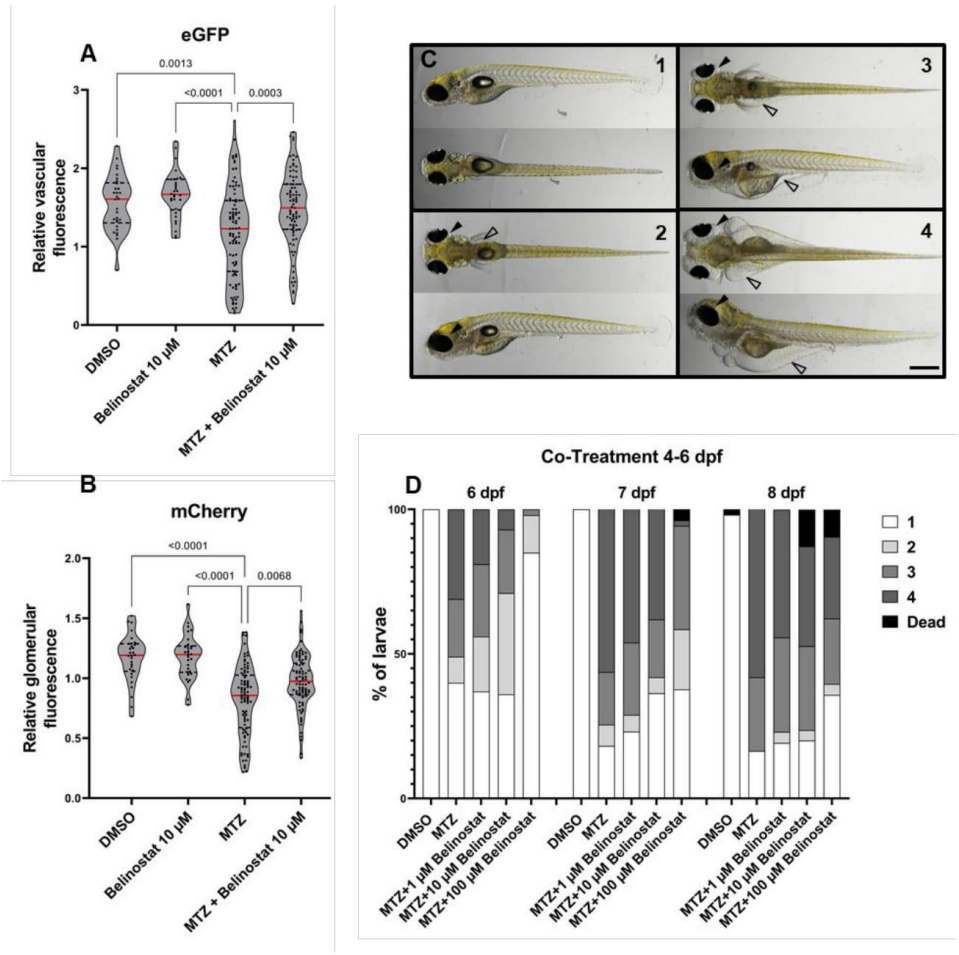

Figure 6: Follow-up experiments with belinostat proved a protective effect on larval podocytes. Treatment with 10 µM belinostat had no harmful effect on the glomerular filtration barrier or podocyte vitality. The podocyte injury by MTZ caused a significantly higher glomerular leakage of eGFP and a loss of podocytes. Addition of 10 µM belinostat to the 80 µM MTZ solution could prevent the leakage of the 78 kDa VDP-eGFP. This result was corroborated by a significantly reduced loss of podocyte mCherry fluorescence in the co-treatment group of belinostat and MTZ in comparison to MTZ (DMSO n=30, belinostat n=30, MTZ n=89, MTZ+belinostat n=85, **A, B**). Data distribution was checked via Kolmogorov-Smirnov test and significance was determined by ordinary one-way ANOVA, followed by Dunnet´s

multiple comparison test for **A** and Kruskal-Wallis test, followed by Dunns´s multiple comparison for **B**. The MTZ group served as control, p≤0.05 was considered statistically significant. Following these results, *nphs2:ntr-mCherry* larvae were treated with different concentrations of belinostat in conjunction with MTZ. Depending on the progression of podocyte injury, larvae develop different degrees of edema: 1: no edema, 2: slight edema, 3: moderate edema, 4: severe edema. Black arrowheads show periocular and blank arrowheads depict abdominal edema (**C**). Belinostat had a concentration dependent protective effect on podocytes from MTZ injury until 8 dpf (DMSO n= 52, MTZ n=55, MTZ+1 µM belinostat n=52, MTZ+10 µM belinostat n=55, MTZ+100 µM belinostat n=53, **D**). These results strongly hint towards a protective effect of belinostat on podocytes. Scale bar in (**C**): 500 µm.

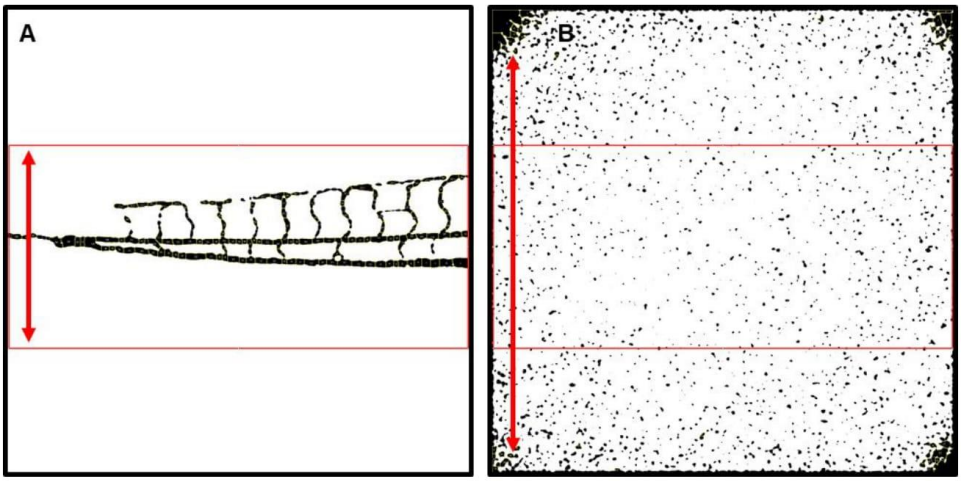

Figure S1: Control of the segmentation process. A successful segmentation automatically detects the vasculature by moving erythrocytes. All segmented areas fit into a bounding rectangle (red) with a restricted size on the Y-axis of 900 pixels (585 µM, the size of the agarose cavity, A). In case of no detected blood flow (no movement) within 10 brightfield frames, the FIJI macro detects the highest pixel change in the corners and segments the corners due to detector noise. These ROIs combined do not fit into the 900 pixels rectangle which leads to exclusion of larvae with no peripheral blood flow (B).

Supplemental table of contents

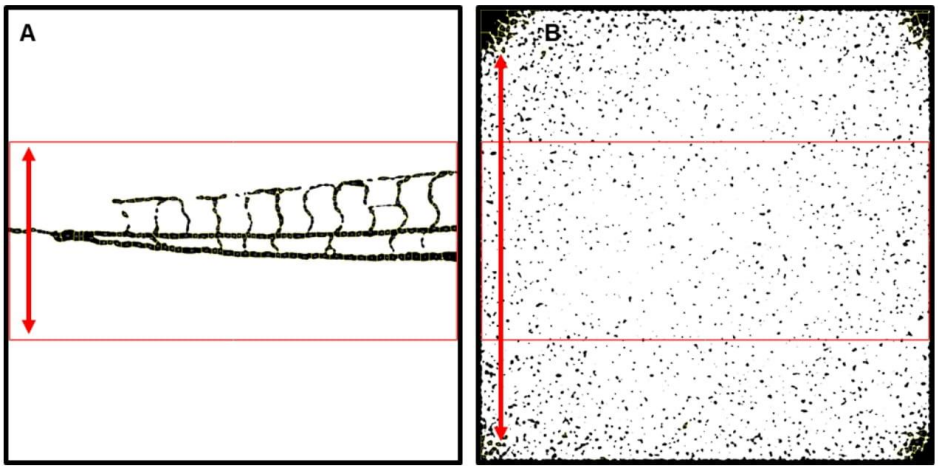

Figure S1: Control of the segmentation process. A successful segmentation automatically detects the vasculature by moving erythrocytes. All segmented areas fit into a bounding rectangle (red) with a restricted size on the Y-axis of 900 pixels (585 µM, the size of the agarose cavity, A). In case of no detected blood flow (no movement) within 10 brightfield frames, the FIJI macro detects the highest pixel change in the corners and segments the corners due to detector noise. These ROIs combined do not fit into the 900 pixels rectangle which leads to exclusion of larvae with no peripheral blood flow (B).

CJASN Clinical Journal of the American Society of Nephrology JASN JOURNAL OF THE AMERICAN SOCIETY OF NEPHROLOGY Kidney360

Checklist for Reporting of Race and Ethnicity in Medical and Science Journals modified from JAMA.*

Manuscript ID:

Section in JAMA Article	Checklist Item	Response
Concerns, Sensitivities, and Controversies in Health Care and Research	Demographic information assessed in the main article, in an online supplement, or both are reported. If any demographic characteristics that were collected are not reported, the reason is stated. Summary demographic information (e.g., baseline characteristics of study participants) is reported in the **Abstract**.	N/A
Concerns, Sensitivities, and Controversies in Health Care and Research	Demographic variables collected for a specific study are indicated in **Methods**.	N/A
Concerns, Sensitivities, and Controversies in Health Care and Research	An explanation of who identified participant race and ethnicity and the source of the classifications used (e.g., self-report or selection, investigator observed, database, electronic health record, survey instrument) is included in **Methods**.	N/A
Concerns, Sensitivities, and Controversies in Health Care and Research	The reasons race and ethnicity categories were collected for a study are included. If collection of data on race and ethnicity was required by the funding agency, it is noted in **Methods**.	N/A
Concerns, Sensitivities, and Controversies in Health Care and Research	Racial and ethnic categories are used instead of collective terms (e.g., *people of color*), when possible, and reported in **Results**. (Specific categories have been used, when possible, understanding that these categories will differ based on 1) the databases or surveys used, 2) the requirements of funders, and 3) the geographic location of data collection or study participants. Categories included in groups labeled as "other" are defined.	N/A
Concerns, Sensitivities, and Controversies in Health Care and Research	Demographic information is listed in alphabetical order (e.g., *Black patients, Latinx patients, and White patients*) in **text and tables**.	N/A
Additional Guidance for Use of Racial and Ethnic Collective Terms	Specific groups are named when comparing racial and ethnic groups, rather than using a collective reference like "non-White."	N/A
Additional Guidance for Use of Racial and Ethnic Collective Terms	"Multiracial" and "multiethnic" are used only if the specific categories these terms comprise are defined, or if the terms were predefined in a study or database to which participants self-selected.	N/A
Capitalization	The names of races, ethnicities, and tribes are capitalized (e.g., *African American, Alaska Native, American Indian, Asian, Black, Cherokee Nation, Hispanic, Kamba, Kikuyu, Latino, and White*).	N/A
Adjectival Usage for Specific Categories	Racial and ethnic terms are not used in noun form *(e.g., Asians, Blacks, Hispanics, or Whites);* the adjectival form is used instead *(e.g., Asian participants).*	N/A
Geographic Origin and Regionalization Considerations	The term *African American or Black* is used to describe participants in studies involving populations in the United States, following how such information was recorded or collected for the study. However, the 2 terms are not used interchangeably in reports of research unless both terms were formally used in the study, and the terms are used consistently throughout the article.	N/A
Geographic Origin and Regionalization Considerations	In reference to persons indigenous to North America (and their descendants), *American Indian or Alaska Native* is used, when possible, instead of *Native American.* However, the term Indigenous is also acceptable. There are also other specific designations for people from other locations, such as *Native Hawaiian* and *Pacific Islander,* which are used when appropriate. The nation or peoples are specified when possible (e.g., *Inuit, Iroquois, Mayan, Navajo, Nez Perce, Samoan*).	N/A
Geographic Origin and Regionalization Considerations	*Hispanic, Latino or Latina, Latinx,* and *Latine* are used for people living in the United States of Spanish-speaking or Latin American descent or heritage, but as with other terms, they can include people from other geographic locations.	N/A
Geographic Origin and Regionalization Considerations	The term *Asian American* is used when describing those who identify with Asian descent among the US population. However, reporting of individuals' self-identified countries of origin is included when known.	N/A
Geographic Origin and Regionalization Considerations	Persons of Asian ancestry are described according to their country or regional area of origin (e.g., *Cambodian, Chinese, Indian, Japanese, Korean, Sri Lankan, East Asian, Southeast Asian*) when possible. Study participants from the Middle Eastern and North African region are described using their nation of origin (e.g., *Egyptian, Iranian, Iraqi, Israeli, Lebanese*) when possible.	N/A
Abbreviations	Abbreviations of categories for race and ethnicity were avoided unless there were space constraints (e.g., in tables and figures) or to avoid long, repetitive strings of descriptors.	N/A

Source: Flanagin A, Frey T, Christiansen SL. Updated guidance on the reporting of race and ethnicity in medical and science journals. JAMA. 2021;326(7):621. doi:10.1001/jama.2021.13304

*This checklist has been adapted by the ASN journals for author and editor use.

7 Discussion

Podocytes are postmitotic cells with a unique cytoarchitecture that form the final filtration barrier in the kidney [1]. Any alteration of the complex 3D morphology of the interdigitating foot processes or the detachment of podocytes directly leads to the loss of the size-selectivity of the renal filtration barrier [38]. Moreover, podocyte injury may lead to severe kidney diseases such as FSGS, often resulting in the loss of the entire organ [39]. Until now, it is still controversial whether podocytes have a relevant regenerative potential and it is generally accepted that regeneration is only possible to a very limited extent [40–42]. Unfortunately, to date, there are no curative drugs available to treat podocytopathies such as FSGS [27] and therefore high-dose immunosuppressants e.g. glucocorticoids or calcineurin inhibitors have to be used [43, 44]. These treatments are rather unspecific and especially systemic suppression of the immune system might cause severe side-effects [45]. Expanding the knowledge of pathways and substances that might stimulate protection and/or regeneration of podocytes *in vivo* is highly relevant. Therefore, the aim of this work was the establishment of a high-content screening system to identify podocyte-protective small molecules or compounds. To this end, our group uses transgenic zebrafish larvae as *in vivo* model since it offers the possibility to combine high-throughput with the advantages of an animal model. A high fecundity, optical transparency, transgenic expression of fluorescent reporters and a high homology of the glomerular filtration unit are essential benefits of the zebrafish larva as a model to study podocyte biology in detail and *in vivo* [10, 15, 46].

In order to generate a robust high-content screening system, this work can be split into two main parts: i) Establishment of a reliable and rapid podocyte injury model in

zebrafish larvae that mimics FSGS, and ii) the development of a high-content, imaging-based *in vivo* screening pipeline. It has been previously described that morpholino injections into fertilized zebrafish eggs successfully damage larval podocytes [16, 20, 47]. However, morpholinos - small oligonucleotides - must be injected at a very early stage of development, i.e. at the one-cell stage [48, 49]. Since the development of zebrafish embryos is quite rapid, there is only a small window of opportunity for injections and morpholino induced gene knockdowns rather mimic developmental defects.Another option was the use of PAN which is already described to induce a severe podocyte phenotype and an impairment of the filtration barrier in rodents [50]. Müller-Deile and colleagues claimed that addition of PAN to the larval medium at 46 hours post fertilization (hpf) causes proteinuria and foot process effacement in zebrafish larvae [51]. On the one hand, however, PAN is an expensive molecule and treatment of hundreds of larvae with the suggested concentrations would break any financial framework. On the other hand, it was not possible to recapitulate the results of Müller-Deile and colleagues in preliminary experiments. Furthermore, it has been reported that intravenous injections of PAN into the cardiac sinus venosus results in glomerular injury in zebrafish larvae [37, 52]. Nevertheless, injection-based approaches are not scalable to a high-content and we excluded this method for our aims. Another substance that is used to induce podocyte injury is ADR [53]. ADR, a DNA-intercalating anthracycline, inhibits the topoisomerase II activity and is clinically used as a cytostatic drug [54]. ADR is reported to induce FSGS with varying reliability, depending on species and strain [34, 55]. For example, ADR has been shown to damage podocytes in many rat strains, but only in a few mouse strains [56]. Zennaro and colleagues demonstrated that treatment of zebrafish embryos for 7 hours with ADR starting at 3 hpf causes

severe developmental defects of podocytes, suggesting a general susceptibility of larval podocytes to ADR [36]. Since we wanted to avoid unspecific developmental defects, we administered ADR at a later developmental stage. Addition of three different concentrations of ADR to the medium at 7 dpf, a state in which larval podocytes are already highly differentiated, caused no podocyte injury within the timeframe of 48 hours [57]. Treated larvae did not develop proteinuria, a hallmark for glomerular injury in zebrafish larvae [16], demonstrated by vascular eGFP measurement in the *cade* strain. ADR treated larvae retained the circulating 78 kDa VDP-eGFP fusion protein in the vasculature, which indicates an intact GFB [57]. Additionally, immunohistological and ultrastructural analysis of ADR-treated larvae demonstrated healthy podocytes as well as an unscathed GFB [57]. One explanation for the difference in susceptibility to ADR of rodents and fish could be given by the report of Zheng and colleagues [58]. Accordingly, ADR susceptibility appears to be dependent on the expression of protein arginine methyltransferase 7 (*Prmt7*), implying that a low expression level increases ADR susceptibility. In this context, it was already shown that zebrafish embryos express *prmt7* even at very early developmental stages [59]. Furthermore, intraperitoneal injection of ADR in adult zebrafish resulted in renal tubular but not podocyte injury [60]. This supports our results that differentiated zebrafish podocytes are not susceptible to ADR injury [57]. An elegant alternative to ADR and PAN treatment is the pharmacogenetic and cell-specific NTR/MTZ ablation model [61]. After addition of MTZ to the medium, only NTR-expressing cells convert the prodrug MTZ into a toxin that induces apoptosis. In the past, Zhou and Hildebrandt have generated a zebrafish strain which expresses the NTR together with the fluorophore mCherry exclusively in podocytes [62]. Recently, our group has demonstrated that high doses of MTZ (≥ 1 mM) in the

medium cause acute podocyte detachment accompanied with proteinuria in the *cherry* strain [23, 63]. In order to find a suitable degree of podocyte injury as basis for a protective screening, the MTZ concentration needed to be reduced to avoid a complete loss of podocytes and generation of a non-reversible phenotype. To this end, we treated *cherry* larvae with 80 µM MTZ for 48 hours from 4 to 6 dpf. Extensive analysis of edema assessment, histological stainings, immunofluorescence stainings and transmission electron microscopy revealed that 80 µM MTZ induced a partial podocyte depletion [64]. Furthermore, MTZ induced podocyte foot process effacement, an activation of parietal epithelial cells (PECs), parieto-visceral adhesions and an accumulation of extracellular matrix in the GBM [64]. Smeets and colleagues found that PECs and their activation play a key role in the formation of sclerotic lesions in FSGS [65]. Moreover, MTZ treatment induced a morphological change of PECs from a flat to a cuboidal phenotype in *cherry* larvae upon podocyte depletion which was already observed in a rodent model of FSGS [64, 66]. These results strongly suggest that low dose MTZ treatment of *cherry* larvae via the medium reliably mimics mammalian FSGS and is therefore a suitable injury inductor and an excellent basis for a protective screening system [64].

Since transgenic zebrafish larvae are ideally suited for *in vivo* microscopy, we aimed to establish an imaging-based, high-throughput screening system on the basis of the MTZ-sensitive *cherry* strain. Therefore, we used the s*creeFi* strain which is a cross of the *cherry* and the *cade* strain. In this strain, MTZ induces podocyte depletion, accompanied by a quantifiable loss of podocyte specific mCherry fluorescence and a quantifiable loss of intravascular eGFP fluorescence due to a pathological glomerular excretion of the 78 kDa VDP-eGFP [23, 62]. Hence, the loss of mCherry fluorescence depicts the degree of podocyte injury and the loss of vascular eGFP

fluorescence depicts the degree of proteinuria [67]. First, an imaging protocol had to be established which reliably acquires the vascular eGFP signal and the glomerular mCherry signal. Hanke and colleagues established a fluorescence measurement of the retinal plexus to quantify eGFP fluorescence in proteinuric zebrafish larvae [67]. However, the objective and the ocular lens have to align perfectly to obtain images of high quality. Therefore, we excluded this method and decided to acquire the peripheral vasculature in the tail region. The larval tail is almost two-dimensional in contrast to more cranial regions which is advantageous for automatic focus plane detection. For this reason, our group uses a lateral orientation of larvae which combines microscopic access to the vasculature in the tail as well as the mCherry in podocytes [67]. Automated segmentation to accurately detect the region of interest is crucial to analyze large amounts of imaging data. Here, we developed custom codes to automatically segment and measure the fluorescence in the vasculature and podocytes of the *screeFi* strain [67]. After system calibration, a 138 compounds epigenetic drug library was screened for protective effects, since recent findings pointed out that epigenetic changes play an important role in patients with podocytopathies and diabetic nephropathy [68–70]. 7 compounds had an initial protective effect in the screening experiments. These candidates were further validated with a higher larvae count [67]. Out of these candidates, belinostat could be confirmed as protective for larval podocytes in a dose-dependent manner in this injury model. Belinostat reliably delayed edema formation, reduced podocyte depletion and prevented proteinuria [67]. Belinostat is a pan-HDAC (histone deacetylase) inhibitor that has an FDA-approval for the treatment of peripheral T-cell lymphoma [71]. Interestingly, nephroprotective effects of HDAC inhibition have already been reported for acute kidney injury [72, 73]. Additionally, it is known that

HDACs do not only regulate gene expression but modify immune responses as well [74]. Furthermore, belinostat has effects on GSK3 signaling and the Hippo-pathway, which play an important role in podocytes homeostasis [75–77]. In order to exclude an injury model or species-specific protective effect of belinostat, e.g. direct interactions with MTZ or the NTR, this drug will be tested in rodent models of podocyte diseases in the near future. This work lead to a patent filing of belinostat for kidney diseases by our group (Application number: EP22179045.4)

In summary, we established a high-content, imaging-based *in vivo* screening pipeline to identify and to study podocyte-protective small molecules/compounds by using a well-established zebrafish disease model. To achieve this end, it was necessary i) to establish an elaborate image acquisition, ii) to generate an automatic target structure segmentation and iii) to subsequently quantify fluorescence signals by custom code writing. Direct application of this high-content screening system led to identification of belinostat as a substance that prevents podocyte injury in a short-term treatment which suggests the modulation of important podocyte-specific signaling pathways.

8 Disclosure of shares in the cumulative dissertation

1) Adriamycin does not damage podocytes of zebrafish larvae

PLoS One. 2020 Nov 13;15(11):e0242436. doi: 10.1371/journal.pone.0242436. eCollection 2020.

Maximilian Schindler, Antje Blumenthal, Marcus Johannes Moeller, Karlhans Endlich, Nicole Endlich

	Data collection	Data analysis	Manuscript writing
MS	80%	70%	60%
AB	10%	0%	5%
MJM	0%	5%	5%
KE	0%	10%	10%
NE	10%	15%	20%

2) Prolonged podocyte depletion in larval zebrafish resembles mammalian focal and segmental glomerulosclerosis

FASEB J. 2020 Dec;34(12):15961-15974. doi: 10.1096/fj.202000724R. Epub 2020 Oct 18.

Kerrin Ursula Ingeborg Hansen, Florian Siegerist, Sophie Daniel, **Maximilian Schindler**, Anna Lervolino, Antje Blumenthal, Christoph Daniel, Kerstin Amann, Weibin Zhou, Karlhans Endlich, Nicole Endlich

	Data collection	Data analysis	Manuscript writing
KUIH	40%	40%	30%
FS	20%	30%	30%
SD	5%	5%	5%
MS	10%	5%	5%
AL	5%	5%	0%
AB	5%	0%	0%
CD	0%	5%	0%
KA	5%	0%	0%
WZ	5%	0%	0%
KE	0%	5%	5%
NE	5%	5%	25%

3) A novel high-content screening assay identified belinostat to be protective in a FSGS-like zebrafish model

Submitted to the Journal of the American Society of Nephrology: JASN 2022 at 5th July 2022.

Maximilian Schindler, Florian Siegerist, Tim Lange, Sophia-Marie Bach, Jochen Gehrig, Sheraz Gul, Nicole Endlich

	Data collection	Data analysis	Manuscript writing
MS	60%	60%	50%
FS	10%	10%	5%
TL	0%	10%	5%
SMB	20%	0%	0%
JG	0%	5%	5%
SG	0%	5%	5%
NE	10%	10%	30%

Signature of the supervisor(s)

Signature of the doctoral candidate

9 References

1. **Rodewald R, Karnovsky MJ**. Porous substructure of the glomerular slit diaphragm in the rat and mouse. *The Journal of cell biology*. 1974; 60: 423–33.
2. **Breshears MA, Confer AW**. The Urinary System. In: Pathologic Basis of Veterinary Disease: Elsevier; 2017. 617-681.e1.
3. **Reiser J, Kriz W, Kretzler M, Mundel P**. The glomerular slit diaphragm is a modified adherens junction. *Journal of the American Society of Nephrology : JASN*. 2000; 11: 1–8.
4. **Roselli S, Gribouval O, Boute N, Sich M, Benessy F, Attié T*, et al.*** Podocin Localizes in the Kidney to the Slit Diaphragm Area. *The American journal of pathology*. 2002; 160: 131–39.
5. **D'Amico G, Bazzi C**. Pathophysiology of proteinuria. *Kidney international*. 2003; 63: 809–25.
6. **Bauer B, Mally A, Liedtke D**. Zebrafish Embryos and Larvae as Alternative Animal Models for Toxicity Testing. *International journal of molecular sciences*. 2021; 22.
7. **Crouzier L, Richard EM, Sourbron J, Lagae L, Maurice T, Delprat B**. Use of Zebrafish Models to Boost Research in Rare Genetic Diseases. *International journal of molecular sciences*. 2021; 22.
8. **Wang J, Cao H**. Zebrafish and Medaka: Important Animal Models for Human Neurodegenerative Diseases. *International journal of molecular sciences*. 2021; 22.
9. **Cornuault JK, Byatt G, Paquet M-E, Koninck P** de**, Moineau S**. Zebrafish: a big fish in the study of the gut microbiota. *Current opinion in biotechnology*. 2022; 73: 308–13.
10. **Howe K, Clark MD, Torroja CF, Torrance J, Berthelot C, Muffato M*, et al.*** The zebrafish reference genome sequence and its relationship to the human genome. *Nature*. 2013; 496: 498–503.
11. **Drummond IA, Majumdar A, Hentschel H, Elger M, Solnica-Krezel L, Schier AF*, et al.*** Early development of the zebrafish pronephros and analysis of mutations affecting pronephric function. *Development (Cambridge, England)*. 1998; 125: 4655–67.
12. **Drummond IA**. The zebrafish pronephros: a genetic system for studies of kidney development. *Pediatric nephrology (Berlin, Germany)*. 2000; 14: 428–35.
13. **Wingert RA, Davidson AJ**. The zebrafish pronephros: a model to study nephron segmentation. *Kidney international*. 2008; 73: 1120–27.
14. **Jobst-Schwan T, Hoogstraten CA, Kolvenbach CM, Schmidt JM, Kolb A, Eddy K*, et al.*** Corticosteroid treatment exacerbates nephrotic syndrome in a zebrafish model of magi2a knockout. *Kidney international*. 2019; 95: 1079–90.

15. **Kramer-Zucker AG, Wiessner S, Jensen AM, Drummond IA**. Organization of the pronephric filtration apparatus in zebrafish requires Nephrin, Podocin and the FERM domain protein Mosaic eyes. *Developmental biology*. 2005; 285: 316–29.
16. **Müller T, Rumpel E, Hradetzky S, Bollig F, Wegner H, Blumenthal A*, et al.*** Non-muscle myosin IIA is required for the development of the zebrafish glomerulus. *Kidney international*. 2011; 80: 1055–63.
17. **Endlich N, Simon O, Göpferich A, Wegner H, Moeller MJ, Rumpel E*, et al.*** Two-photon microscopy reveals stationary podocytes in living zebrafish larvae. *Journal of the American Society of Nephrology : JASN*. 2014; 25: 681–86.
18. **Kotb AM, Müller T, Xie J, Anand-Apte B, Endlich K, Endlich N**. Simultaneous assessment of glomerular filtration and barrier function in live zebrafish. *American journal of physiology. Renal physiology*. 2014; 307: F1427-34.
19. **Kawakami K**. Tol2: a versatile gene transfer vector in vertebrates. *Genome biology*. 2007; 8 Suppl 1: S7.
20. **Perner B, Englert C, Bollig F**. The Wilms tumor genes wt1a and wt1b control different steps during formation of the zebrafish pronephros. *Developmental biology*. 2007; 309: 87–96.
21. **Albadri S, Del Bene F, Revenu C**. Genome editing using CRISPR/Cas9-based knock-in approaches in zebrafish. *Methods (San Diego, Calif.)*. 2017; 121-122: 77–85.
22. **Xie J, Farage E, Sugimoto M, Anand-Apte B**. A novel transgenic zebrafish model for blood-brain and blood-retinal barrier development. *BMC developmental biology*. 2010; 10: 76.
23. **Siegerist F, Zhou W, Endlich K, Endlich N**. 4D in vivo imaging of glomerular barrier function in a zebrafish podocyte injury model. *Acta physiologica (Oxford, England)*. 2017; 220: 167–73.
24. Global, regional, and national burden of chronic kidney disease, 1990-2017: a systematic analysis for the Global Burden of Disease Study 2017. *Lancet (London, England)*. 2020; 395: 709–33.
25. **Wiggins RC**. The spectrum of podocytopathies: a unifying view of glomerular diseases. *Kidney international*. 2007; 71: 1205–14.
26. **Bose B, Cattran D**. Glomerular diseases: FSGS. *Clinical journal of the American Society of Nephrology : CJASN*. 2014; 9: 626–32.
27. **Vriese AS** de**, Wetzels JF, Glassock RJ, Sethi S, Fervenza FC**. Therapeutic trials in adult FSGS: lessons learned and the road forward. *Nature reviews. Nephrology*. 2021; 17: 619–30.
28. **Ebrahimi V, Khademian MH, Masoumi SJ, Morvaridi MR, Ezzatzadegan Jahromi S**. Factors influencing survival time of hemodialysis patients; time to event analysis using parametric models: a cohort study. *BMC nephrology*. 2019; 20: 215.
29. **Liabeuf S, Sajjad A, Kramer A, Bieber B, McCullough K, Pisoni R*, et al.*** Guideline attainment and morbidity/mortality rates in a large cohort of European

haemodialysis patients (EURODOPPS). *Nephrology, dialysis, transplantation : official publication of the European Dialysis and Transplant Association - European Renal Association*. 2019; 34: 2105–10.

30. **Vriese AS** de**, Sethi S, Nath KA, Glassock RJ, Fervenza FC**. Differentiating Primary, Genetic, and Secondary FSGS in Adults: A Clinicopathologic Approach. *Journal of the American Society of Nephrology : JASN*. 2018; 29: 759–74.
31. **Wada T, Pippin JW, Marshall CB, Griffin SV, Shankland SJ**. Dexamethasone prevents podocyte apoptosis induced by puromycin aminonucleoside: role of p53 and Bcl-2-related family proteins. *Journal of the American Society of Nephrology : JASN*. 2005; 16: 2615–25.
32. **Bejoy J, Qian ES, Woodard LE**. Tissue Culture Models of AKI: From Tubule Cells to Human Kidney Organoids. *Journal of the American Society of Nephrology : JASN*. 2022; 33: 487–501.
33. **Agarwal S, Sudhini YR, Reiser J, Altintas MM**. From Infancy to Fancy: A Glimpse into the Evolutionary Journey of Podocytes in Culture. *Kidney360*. 2021; 2: 385–97.
34. **Fogo AB**. Animal models of FSGS: lessons for pathogenesis and treatment. *Seminars in nephrology*. 2003; 23: 161–71.
35. **Yang JW, Dettmar AK, Kronbichler A, Gee HY, Saleem M, Kim SH*, et al.*** Recent advances of animal model of focal segmental glomerulosclerosis. *Clinical and experimental nephrology*. 2018; 22: 752–63.
36. **Zennaro C, Mariotti M, Carraro M, Pasqualetti S, Corbelli A, Armelloni S*, et al.*** Podocyte developmental defects caused by adriamycin in zebrafish embryos and larvae: a novel model of glomerular damage. *PloS one*. 2014; 9: e98131.
37. **Rider SA, Bruton FA, Collins RG, Conway BR, Mullins JJ**. The Efficacy of Puromycin and Adriamycin for Induction of Glomerular Failure in Larval Zebrafish Validated by an Assay of Glomerular Permeability Dynamics. *Zebrafish*. 2018; 15: 234–42.
38. **Campbell KN, Tumlin JA**. Protecting Podocytes: A Key Target for Therapy of Focal Segmental Glomerulosclerosis. *American journal of nephrology*. 2018; 47 Suppl 1: 14–29.
39. **Fogo AB**. Causes and pathogenesis of focal segmental glomerulosclerosis. *Nature reviews. Nephrology*. 2015; 11: 76–87.
40. **Shankland SJ, Pippin JW, Duffield JS**. Progenitor cells and podocyte regeneration. *Seminars in nephrology*. 2014; 34: 418–28.
41. **Grahammer F, Wanner N, Huber TB**. Podocyte regeneration: who can become a podocyte? *The American journal of pathology*. 2013; 183: 333–35.
42. **Kriz W**. The Inability of Podocytes to Proliferate: Cause, Consequences, and Origin. *Anatomical record (Hoboken, N.J. : 2007)*. 2020; 303: 2588–96.
43. **Rovin BH, Adler SG, Barratt J, Bridoux F, Burdge KA, Chan TM*, et al.*** Executive summary of the KDIGO 2021 Guideline for the Management of Glomerular Diseases. *Kidney international*. 2021; 100: 753–79.

44. **Diefenhardt P, Osterholt T, Brinkkötter P**. Nephrotisches Syndrom: Überblick und Basis. *Deutsche medizinische Wochenschrift (1946)*. 2022; 147: 332–36.
45. **Rice JB, White AG, Scarpati LM, Wan G, Nelson WW**. Long-term Systemic Corticosteroid Exposure: A Systematic Literature Review. *Clinical therapeutics*. 2017; 39: 2216–29.
46. **Gerlach GF, Wingert RA**. Kidney organogenesis in the zebrafish: insights into vertebrate nephrogenesis and regeneration. *Wiley interdisciplinary reviews. Developmental biology*. 2013; 2: 559–85.
47. **Kroeger PT, Drummond BE, Miceli R, McKernan M, Gerlach GF, Marra AN*, et al.*** The zebrafish kidney mutant zeppelin reveals that brca2/fancd1 is essential for pronephros development. *Developmental biology*. 2017; 428: 148–63.
48. **Nasevicius A, Ekker SC**. Effective targeted gene 'knockdown' in zebrafish. *Nature genetics*. 2000; 26: 216–20.
49. **Kim S, Radhakrishnan UP, Rajpurohit SK, Kulkarni V, Jagadeeswaran P**. Vivo-Morpholino knockdown of alphaIIb: A novel approach to inhibit thrombocyte function in adult zebrafish. *Blood cells, molecules & diseases*. 2010; 44: 169–74.
50. **Whiteside CI, Cameron R, Munk S, Levy J**. Podocytic cytoskeletal disaggregation and basement-membrane detachment in puromycin aminonucleoside nephrosis. *The American journal of pathology*. 1993; 142: 1641–53.
51. **Müller-Deile J, Schenk H, Niggemann P, Bolaños-Palmieri P, Teng B, Higgs A*, et al.*** Mutation of microphthalmia-associated transcription factor (mitf) in zebrafish sensitizes for glomerulopathy. *Biology open*. 2019; 8.
52. **Hentschel DM, Mengel M, Boehme L, Liebsch F, Albertin C, Bonventre JV*, et al.*** Rapid screening of glomerular slit diaphragm integrity in larval zebrafish. *American journal of physiology. Renal physiology*. 2007; 293: F1746-50.
53. **Weening JJ, Rennke HG**. Glomerular permeability and polyanion in adriamycin nephrosis in the rat. *Kidney international*. 1983; 24: 152–59.
54. **Bonadonna G, Monfardini S, Lena M** de**, Fossati-Bellani F**. Clinical evaluation of adriamycin, a new antitumour antibiotic. *British medical journal*. 1969; 3: 503–06.
55. **Wang Y, Wang YP, Tay YC, Harris DC**. Progressive adriamycin nephropathy in mice: sequence of histologic and immunohistochemical events. *Kidney international*. 2000; 58: 1797–804.
56. **Lee VWS, Harris DCH**. Adriamycin nephropathy: a model of focal segmental glomerulosclerosis. *Nephrology (Carlton, Vic.)*. 2011; 16: 30–38.
57. **Schindler M, Blumenthal A, Moeller MJ, Endlich K, Endlich N**. Adriamycin does not damage podocytes of zebrafish larvae. *PloS one*. 2020; 15: e0242436.
58. **Zheng Z, Schmidt-Ott KM, Chua S, Foster KA, Frankel RZ, Pavlidis P*, et al.*** A Mendelian locus on chromosome 16 determines susceptibility to doxorubicin

nephropathy in the mouse. *Proceedings of the National Academy of Sciences of the United States of America*. 2005; 102: 2502–07.

59. **Zhang W-W, Zhang Y-B, Zhao X-X, Hua Y, Wu Z-L, Yan Y-C*, et al.*** Prmt7 regulates epiboly by facilitating 2-OST and modulating actin cytoskeleton. *Journal of molecular cell biology*. 2015; 7: 489–91.
60. **Kato Y, Tonomura Y, Hanafusa H, Nishimura K, Fukushima T, Ueno M**. Adult Zebrafish Model for Screening Drug-Induced Kidney Injury. *Toxicological sciences : an official journal of the Society of Toxicology*. 2020; 174: 241–53.
61. **Davison JM, Akitake CM, Goll MG, Rhee JM, Gosse N, Baier H*, et al.*** Transactivation from Gal4-VP16 transgenic insertions for tissue-specific cell labeling and ablation in zebrafish. *Developmental biology*. 2007; 304: 811–24.
62. **Zhou W, Hildebrandt F**. Inducible podocyte injury and proteinuria in transgenic zebrafish. *Journal of the American Society of Nephrology : JASN*. 2012; 23: 1039–47.
63. **Siegerist F, Blumenthal A, Zhou W, Endlich K, Endlich N**. Acute podocyte injury is not a stimulus for podocytes to migrate along the glomerular basement membrane in zebrafish larvae. *Scientific reports*. 2017; 7: 43655.
64. **Hansen KUI, Siegerist F, Daniel S, Schindler M, Iervolino A, Blumenthal A*, et al.*** Prolonged podocyte depletion in larval zebrafish resembles mammalian focal and segmental glomerulosclerosis. *FASEB journal : official publication of the Federation of American Societies for Experimental Biology*. 2020; 34: 15961–74.
65. **Smeets B, Kuppe C, Sicking E-M, Fuss A, Jirak P, van Kuppevelt TH*, et al.*** Parietal epithelial cells participate in the formation of sclerotic lesions in focal segmental glomerulosclerosis. *Journal of the American Society of Nephrology : JASN*. 2011; 22: 1262–74.
66. **Suzuki T, Matsusaka T, Nakayama M, Asano T, Watanabe T, Ichikawa I*, et al.*** Genetic podocyte lineage reveals progressive podocytopenia with parietal cell hyperplasia in a murine model of cellular/collapsing focal segmental glomerulosclerosis. *The American journal of pathology*. 2009; 174: 1675–82.
67. **Schindler M, Siegerist F, Lange T, Bach S-M, Gehrig J, Gul S*, et al.*** A novel high-content screening assay identified belinostat to be protective in a FSGS-like zebrafish model. Submitted 05.07.2022. *Journal of the American Society of Nephrology : JASN*. 2022.
68. **Hanke N, King BL, Vaske B, Haller H, Schiffer M**. A Fluorescence-Based Assay for Proteinuria Screening in Larval Zebrafish (Danio rerio). *Zebrafish*. 2015; 12: 372–76.
69. **Liu M, Liang K, Zhen J, Zhou M, Wang X, Wang Z*, et al.*** Sirt6 deficiency exacerbates podocyte injury and proteinuria through targeting Notch signaling. *Nature communications*. 2017; 8: 413.
70. **Allison SJ**. Epigenetics: H3K27me3 in glomerular disease. *Nature reviews. Nephrology*. 2018; 14: 143.

71. **Kuo F-C, Chao C-T, Lin S-H**. The Dynamics and Plasticity of Epigenetics in Diabetic Kidney Disease: Therapeutic Applications Vis-à-Vis. *International journal of molecular sciences*. 2022; 23.
72. **Lee H-Z, Kwitkowski VE, Del Valle PL, Ricci MS, Saber H, Habtemariam BA*, et al.*** FDA Approval: Belinostat for the Treatment of Patients with Relapsed or Refractory Peripheral T-cell Lymphoma. *Clinical cancer research : an official journal of the American Association for Cancer Research*. 2015; 21: 2666–70.
73. **Hyndman KA**. Histone Deacetylases in Kidney Physiology and Acute Kidney Injury. *Seminars in nephrology*. 2020; 40: 138–47.
74. **Zhang L, Cao W**. Histone deacetylase 3 (HDAC3) as an important epigenetic regulator of kidney diseases. *Journal of molecular medicine (Berlin, Germany)*. 2022; 100: 43–51.
75. **Jeong Y, Du R, Zhu X, Yin S, Wang J, Cui H*, et al.*** Histone deacetylase isoforms regulate innate immune responses by deacetylating mitogen-activated protein kinase phosphatase-1. *Journal of leukocyte biology*. 2014; 95: 651–59.
76. **Wennmann DO, Vollenbröker B, Eckart AK, Bonse J, Erdmann F, Wolters DA*, et al.*** The Hippo pathway is controlled by Angiotensin II signaling and its reactivation induces apoptosis in podocytes. *Cell death & disease*. 2014; 5: e1519.
77. **Hurcombe JA, Hartley P, Lay AC, Ni L, Bedford JJ, Leader JP*, et al.*** Podocyte GSK3 is an evolutionarily conserved critical regulator of kidney function. *Nature communications*. 2019; 10: 403.
78. **Basu D, Reyes-Múgica M, Rebbaa A**. Histone acetylation-mediated regulation of the Hippo pathway. *PloS one*. 2013; 8: e62478.

10 Eigenständigkeitserklärung

Hiermit erkläre ich, dass diese Arbeit bisher von mir weder an der Mathematisch-Naturwissenschaftlichen Fakultät der Universität Greifswald noch einer anderen wissenschaftlichen Einrichtung zum Zwecke der Promotion eingereicht wurde.

Ferner erkläre ich, dass ich diese Arbeit selbstständig verfasst und keine anderen als die darin angegebenen Hilfsmittel und Hilfen benutzt und keine Textabschnitte eines Dritten ohne Kennzeichnung übernommen habe.

Datum Unterschrift Promovend

11 Scientific achievements

Publications:

- Kliewe F, Kaling S, Lötzsch H, Artelt N, **Schindler M**, Rogge H, Schröder S, Scharf C, Amann K, Daniel C, Lindenmeyer MT, Cohen CD, Endlich K, Endlich N.
  Fibronectin is up-regulated in podocytes by mechanical stress. The FASEB Journal 2019, DOI: 10.1096/fj.201900978RR.

- **Schindler M**, Blumenthal A, Moeller MJ, Endlich K, Endlich N.
  Adriamycin does not damage podocytes of zebrafish larvae. PloS One 2020, DOI: 10.1371/journal.pone.0242436.

- Hansen KUI, Siegerist F, Daniel S, **Schindler M**, Iervolino A, Blumenthal A, Daniel C, Amann K, Zhou W, Endlich K, Endlich N.
  Prolonged podocyte depletion in larval zebrafish resembles mammalian focal and segmental glomerulosclerosis. The FASEB Journal 2020, DOI: 10.1096/fj.202000724R.

- Michalik S, Siegerist F, Palankar R, Franzke K, **Schindler M**, Reder A, Seifert U, Cammann C, Wesche J, Steil L, Hentschker C, Gesell-Salazar M, Reisinger E, Beer M, Endlich N, Greinacher A, Völker U. Comparative analysis of ChAdOx1 nCoV-19 and Ad26.COV2.S SARS-CoV-2 vector vaccines. Haematologica 2022, DOI: 10.3324/haematol.2021.280154.

- **Schindler M**, Siegerist F, Lange T, Bach SM, Gehrig J, Gul S, Endlich N. A novel high-content screening assay identified belinostat to be protective in a FSGS-like zebrafish model. Submitted to the Journal of the American Society of Nephrology.

Contributions to scientific conferences

- "Adriamycin does not induce podocyte damage *per se* in zebrafish larvae". 30th Meeting of the European Renal Cell Study Group, Florence, Italy, 2018 (oral presentation)
- "Adriamycin does not induce podocyte damage *per se* in zebrafish larvae". 113th Meeting of the Anatomische Gesellschaft, Rostock, Germany, 2018 (oral presentation)
- "Establishment of an *in vivo* high-throughput drug screening assay combining assessment of glomerular barrier function and podocyte vitality on zebrafish larvae". 13th Meeting of the Deutschen Gesellschaft für Nephrologie (DGfN), Rostock, Germany, 2021 (oral presentation)
- "Development of a high-throughput *in vivo* drug screening assay using a FSGS-like zebrafish model". 59th ERA (European Renal Association) Congress, Paris, France, 2022 (free communication / oral presentation)

Grants

- Travel grant for the 30th Meeting of the European Renal Cell Study Group, Florence, Italy, 2018 from the FVMM ("Forschungsverbund Molekulare Medizin").

12 Acknowledgements

Firstly, I want to thank **Prof. Dr. Nicole Endlich** for her endless support, for her impressive and catching scientific drive, for providing outstanding research possibilities and especially for our trustful relationship throughout the whole project.

Furthermore, **Prof. Dr. Steffen Harzsch** guided me perfectly through this work, I always felt welcome and respected. The whole AG CytoEvo is a friendly and inspirational group of biologists and we had a great time on Hiddensee.

The whole **AG Endlich** supported this work outstandingly and I want to thank the following colleagues in detail:

- **Dr. Tim Lange** you are just awesome as a whole. Nothing to add.
- **Dr. Florian Siegerist** did the groundwork for this project from scratch. You are an outstanding scientist and an inspiration. You always have the answer, prego!
- **Sophia-Marie Bach** is an awesome lab technician, hard-working and very funny. You helped me a lot and there is no one who gently pushes larvae better than you.
- **Oliver Zabel and Steffen Prellwitz**, the animal husbandry is awesome. Thank you so much for always being there, even at weekends and on holidays. Cheers.

Next, I want to thank my parents and especially my siblings who always supported me unconditionally.At last, I want to thank my own little family.

Anne, thank you so much for always having my back no matter what and for giving birth to our two awesome sons, **Emil** and **Finn**.

I love you!